Slope Stability Analysis and Remedial Measures for Selected Sections of Qune-Bedesa Road, West Harerghe Zone.

Ketema Belayneh Degu

A Thesis Submitted to Department of Civil Engineering

School of Civil Engineering and Architecture

Presented in Partial Fulfillment of the Requirement for the Degree of Master's in

Geotechnical Engineering

Office of Graduate Studies

Adama Science and Technology University

November, 2024

Adama, Ethiopia

Slope Stability Analysis and Remedial Measures for Selected Sections of Qune-Bedesa Road, West Harerghe Zone.

Ketema Belayneh Degu

Advisor: Argaw Asha (PhD)

A Thesis Submitted to Department of Civil Engineering

School of Civil Engineering and Architecture

Department of Civil Engineering

Presented in Partial Fulfillment of the Requirement for the Degree of Master's in Geotechnical Engineering

Office of Graduate Studies

Adama Science and Technology University

November, 2024

Adama, Ethiopia

APPROVAL PAGE

We, the advisors of the thesis entitled "Slope Stability Analysis and Remedial Measures for Selected Sections of Qune-Bedesa Road Project, West Harerghe Zone" developed by Ketema Belayneh, hereby certify that the recommendation and suggestions made by the board of examiners are appropriately incorporated into the final version of the thesis.

Dr. Argaw Asha (PhD)	____________________	______________
Major Advisor	Signature	Date

Approval sheet of Examiners

We, the undersigned, members of the Board of Examiners of the final open defense by Ketema Belayneh have read and evaluate his thesis entitled "Slope Stability Analysis and Remedial Measures for Selected Sections of Qune-Bedesa Road Project, West Harerghe Zone" and examined the candidate. This is, therefore, to certify that the thesis has been accepted in partial fulfillment of the requirement of the Degree of Masters in Civil Engineering (Geotechnical Engineering).

Name	Signature	Date
Ketema Belayneh Name of student	______________	____________
____________________ Chairperson	______________	____________
____________________ Internal Examiner	______________	____________
____________________ External Examiner	______________	____________
____________________ Head of Department	______________	____________
____________________ School Dean	______________	____________
____________________ Post Graduate Dean	______________	____________

DECLARATION

I hereby declared that this MSc thesis entitled "Slope Stability Analysis and Suggestion of Remedial Measures for Selected Sections of Qune-Bedesa Road Project, West Harerghe Zone" is my own work. That is, it has not been submitted for the award of any academic degree, diploma or certificate in any other university. All sources of material that are used for this thesis have been duly acknowledged through citation.

Ketema Belayneh	______________________	_______________
Name of student	Signature	Date

DECLARATION

This MSc thesis has been submitted for examination with my approval as a thesis advisor.

Name: Dr. Argaw A. (PHD)

Signature: _________________

Date of submission: _________________________

ACKNOWLEDGEMENT

First of all, I would like to thank a lot the Almighty God for his gift that cannot be described in words, protection and help. Next to that I would like to thanks Oda Bultum University to giving me the chance of studying my MSc degree and sponsoring me. Likewise, the deepest gratitude goes to my Instructor's Dr. Argaw Asha for giving me the opportunity to do this Theses under his faithful and immense devotion and to help me for the accomplishment of the research work, for his kindness and tolerance while carrying this thesis write through giving his valuable advice, encouragement and supports of all kind throughout the research writing period.

I want to express my deep appreciation to all of my classmates and friends for our great discussion about research report writing. and the Alasab-Est General contractor and Transportation for allowing me to use their Laboratory.

Finally, I would like to express my appreciation for my family for their encouragement and unlimited support.

TABLE OF CONTENT

LIST OF TABLES

LIST OF FIGURES

LIST OF ACRONYMS AND ABBREVIATIONS

ASTM____ American Society for Testing and Materials

ERA ____ Ethiopian Roads Authority

EBCS____ Ethiopian Building Code Standard

FOS____ Factor of Safety

C____ Cohesion

E____ Modulus of elasticity

FEM ____ Finite Element Method

LEM____ Limit Equilibrium Method

SS____ Soil slope section

SRF____ Strength Reduction Factor

V____ Poisons Ratio

$\emptyset$ ____ The angle of internal friction

ψ ____ angle of dilatancy

ABSTRACT

This study aimed to investigate the slope stability condition along selected failed Qune -Bedesa sections of Arbereketi-Micheta road upgrading project. Finite element and limit equilibrium stability analysis methods were performed on four Soil slope sections (SS1, SS2, SS3 and SS4) using PLAXIS 2D software with the Mohr-Coulomb strength criterion under static dry and static wet conditions. The results indicated that the soils in the study area have a medium to high plasticity index and a high liquid limit, with moisture content ranging from 12.95% to 26.25%. The limit equilibrium analysis revealed the following factors of safety (FOS) for SS1: 1.452 under static dry conditions, 0.904 under static wet conditions. The strength reduction factor (SRF) analysis showed a decrease of 4.6% from static dry to static wet conditions. These findings provide comprehensive and accurate information on the engineering geological and slope stability conditions of the study area, enabling informed decision-making and appropriate measures to mitigate potential slope failures along the road corridor. Finaly after taking effective remedial measure accordingly, slope angle reduction to 43^o, and 38^o improves FOS to 1.398 and 1.442 for SS4 and SS2 respectively, using 2 bench slopes cutting improves FOS to 1.344 and 1.314 for SS2 and SS3 respectively and soil slope nailing makes FOS 1.666 and 1.502 for SS1 and SS2 respectively.

Keywords: Slope Stability analysis, PLAXIS 2D, SS, SRF and FOS

CHAPTER 1. INTRODUCTION

1.1 Background

A slope is an inclined ground surface formed naturally or by human activities through excavation for different purposes. Throughout the world, slope instabilities are the challenging problems mainly to the civil engineering structure such as road, tunnels, dams, and open pit mines (Siddique, Pradhan, Vishal, & Mondal, 2019; Dietze, et al., 2022). It occurs in the form of rotational, translational and wedge mode of failure causing different impact on properties, lives, and blocking traffic (Pantelidis, 2009).

Instability of slopes can occur due to the combination of internal and external factors which causes an immediate or near immediate slope failure either by reducing the shear strength of slope material or by increasing the shear stress on the slope (Kumar, 2022). Rainfall, increase in groundwater table, change in stress conditions, changing geometry, rock discontinuity characteristics, deep weathering, surcharge, and dynamic force like earthquakes are among the common factors responsible for slope instability (Abbate, Longoni, Ivanov, & Papini, 2019; Chen, Qin, Xue, & Xu, 2021). The mechanism of slope failure varies and takes place as speed or slow rate, and it depends on the type of material, slope geometry, and types of triggering factors. As both natural and human activities are responsible for the failure of slopes, it is difficult to prevent the problem entirely. However, the level of damage can be significantly reduced by assessing the stability condition and adopting different preventive measures on it. There are various remedial measures used to reduce the impact of slope failures and these can be grouped into four general classes (i.e., geometric modification, drainage control, slope reinforcement, and retaining structure) (Popescu, 2001). It must be noted that, to design safe and economical slopes, assess the stability of existing slopes, and adopt suitable remedial measures on it, understanding the cause of failure, mode of failure, and methods of stability analysis approaches are necessary.

Ethiopia is one of developing country that undertaking massive civil engineering infrastructural development like Highway, railways, Building, and etc. Among these infrastructures Ethiopian Roads Authority (ERA) has constructing many roads throughout the country accelerate the growth of the country because road is a key factor for transportation and development. Slope instability problems are widespread along roads that pass through mountainous terranes/gorges. Most of the Ethiopian plateau in the north, south, west and eastern parts of the country have a history of slope instability problems both at superficial materials and bedrock levels due to steep mountains and road cuts (Bekele & Meten, 2022). The current study is situated along the eastern highland plateau very close to the Eastern Rift Margin and partly lies within the northwestern extreme end of Ogaden basin. Since it is difficult to stop this slope failure problem, geotechnical engineers have responsibility for these issues for investigating, analyses and propose remedial measure. In this way, the main motivation of these research is to conduct stability analyses along road section and to suggest possible remedial measure in order to save human lives, reduce property damages and provide continuous services along roadway. Hence, stability analysis of cut slope needs to be performed to have information on the slope deformation, state of stresses at critically unstable failure zones, different mode failures and safe functional design of excavated slopes using different slope stability analysis methods.

In the past, many geotechnical engineers and engineering geologists have performed slope stability analyses using different techniques. In geo-mechanical engineering, to asses and analyze stability of the slope, some of the methods such as: Limit equilibrium method, Finite element method, Kinematic analysis and Rock mass classification systems, Deterministic, Probabilistic and Numerical methods (Vanneschi, Rindinella, & Salvini, 2022; Pandit, Singh, Sharma, Sandhu, & Sahoo, 2021) are used frequently.

The present study was conducted to evaluate the stability of slope along selected section of Qune-Bedesa road using limit equilibrium and finite element method. For this purpose, determining the engineering properties of soils through extensive field survey, in situ tests, literature review and correlation, sampling and laboratory experiments were performed in order to extract necessary data. Finally, appropriate remedial measures were recommended based on the analysis results.

1.2 Statement of problem

The construction of highway and railways are growing rapidly in Ethiopia to give access road connection between different zonal and regional government and furtherly to connect the country with ports of neighboring countries. But, due to the difficulty of geographical locations along road alignments, the construction of these infrastructures (highways and railways) needs cutting of slopes and construction of embankments which leads to slope instability problems along this road side. The failure of these roadside slopes is currently an issue in Ethiopia causing considerable damage to the life, natural and manmade assets (Gao, Yang, Hu, & Hu, 2022). Hence, slope stability analysis is crucial to identify critical slope sections and apply different remedial measures.

The Qune – Bedesa upgrading road project is currently an ongoing project around the eastern parts of the country West Harerghe zone Oromia region. However, some slope failures are experienced at different mountainous sections of this road stretch. In connection to this the contractor is forced to stop the works in these sections. Not only road section under construction but also some road sections which are constructed and opened to service are also starting to experience massive landslides. Due to these problems which experienced during field survey, this work aims to fill this gap by studying geological and geotechnical condition of materials of the slope section to identify, locate and analyze slope stability problems along selected road section using Limit equilibrium and Finite element methods. Finally, appropriate remedial measures were recommended based on the analysis results.

1.3 Research Questions (Hypothesis)

After investigation this study would answer the following research questions:

- What's are the main causes or factors that contribute to slope instability along selected failed sections and how does these factors affect slope stability?
- What types of failure modes or classification of landslide is it in these sections?
- What's are values of factor of safety (FOS) for selected failed sections?
- What's are the remedial measures for these failed slope sections?

1.4 Objectives of the study

1.4.1 General objective

The primary purpose of this study is to investigate and evaluate the slope stability condition and suggesting remedial measures along selected section of Qune – Bedesa road upgrading project.

1.4.2 Specific Objectives

The specific objectives of the research are;

- To determine the index and engineering properties of soils found in failed slope sections.
- To determine the factor of safety and failure probability of the critical slope sections.
- To identify causes of failure and Classifications of slope failure at those selected failed locations.
- To take effective remedial measures on identified failed slope sections.

1.5 Significance of the study

The landslide events were very devastating and it has severely influence transportation activity.

Qune – Bedesa road which links many important growing towns of eastern part to the central parts of Ethiopia was coming into traffic volume problem from time to time due to chat and related other marketing activities. However, the road section around mountainous region has slope instability problems that hinder these marketing activities which is among major economic backbone for the country as whole. Therefore, this study is very important from the point of view of identifying and understanding the possible causes of the slope instabilities along the road. Furthermore, for those slopes where the results of the stability analysis indicate that the roadway slope do not meet the factor of safety requirement, remedial measures need to be proposed on these slope sections. Additionally, since there is no previous study along these areas this research may be used as input data for future researcher who study on stability of this failed slopes.

1.6 Scope and limitation of the study

The scope of this study is limited to the road cut slope stability analysis and remedial measure of slope profiles for roads constructed from Qune – Bedesa road section. The analysis was carried using both finite element method and limit equilibrium method by using plaxis 2D and slide software respectively on four critical road cut sections only. This study not includes effect of ground water table. Suitable data for the analysis was obtained from laboratory tests, and correlations using the literature. A comparative study was made on slope profiles (single slope and bench slope) and soil nailing in the selected slope section. The modeling results are evaluated in terms of deformation and factor of safety using plaxis 2D and slide software.

1.7 Organization of the study

This Research reports have seven Chapters as listed below.

Chapter 1: Provides a general introduction of slope stability, statement of the problem, the research objectives and significance of the study.

Chapter 2: Presents a literature review about slope failure and its stability analysis, Various types and causes of failure, shear strength criteria, and different stability analysis approaches are discussed. Further slope stability studies, stabilization methods, and software applications also included in this chapter.

Chapter 3: Presents the description of the study area, material and methodology followed to attain the objectives of the study and material used in this research.

Chapter 4: Presents data processing and tabulation of data used for numerical modeling from field investigation and laboratory work.

Chapter 5: Presents the numerical modeling procedures of critical slope sections in both FEM (PLAXIS software) and LEM (SLIDE). Modeling of geometric profiles for performance evaluation and validation of numerical models using previous works also included in this chapter.
Chapter 6: Presents the result and discussions of numerical analysis. Discussions on the stability conditions of slope and comparisons of analysis methods are presented. Discussions also included the performance of geometric profiles, comparison of FEM and LEM, remedial measures taken and suitable conditions for them. Finally,
Chapter 7: Provides a general conclusion and recommendation of the study.

CHAPTER 2. LITERATURE REVIEW

2.1 Introduction

Slope failure is an ongoing problem all over the world causing damages to infrastructures, loss of human life, and damages to natural resources. Slope instability problems damage civil engineering structures such as buildings, dams, irrigation canals, roads, railway, etc. in the world (Bekele, A., & Meten, M., 2022). Slope instability problem is one of the geological and geotechnical problems which are a complex natural phenomenon that constitutes a serious natural hazard in many countries. Slope failures are generally considered as fairly well predictable hazards and economic losses due to such hazards can be reduced significantly (Hansen, 1984.) Especially in recent years, there have been advances in better understanding of the initiations of landslides and in techniques of slope instability hazard assessments, prediction and mitigation (Hansen, 1984.) In recent years, growing population and expansion of settlements and life-lines over hazardous areas have largely increased the impact of natural disasters both in industrialized and developing countries. Third world countries have difficulty meeting the high costs of controlling natural hazards through major engineering works and rational land-use planning. Industrialized societies are increasingly reluctant to invest money in structural measures that can reduce natural risks. Hence, the new issue is to implement warning systems and land utilization regulations aimed at minimizing the loss of lives and property without investing in long-term, costly projects of ground stabilization.(Alberto, 1991).

The primary concern of slope stability studies is to contribute to the safe and economic design of new slope and stability assessment of existing slopes. The engineering solutions to slope stability problems require a good understanding of cause and mechanisms of slope failure, analytical methods, investigative tools, and stabilization measures. Hence, in this section review was made on factors affecting slope stability, type of slope failures**,** causes and mechanisms of failure, shear strength criteria of soils and rocks, analysis methods, previous stability assessments, stabilization methods, and software applications.

2.2 Factors Affecting Slope Stability

The majority of soil and rock slope instability in the past has been driven by natural processes (Savi, Comiti, & Strecker, 2021). Slope failure occurs when the downward movements of material due to gravity and shear stresses exceed the shear strength. Instability of the slope deals with the relationship between shear stress and shear strength forces(Kumar & Kumar, 2022). Therefore, factors that tend to increase the shear stresses or decrease the shear strength increase the chances of failure of a slope. Different processes can lead to a reduction in shear strengths. Increased pore pressure, cracking, swelling, decomposition of clayey rock fills, creep under sustained loads, leaching, weathering, and cyclic loading are common factors that decrease the shear strength. In contrast to this, the shear stress in slopes may increase due to additional loads at the top of the slope, increase in water pressure, increase in soil weight due to increased water content, excavation at the bottom of the slope, and seismic effects (Searom, 2017). In addition to these reasons factors contributing to the failure of slope include slope geometry, state of stress, and erosion. The factors affecting slope failure have been shown in Table 2.1 and important factors have been described in this chapter.

Factors affecting slope stability

Table 2.1 Factors affecting slope stability (Fentahun. A, 2020)

S. No	*Name of the parameters*	*Descriptions*
1	*Geometry of the slope*	*Height of slope, angle of slope, and slope profiles*
2	*Rock discontinuities*	*Fault, Joint, bedding plane properties*
3	*Rock and Soil properties*	*Index and strength properties (density, grain size, Atterberg limit, UCS, tensile strength, and shear strength parameters).*
4	*Rainfall and groundwater*	*Rainfall, drainage pattern, permeability, and groundwater conditions.*
5	*Dynamic forces*	*Blasting and Seismic activity*
6	*Excavation*	*Cutting, drilling and other human activities*

2.2.1 Geometry of the slope

The basic geometrical slope design parameters such as slope angle, slope height, slope profile, dip, and dip direction play a key role in slope stability. The steeper slope will be more susceptible than the gentler slope for instability (Hamza & Raghuvanshi, 2017). The overall angle increases the possible extent of the development of any failure to the rear of the crests increases and it should be considered so that the ground deformation at the mine peripheral area can be avoided. Similarly, the possibility of slope failure or landslide occurrence will increase with increasing slope relative relief or height. Moreover, the inappropriate selection and design of slope profile (i.e., single slope, multi slope, or benched slope) lead to slope instability problems. One of the factors which determine the stability of the rock and soil slope is the potential failure plane. The characteristics of discontinuities and their inter-relationship with the slope geometry affect the stability condition of rock slopes (Havaej & Stead, 2016). The main characteristics of discontinuities that control the stability of rock slopes are spacing, orientation, persistence, surface characteristics, separation of discontinuity surface, and thickness of material filled in discontinuities. Similarly, in soil slopes weak layers of soil which sometimes rest on hard strata serve as failure planes.

2.2.2 Geotechnical properties of Soils

Geotechnical factors like porosity, gradation factors, dry density, saturated permeability, and shear strength have been identified to contribute to the predictions of slope failures from the physical-based approach (Gidday, Ayothiraman, Ramaiah, & Ramana, 2023; Gutierrez-Martin, 2020). The soil composition depth shear strength (which is dependent on density, cohesion, plasticity, dilatancy, and the angle of internal friction), porosity, permeability, grading, moisture content, and organic matter content are some of the important geotechnical parameters of soils that control slope stability(Kamal et al., 2022). The strength parameters of the rock change by mechanical and chemical weathering. The cohesion and angle of internal friction are the shear strength parameters of the slope material, and they are the key factors that define resisting force acting normal to the failure plane (Raghuvanshi T. K., 2017). Lithology is strongly related to slope instability by weathering processes, water percolation, and interaction of rock mass. Weathered rock mass allows percolation of water via joints and fractures which can promote slope failure. The properties of rock materials such as strength and permeability are related to the degree of weathering and internal structure of the rock.

2.2.3 Rainfall and groundwater condition

Most of the time, the main reason for slope failure occurrence is the influence of rainfall which is one of the external and triggering factors of slope instability (Abbate, Longoni, Ivanov, & Papini, 2019; Chen, Qin, Xue, & Xu, 2021). Rainfall and groundwater cause slope failure by altering the cohesion and frictional parameters and reducing the normal effective stress. Groundwater causes increased up thrust and driving water forces and has an adverse effect on the stability of the slopes.

Physical and chemical effects of pore water pressure in joints filling material can thus alter the cohesion and friction of the discontinuity surface. This will reduce the shearing resistance along the potential failure plane by reducing the effective normal stress acting on it. Physical and chemical effects of the water pressure in the pores of the rock cause a decrease in the compressive strength, particularly where confining stress has been reduced. An increase in the groundwater table along the potential failure surface reduces the shear strength and lubricates the surface facilitating the sliding process (Raghuvanshi T. K., 2017). The water within rock discontinuity develops water forces in discontinuities leading to rock mass sliding. Whereas groundwater increases in soil slope result development of pore water pressure which reduces the shear strength in the soil mass (Ermias et al., 2017).

Many soil and rock slope failures in Ethiopia are associated with rainfall. Numerous case studies in different places (Fathiyah, 2017). show that rainfall infiltration reduces FOS of slope significantly. The rainfall, which infiltrate into the slope, increase the instability of the potential failure plane by reducing shear strength (Gallage, Abeykoon, & Uchimura, 2021; Raghuvanshi T. K., 2017). According to studies (Fathiyah, 2017).and (Shi, 2019), the intensity and duration of rainfall also play a major role in the mechanism and amount of slide. Small landslides like soil slips and debris flow occur during heavy rainfall of a short period as it affects only the near-surface material. Whereas Bedrock and deeper slides in unconsolidated materials will be triggered by the cumulative effects of a series of storms. Heavy rainfall increases the water pressure on materials laying on the bed slope temporarily, which is enough to decrease strength and leading to debris slips and flows. Many roadside slope failures like debris/earth slides, debris/earth flows, and rockslides in Ethiopia have occurred during the time of continued and heavy rainfalls (Woldearegay, 2013). The increased pore water pressure along potential failure plane can reduce the shear strength, and the water can also lubricate the surface, making it easier for things to slide around (Liang, 2023). According to (Mebrahtu, Banning, Girmay, & Wohnlich, 2021) increases in groundwater in soil slope results in the development of pore water pressure which reduces the shear strength in the soil mass.

2.2.4 The seismicity

Seismic activity is another triggering factor of slope stability especially in active seismic zone (Mebrahtu, Heinze, Wohnlich, & Alber, 2022). According to (Zhao, L., & Karim, M. A ., 2018), slope failures that happened by the earthquake may occur due to an increase in driving movement and reducing the shear strength. The slopes which are stable during static conditions may fail during dynamic seismic loading. The minimum magnitude of an earthquake to cause slope failure is approximately 4-5MM (BAYOU, 2020). From the safety point of view, it is recommended that seismicity is taken into consideration for critical structures like steep slopes (Caroles, 2023). Since horizontal seismic acceleration adds to driving force along failure plane, planar mode of rock slope failures will be easily destabilized under seismic loading conditions (Raghuvanshi T. K., 2017). Ethiopia is in the East African Rift Valley region, which has a history of generating large earthquakes. This can cause damages on infrastructures of active seismic zones (i.e., Afar Triangle, Main Ethiopian Rift (MER), and Southern Most Rift (SMR)) (Eleyas, 2016). For example, the 1961 Karakore earthquake (M=6.1) destroyed the town of Majete and produces cracks, fissures, rockslides, and subsidence of up to 1m deep on the Addis Ababa –Asmara highway.

2.2.5 Excavation and Other human activities

Human activity like improper modifications and excavations of the slope can trigger the stability of the slope. Most of the time human activities which can cause the slope to fail are: cutting the slope in an unplanned manner, steepening the slope gradient, improper excavation on the toe of the slope, and adding an extra load (Raghuvanshi T. K., 2017). The natural slope stability is disturbed and loses its stability in slope due to man-made activities.

2.2.6 Shear strength parameter of the slope material

Shear strength parameters of the slope material (i.e., cohesion and angle of internal friction) are the key factors that define resisting force acting normal to the failure plane (Raghuvanshi T. K., 2017). Hence any reduction of these shear strength parameters will significantly affect the stability of slopes. For example, shear strength parameters of rock change when the strength of intact rock and conditions of discontinuities like roughness, aperture, and filling changes (Lamesa & Meten, 2021). As discussed in the strength creations both discontinuity and rock mass shear strength parameters are responsible for rock slope failures.

2.2.7.1 Cohesion

It is the characteristic property of a rock or soil that measures how well it resists being deformed or broken by forces such as gravity. In soils/rocks true cohesion is caused by electrostatic forces in stiff over consolidated clays, cementing by Fe_2O_3, $CaCO_3$, $NaCl$, etc. and root cohesion. However, the apparent cohesion is caused by negative capillary pressure and pore pressure response during undrained loading. Slopes having rocks/soils with less cohesion tend to be less stable. The factors that strengthen cohesive force include, a) Friction b) Stickiness of particles can hold the soil grains together. c) Cementation of grains by calcite or silica deposition can solidify earth materials into strong rocks. d) Man-made reinforcements can prevent some movement of material. The factors that weaken cohesive strength include, a) High water content can weaken cohesion because abundant water both lubricates (overcoming friction) and adds weight to a mass. b) Alternating expansion by wetting and contraction by drying of water reduces the strength of cohesion, just like alternating expansion by freezing and contraction by thawing. c) Undercutting in slopes. d) Vibrations from earthquakes, sonic booms, blasting that create vibrations which overcome cohesion and cause mass movement.

2.2.7.2 Internal Friction Angle

Internal friction angle is measured between the normal force and resultant force, that is attained when failure just occurs in response to shearing stress. It is a measure of the ability of a unit of rock or soil to withstand shear stress. This is affected by particle roundness and particle size. Lower roundness or larger median particle size results in a larger friction angle.

2.3 Type of Slope Failures

Slope failures can occur in a variety of ways depending on the cause of failure, geometry, materials properties and rate of movement (Aydan, 2016). Slope failure can be classified into different types on the basis of the type of movement. This type of movement describes the actual internal mechanics of how the landslide mass is displaced: fall, topple, slide, spread, or flow (Highland, L. M., and Bobrowsky, Peter,, 2008)

1. Falls: A fall begins with the detachment of soil or rock, or both. It involves the collapse of material from a cliff or steep slope along a surface on which little or no shear displacement has occurred. The material subsequently descends mainly by falling, bouncing, or rolling as shown on figure 2.1 below.

It consists of rapid movement of material that becomes detached from steep slopes or cliffs. Separation occurs along discontinuities such as fractures, joints, and bedding planes, while the movement occurs by free-fall, bouncing, and rolling. Falls are usually of a small volume (a few individual blocks). Rock (and soil) falls are characterized by the scattered accumulation of material on the ground surface downslope of the zone of depletion and forming a talus slope at the toe. (NZGS, 2023)

2. Topple: A topple is recognized as the forward rotation out of a slope of a mass of soil or rock around a point or axis below the center of gravity of the displaced mass. Topples can consist of rock, debris (coarse material), or earth materials (fine-grained material).

According to (NZGS, 2023) Toppling failures can occur in slopes cut in rock with regularly spaced fractures or bedding planes that strike parallel or subparallel to the slope, and dip into the face. This contrasts with sliding failures which occur when the geological structure dips out of the face. Toppling may be either Flexural, where the rock mass deforms in a plastic fashion by bending and forward rotation on closely spaced defects, or Block, where the stability of thicker, rigid rock blocks is governed by defect orientation.

3. Slides A slide is a downslope movement of a soil or rock mass occurring on surfaces of rupture or on relatively thin zones of intense shear strain. Movement does not initially occur simultaneously over the whole of what eventually becomes the surface of rupture; the volume of displacing material enlarges from an area of local failure. Slides can be a little more complex than falls and the shape of these features is dependent on the type of material in which the slide occurs as well as the amount and direction of movement.

This are characterized by a failure of material at depth and then movement by sliding along a rupture or slip surface. There are two types of slide failure, rotational slides (slumps) and translational (planar) slides. (BGS, 2024).

Rotational Landslide: A landslide on which the surface of rupture is curved upward (spoon-shaped) and the slide movement is more or less rotational about an axis that is parallel to the contour of the slope.

Translational Landslide: The mass in a translational landslide moves out, or down and outward, along a relatively planar surface with little rotational movement or backward tilting. This type of slide may progress over considerable distances if the surface of rupture is sufficiently inclined, in contrast to rotational slides, which tend to restore the slide equilibrium.

4. Spreads: An extension of a cohesive soil or rock mass combined with the general subsidence of the fractured mass of cohesive material into softer underlying material. Types of spreads include block spreads, liquefaction spreads, and lateral spreads. This form of landslide is characterized by lateral extension and accompanied by shear or tensile fractures and usually occurs on very gentle slopes. In soils, failure may be caused by liquefaction of susceptible soils, usually triggered by a strong ground motion from high magnitude earthquake events.

5. Flows: A flow is a spatially continuous movement in which the surfaces of shear are short-lived, closely spaced, and usually not preserved. Flows are landslides that involve the movement of material down a slope in the form of a fluid. Flows often leave behind a distinctive, upside-down funnel shaped deposit where the landslide material has stopped moving.

Debris Flows: A form of rapid mass movement in which loose soil, rock and sometimes organic matter combine with water to form a slurry that flows downslope.

Debris Avalanche: Debris avalanches are essentially large, extremely rapid, often open-slope flows formed when an unstable slope collapses and the resulting fragmented debris is rapidly transported away from the slope.

Earthflow: Earthflows can occur on gentle to moderate slopes, generally in fine-grained soil, commonly clay or silt, but also in very weathered, clay-bearing bedrock. The mass in an earthflow moves as a plastic or viscous flow with strong internal deformation.

Slow Earthflow (Creep): Creep is the informal name for a slow earthflow and consists of the imperceptibly slow, steady downward movement of slope-forming soil or rock.

The following figures 2.1 describe and summarizes the type and mechanism of slope failure in detail.

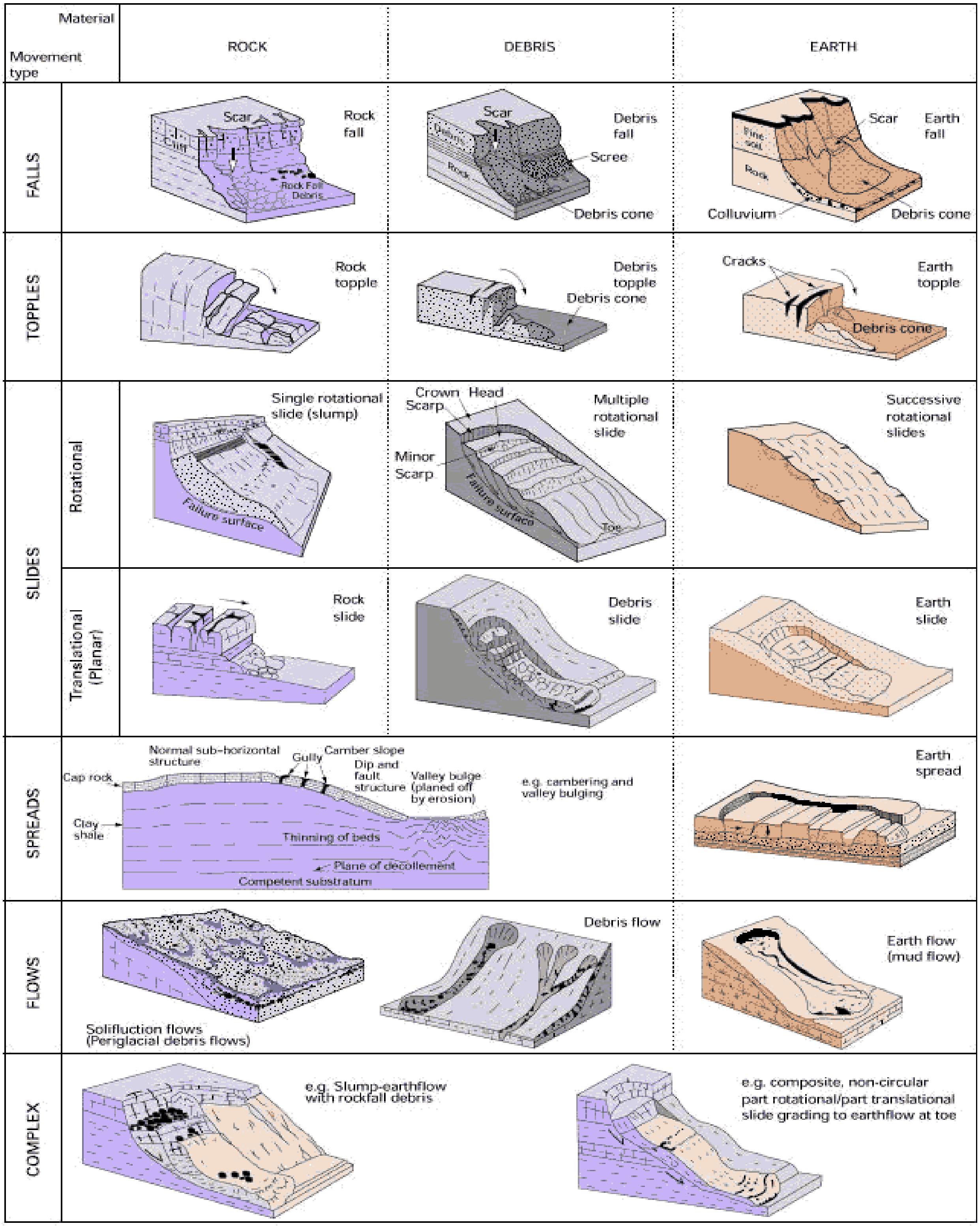

Figure 2-1 Classification of type of landslides modified after Varnes (1978). (Sara, 2012)

2.4 Previous Studies on Slope Failure

(Shiferaw, 2021) Study on the influence of slope height and angle on the factor of safety and shape of failure of slopes based on strength reduction method of analysis using finite element method PLAXIS and concludes that Decreasing slope angle increases the factor of safety of slopes nearly linearly while decreasing slope height increases the factor of safety at different rates. For a particular slope, decreasing the slope angle will increase the factor of safety more efficiently than decreasing the slope while for another slope, decreasing height is more efficient. Understanding the failure mode and influence of geometric alteration on slope factor of safety is useful to adopt the most efficient method to increase the stability of slopes

(Eleyas, 2016) study the cause and mitigation measures of slope instability problems in the case of Ethiopian railways. Accordingly, the hilly terrains in the highlands of Ethiopia remain highly fragile in terms of slope stability whereby any external factors could trigger slope failure. The study states that rainfall, earthquake, and expansive soil are the major causes of slope failures in Ethiopian railways.

(Fathiyah, 2017) Also investigates the effect of rainfall pattern on slope stability with different slope angle. From the result, critical FS for gentle and steep slope is reached under the application of advanced and delayed rainfall patterns respectively. Further FS reduction in gentle slope is found to be higher than the FS reduction in steep slope in any rainfall pattern.

Modification of slope geometry such as removal of driving material, the addition of material to area maintaining stability and change of slope profile provides good slope stabilization technique (Popescu, 2001).

According to (Khan & Wang, 2021) Geotechnical engineers should pay close attention to geology, surface drainage, groundwater and the shear strength of the soil to assess slope stability. Most of these failures are due to the shear strength failure of soil. Shear strength has a very close connection with slope angle, which is also called the angle of repose (β).

2.5 Shear strength criteria of soil

2.5.1 Mohr-Coulomb Failure Criterion for Soil

The Mohr-Coulomb failure criterion is the most common and widely used in soil mechanics. This model is a perfectly elastic-plastic model and has been mostly used in geotechnical applications (Ambassa & Amba, 2022). Mohr-coulomb gives a failure criterion of soil material by using a critical combination of normal and shear stress (Pauli, Kraus, & Siebert, 2021)**.** The linear empirical equation of the Mohr-Coulomb criterion relates the shear strength of the material on the failure plane with the cohesion, normal stress, and angle of internal friction of the material (Eq .2.1).

$\tau f = c + \sigma n \ tan\emptyset$ --Eq.2.1

where, τ = is the shear stress, σ= is the normal stress, c= is the cohesion of the material, and ϕ is the material angle of friction.

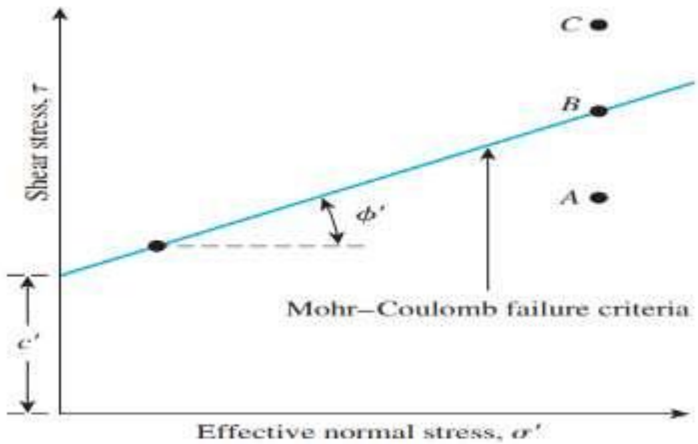

Figure 2-2 Mohr-Coulomb failure criterion (Pauli, Kraus, & Siebert, 2021)

2.6 Slope stability analysis approaches

Slope stability is one of the most common problems in geotechnical engineering. The need for a better understanding of failure mechanism of both man-made and natural earthen slopes is necessary to better assist any remediation measure of potentially moving or failing slopes. Slope stability analysis methods developed over many years and continue to develop as a result of advancement in technology, instrumentations, soil behavior and theories, and new constitutive soil models (Albataineh, 2006).

Many techniques exist for evaluation of the stability of a given slope. Earlier methods for slope stability analysis were generally based on hand-performed and therefore simplified computations. But due to the complexity of problem and taking different factors into account for more accuracy different methods are become more advantageous and get updated. According to (Albataineh, 2006) ,thousands of research articles had been published since the publication of the first method of analysis by Fellenius (1936) that were either related to slope stability or involved slope stability analysis subjects. In relation to this, the two well-known approaches the Limit Equilibrium method (LEM) and the Finite Element Method (FEM) are using by many investigators and researchers.

2.6.1 Limit Equilibrium Methods (LIM)

Limit equilibrium types of analysis to assess stability have been used in geotechnical engineering for decades. The concepts have been widely applied to the stability analysis of earth slopes. The idea of discretizing a potential sliding mass into vertical slices was introduced early in the 20th century. In 1916, Petterson (1955) presented the stability analysis of the Stigberg Quay in Gothenberg, Sweden where the slip surface was taken to be circular and the sliding mass was divided into slices. During the next couple of decades or so, Fellenius (1936) introduced the Ordinary or Swedish method of slices. In the mid-1950s, Janbu (1954) and Bishop (1955) developed advances in the method. The advent of electronic computers in the 1960s made it possible to more readily handle the iterative procedures inherent in the method, which led to mathematically more rigorous formulations such as those developed by Morgenstern and Price (1965) and by Spencer (1967). In order to use the limit equilibrium method effectively, it is useful to have a good understanding of the formulation fundamentals. The formulation is based on principles of limiting equilibrium. It means that forces on a free body are such that it will remain stationary. It satisfies statics, and the summation of moments, horizontal forces, and vertical forces is zero. There are some important assumptions as in the below:

- ✓ The factor of safety is a constant along the slip surface.
- ✓ Each slice has the same factor of safety.
- ✓ The factor of safety is defined as the factor by which the soil strength must be reduced so that the potential sliding mass is a point of limiting equilibrium. That is, the moments and forces must sum to zero. (MIDAS GEOTECH, 2021)

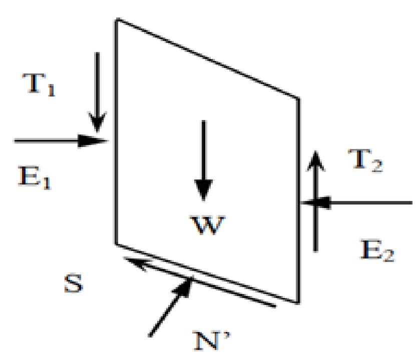

Figure 2-3 Slices and forces in a sliding mass

Various solution techniques for the method of slices have been developed and are in common use. The primary difference among all these methods lies in which equations of statics are considered and satisfied, which interslice normal and shear forces are included, and the assumed relationship between the interslice forces. This table summarizes the conditions for some of the common methods. This table lists which equations of equilibrium are satisfied, whether the interslice normal is included, whether the interslice shear is considered, and what the assumed relationship between the interslice normal and shear forces is. (MIDAS GEOTECH, 2021)

Table 2.2 Summery of LEM (Duncan and Wright. 2005, Abramson et al. 2002, Nash 1987)

Statics satisfied and interslice forces in various methods

Methods	Moment Equilibrium	Force Equilibrium	Shape of Slip surface	Interslice Normal (E)	Interslice Shear (T)	Assumption for T and E
Ordinary (Fellenius)	Yes	No	Circular	No	No	No interslice forces
Bishop's Simplified	Yes	No	Circular	Yes	No	The side forces are horizontal
Janbu's Simplified	No	Yes	Any shape	Yes	No	The side forces are horizontal
Janbu's Generalized	Yes	Yes	Any shape	Yes	Yes	Applied line of thrust and moment equilibrium of slice
Sarma	Yes	Yes	Any shape	Yes	Yes	Interslice shear $T = ch + E \tan \varphi$
Spencer	Yes	Yes	Any shape	Yes	Yes	Constant inclination $T = E \tan \theta$
Morgenstern Price	Yes	Yes	Any shape	Yes	Yes	Defined by f(x), T= f (x)...λ. E

Different types of LEM methods exist differing in how they solve the problem of equilibrium of slices by statics. Advantages and disadvantages of each method are stated in the above table. Bishop's method is most widely used for slope stability analysis and is well suited for clays as cohesive materials often go through the rotational failure of mass volume about a point of rotation. For more complex problems involving, highly heterogeneous ground with different material between adjacent layers, and where the interslice shear force is expected to vary, you can use the Morgenstern-Price method using variable functions for modeling interslice shear forces. (MIDAS GEOTECH, 2021)

2.6.2 Finite Element Method (FEM)

The safety factor registered utilizing the LEM is not particularly decided, in light of the fact that it fluctuates with the suspicion made for the slip surface. The outcome may not be solid if nonhomogeneous and anisotropic stratifications are considered. Effortlessness and generally great outcomes are the benefits of these techniques. Since, the FEM depends on the stress-strain relationship, push redistributions are without a doubt better processed notwithstanding for a confusing issue. (MIDAS GEOTECH, 2021)

The finite element method represents a powerful alternative approach for slope stability analysis which is accurate, versatile and requires fewer a priori assumptions, especially, regarding the failure mechanism. Slope failure in the finite element model occurs 'naturally' through the zones in which the shear strength of the soil is insufficient to resist the shear stresses (D.V. Griffiths, 1999). In this method, the slope is divided into a finite number of regions or elements using appropriate constitutive laws for the materials in the slope and these elements are interconnected at their nodes and predefined boundaries of the continuum. Due to the readily availability of personal computers, the Finite Element method has been increasingly used in slope stability analysis.

The tools required to carry out geotechnical stability analyses based on finite element computed stresses are today readily available. Applying the tools is now not only feasible but also practical. Unforeseen issues will possibly arise in the future, but such details will likely be resolved with time as the method is used more and more in geotechnical engineering practice. Using finite element computed stresses inside a limit equilibrium framework to analyze the stability of geotechnical structures is a major step forward since it overcomes many of the limitations of traditional limit equilibrium methods and yet provides an anchor to the familiarity of limit equilibrium methods so routinely used in current practice.

2.7 REMEDIAL MEASURES FOR SLOPE INSTABILITY PROBLEMS

Before selecting an appropriate slope stabilization method evaluation of the existing slope conditions and considering the prevailing causes are very useful for the instability of the slopes. After the causes of slope stability are identified, the appropriate remedial measure for slope is selected based on feasibility, stability and economy (Kazmi, et al., 2017). According to (Kazmi, et al., 2017) surface protection and drainage, subsurface drainage, slope regarding, retaining structures, structural reinforcement, strengthening of slope-forming material, vegetation and bioengineering, removal of hazards and others are the remedial measures generally considered to stabilize the unstable slope. From the aforementioned methods, some of them are discussed as the following.

2.7.1 Drainage systems

Saturation and pore water pressure building up in the subsoil is the factor that increases the slope failure. According to (Mizal-Azzmi, 2011) by providing a proper drainage system it is possible to stabilize the slope by minimizing the pore water pressure and saturation of subsoil. The drainage system method is usually performed in combination with other methods. The drainage system method is applicable in those conditions where proper maintenance of surface and sub-surface drains is performed. The presences of excess pore water pressure are a major factor causing the instability of the slope. Using the proper design of surface and subsurface drainage system, the pore water pressure build-up in subsoil can be removed and the stability of a slope can be enhanced.

2.7.2 Geometrical Method

In the steep slope, there is a high tendency of sliding of slope material due to the gravitational acceleration and increases its sliding speed (Ibrahim, Salisu, Musa, Abussalam, & Hamza, 2022). The geometrical method is easy and inexpensive; however, it requires adequate space. The stability of the slope can be increased easily by converting the steeper slopes into the gentler slope. This method can be performed by cutting the slope to make the slope free from extra loading. Under this condition, the stability of a slope can be increased by either flatten or backfilling at the toe of the slope (Kazmi, et al., 2017). The method is easy and economical, but it depends very much on the site condition.

2.7.3 Retaining Structures Method

Under this method, the retaining structures are used to resist the downward forces of the soil masses. There are various types of retaining structures such as gravity and cantilever retaining walls, contiguous bored piles and nailing are used to stabilize slopes. Even though the method is more expensive, it is usually the most commonly utilized method due to its flexibility in a constrained site (Kazmi, et al., 2017).

2.8 SOFTWARE APPLICATIONS

2.8.1 Slide software

The software is initially proposed by Rocscience Inc. Toronto Canada and used for slope stability analysis of both soil and rock slopes. The slide software is a computer-based program 2D limit equilibrium that can be used to evaluate the stability for both circular and non-circular failure surfaces (Slide, 2003). This software is easy to perform and possible to model the slopes with various loading conditions such as surcharge, pseudo-static earthquake, groundwater condition, and support conditions. The slope stability analysis can be performed in this software by vertical slice using different types of limit equilibrium method analysis such as Bishop, Spencer, and Ordinary/Fellenies methods Spencer and others as discussed in the above section. In addition, the software has various features such as searching for critical surface, modeling of multiple, anisotropic, and non-linear Mohr-Coulomb materials, defining and analyzing groundwater problem and viewing detailed analysis results (Slide, 2003).

2.8.2 Plaxis software

Plaxis software is a finite element-based which is used for stability analysis deformation and deformation. Using plaxis software model of soil and rock layers, structures, construction stages, loads, and boundary conditions can be done. It is also possible to form an automatic unstructured finite element meshes generation. It has many features such as modeling of spatial beam elements like walls, tunnel lining and shells using plates, modeling of soil structure instruction using interface materials, analysis of slope and excavation supports using anchors, soil reinforcement using geogrids and analysis of circular and non-circular tunnels (Plaxis, 2013). The four features of Plaxis 2D are input, calculation, output, and curves. The importance of Plaxis input is the modeling of geometry, material, and boundary condition with a generation of mesh and initial condition (pore water pressure and initial stress condition). For the analysis of different structures, loading conditions, construction stages, and pore water conditions Plaxis calculation is utilized. Plaxis output and curves are used to observe and display analysis results (Plaxis, 2013).

CHAPTER 3. METHODOLOGY AND MATERIALS

3.1 METHODOLOGY

To obtain accurate and comprehensive information on the engineering geological and slope stability conditions of the study area, different appropriate methods were utilized. The data acquisition processes and general working principles of these techniques are presented in this section. The methods and approaches used in this study included secondary data collection and field survey, detailed fieldwork and sampling, laboratory testing and data processing. Slope stability analysis was conducted using limit equilibrium and finite element methods. The primary and secondary data were integrated to analyze, summarize and present the results. The approaches and some applications of those aforementioned methodologies are discussed in detail as follows.

3.2 Description of the study area

3.2.1 Location of the study area

The study area is located in Eastern part of the Country, Oromia Region West Harerghe Zone which is 343Km from capital Addis Ababa. The project is upgrading the existing gravel road to hot mix concrete asphalt. West Harerghe zone is a busy transportation center due to its chat marketing center and the road also connect the two zones Arsi and west Harerghe. The road under construction titled Arbereketi– Micheta is 105 KM long and 7m wide in rural areas and 14m wide in cities. The road is constructed by Alasab-east general contractor and transportation company through supervision of Ethiopian Road Authority (ERA).

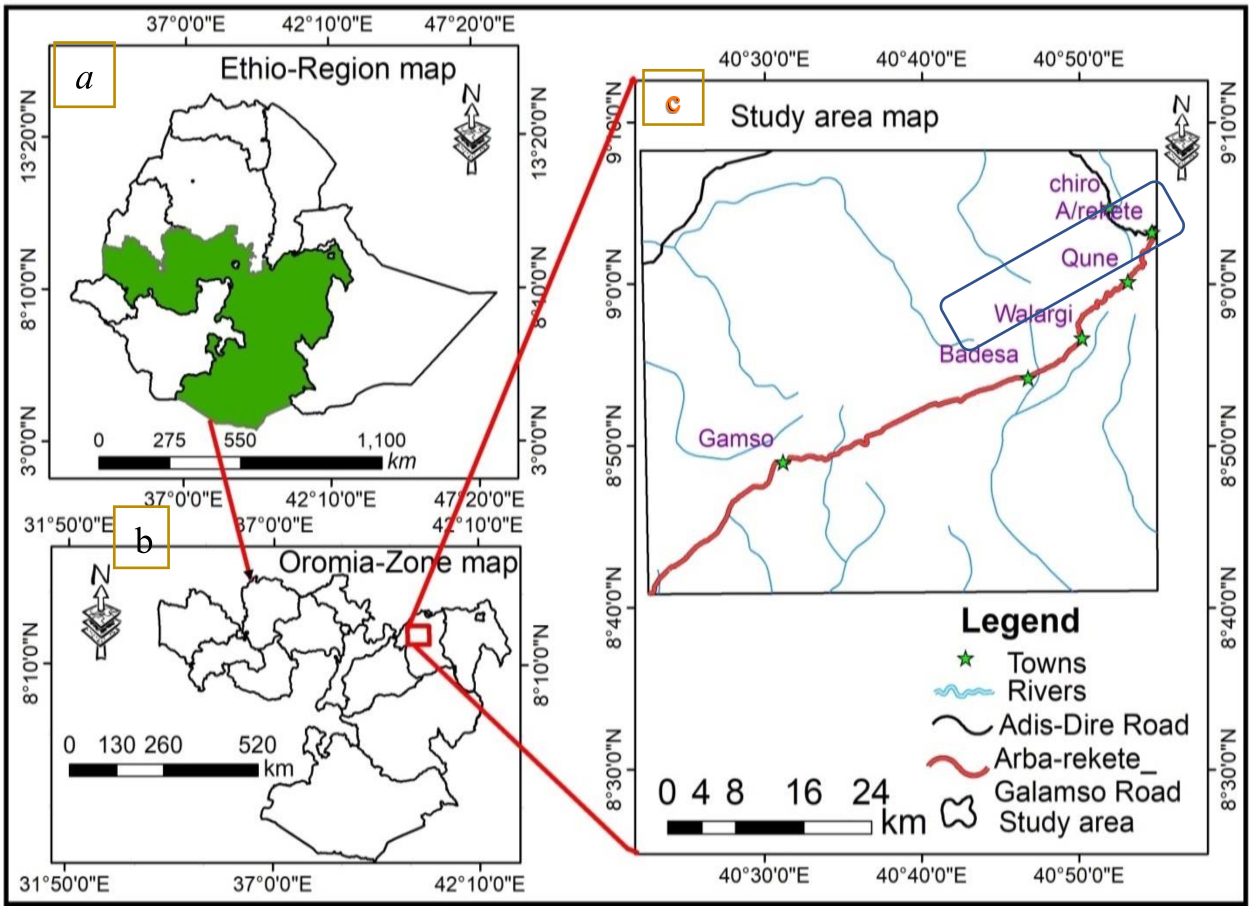

Figure 3-1 Location maps of study area (a) Ethiopian regional boundary b) Oromia zone boundary and c) study area boundary.

3.2.2 Drainage pattern

The study area is located on the eastern highland of Ethiopian plateau which contains the small rivers and their tributaries. Several small tributary streams run through the study area and intersect at various points and drain to Galeyti River. The road pass through the steep slope and the drainages are flow easily from the escarpment to the rivers in the lowland area. All the local drainages in the study area flow towards the southeastern and southern direction. The drainage pattern of the studied area is characterized by parallel to subparallel dendritic patterns. The structures and topographic landscapes of the study area control the flow direction and distribution of the drainage pattern.

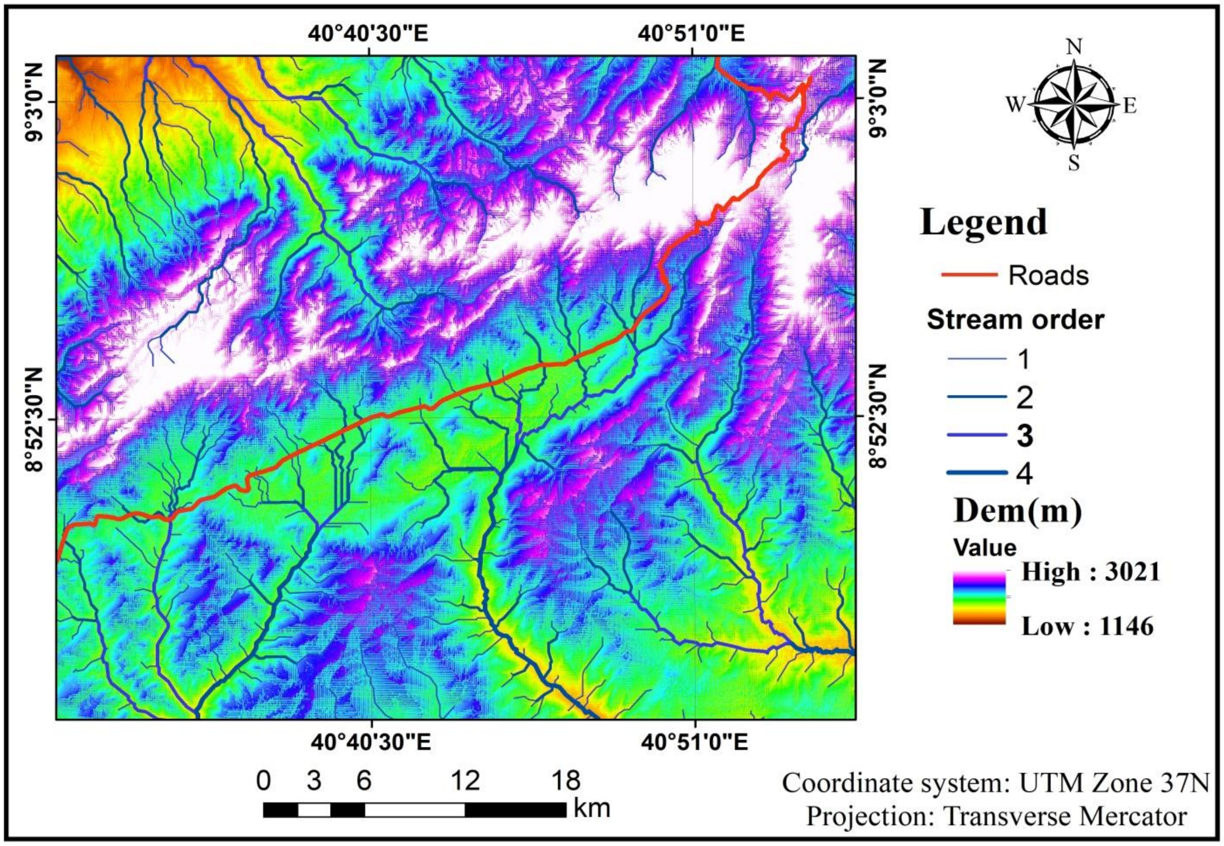

Figure 3-2 Drainage pattern and stream order of the study area.

3.2.3 Seismicity of the study area

Seismic activity is one of the factors that contribute to slope instability, particularly in active seismic zones (Mebrahtu, Heinze, Wohnlich, & Alber, 2022). When rock slopes are subjected to ground accelerations through significant structural discontinuities, the structural discontinuities stretch or open. As a result, shear strength and structural discontinuity is reduced while slope failure increases (He, et al., 2023). The seismic risk map of Ethiopia for a hundred-year return period showed that the present study area falls within the 7 M.M scales as shown in Fig 3-3. The predicted earthquake acceleration is average of 0.07g based on the Modified Mercalli intensity scale (Luna, et al., 2010). Hence, the present study area fell into zones (zone 3) with high seismic hazards. Accordingly, there is a high chance for slope instability problem in the study area which may be triggered by seismic activity.

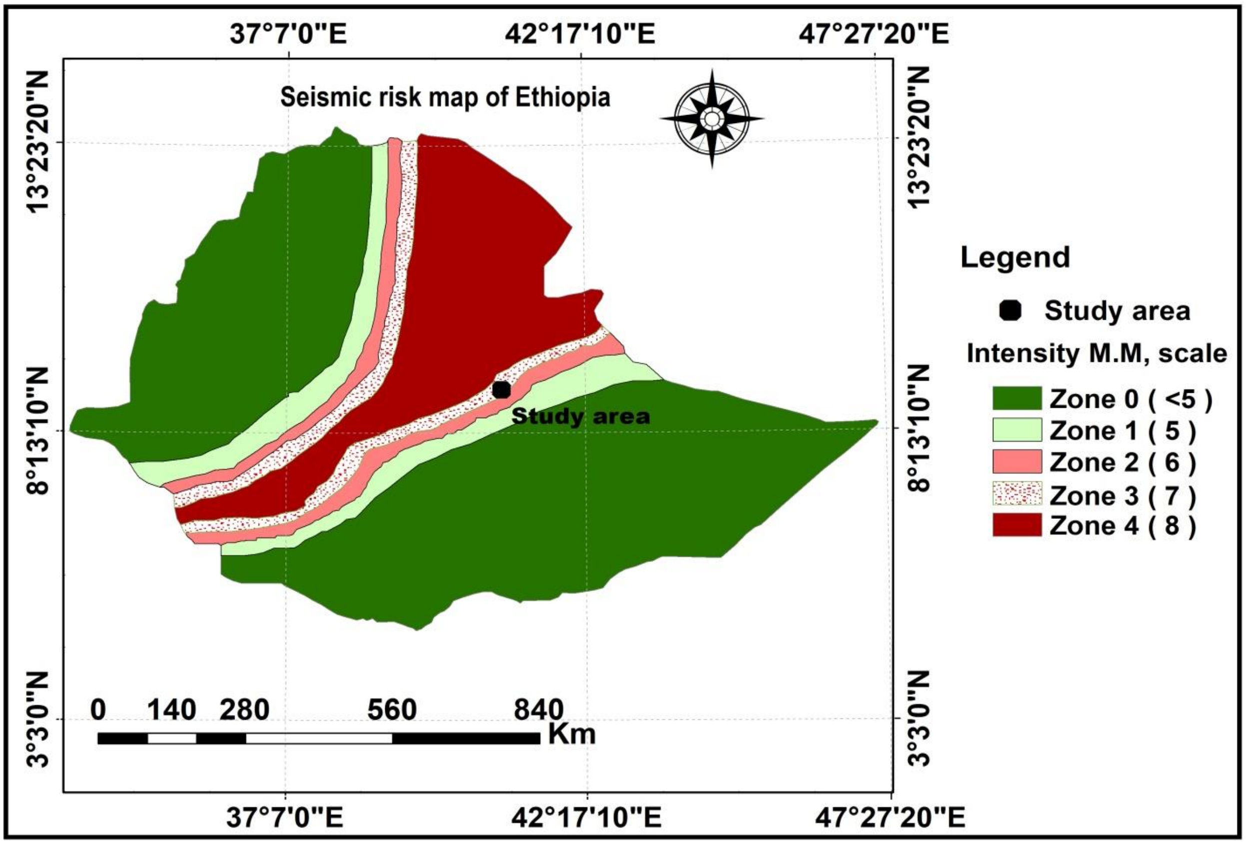

Figure 3-3 Seismic hazard map of Ethiopia for 100-year return period as per EBCS 8: 1995 (Stewart, et al., 2003)

3.2.4 The climate Condition of the study area

The climate of study area contains the average temperature (Fig.3.4) and precipitation conditions (Fig.3.5). Ethiopia has a variety of rainfall distributions. According to (Ayalew, 1999), the Lowland locations have lower precipitation records and the highland areas have over 70% of yearly rainfall. There are two recognized climate components: precipitation amount and distribution of temperature conditions according to (Ayalew, 1999) description.

3.2.4.1 Temperature

The maximum and minimum mean annual temperature data for study area was taken from National Meteorological Agency of Ethiopia for and Bedesa town stations. The maximum and minimum average annual temperature of and Bedesa town stations in the study area includes 31.10ºC to 9.95ºC and 32.33ºC to 6.74ºC respectively as shown in Fig.3.4.

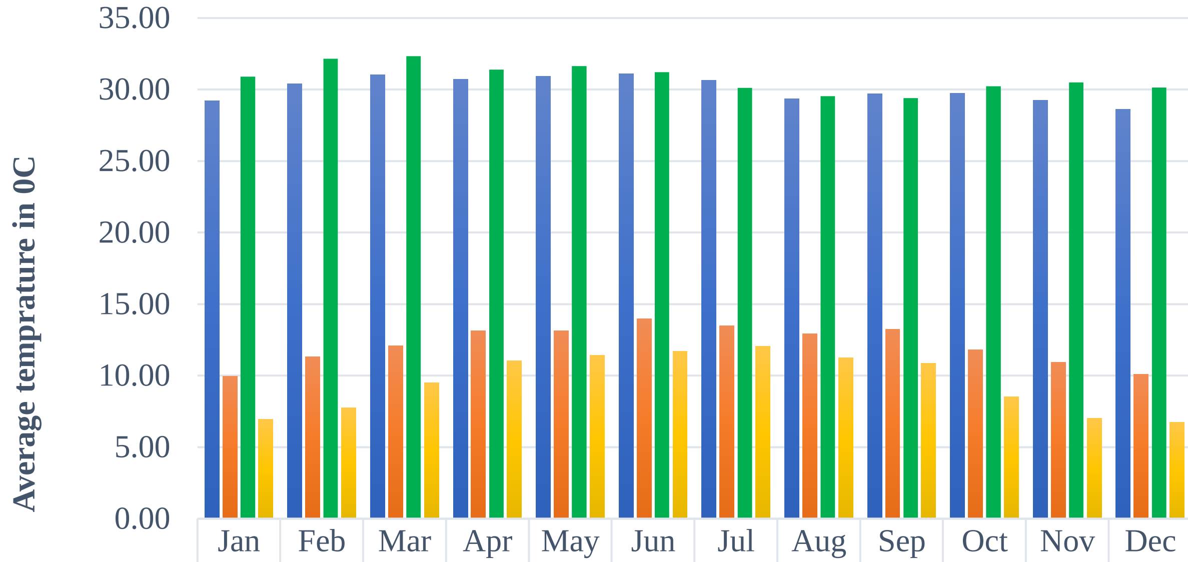

	Jan	Feb	Mar	Apr	May	Jun	Jul	Aug	Sep	Oct	Nov	Dec
Qune max	29.22	30.40	31.02	30.70	30.94	31.10	30.66	29.36	29.70	29.76	29.25	28.61
Qune min	9.95	11.31	12.10	13.14	13.15	13.99	13.47	12.94	13.23	11.81	10.95	10.11
Badesa max	30.91	32.17	32.33	31.40	31.65	31.21	30.12	29.53	29.40	30.22	30.49	30.15
Badesa min	6.95	7.77	9.52	11.03	11.43	11.70	12.04	11.27	10.87	8.52	7.04	6.74

Months

Figure 3-4 Mean average temperature of the study area (2000-2022). (Sources: National Meteorological Agency of Ethiopia).

3.2.4.2 Rainfall of the study area

Heavy rainfall is the most common cause of slope failures (Chango, et al., 2021). The slope instability of the Ethiopian highlands can be affected by a variety of topographical, geological, hydrological, and land use conditions, but most of the landslides were caused by heavy rainfall (Getachew & Meten , 2021). During heavy rainfall events, the pore water pressures distributed in the soil are very different depending on the hydraulic conductivity, the topography, the degree of weathering and the soil types. The meteorological conditions in the present study area range from tropical to subtropical. Furthermore, slope instability in the study area occurs during the rainy season. The rainfall data of study area was collected from the National Meteorological Agency of Ethiopia for Chiro, Kune and Bedesa stations. At Kune station, the maximum and minimum mean monthly rainfall was 197.1mm and 17.68mm respectively (Fig.3.5). At Bedesa stations, the average monthly rainfall varied between 16.47 mm and 155.6mm. The study area rainfall does not the same throughout the year as shown in (Fig.3.6). According to field observations, slope instability in the study area occurs more frequently during months of July and August where heavy rainfalls (Fig.3.5).

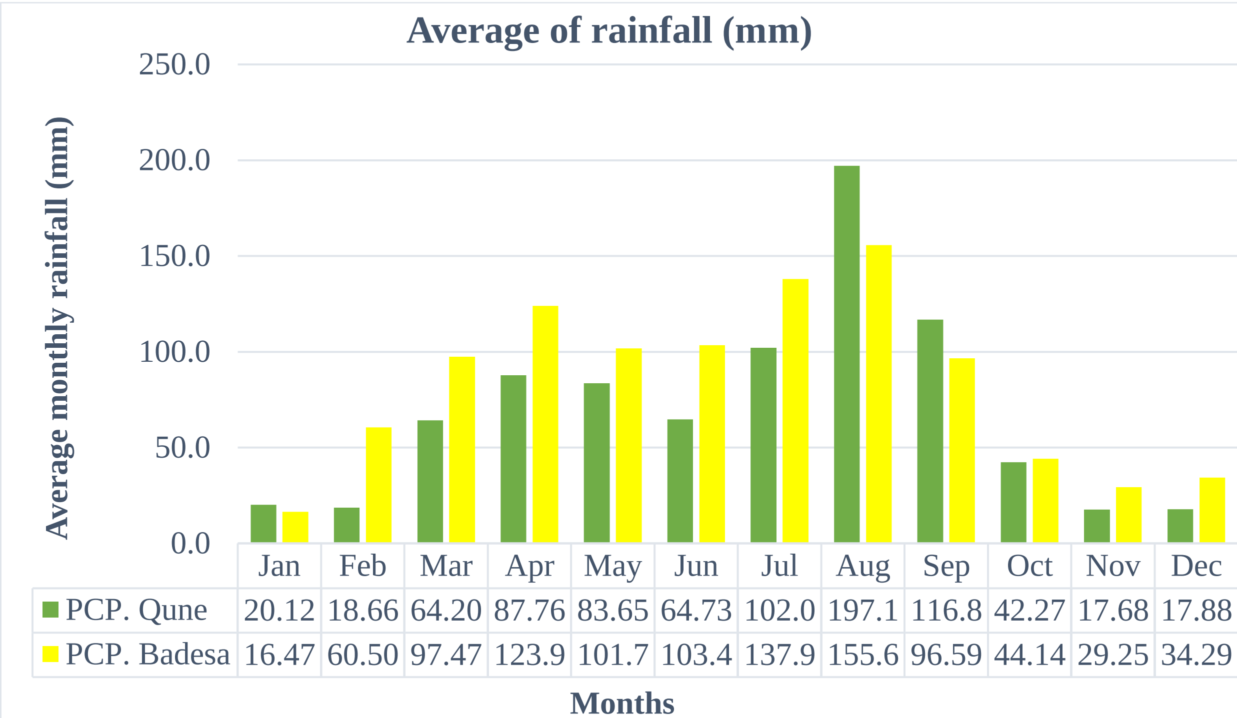

	Jan	Feb	Mar	Apr	May	Jun	Jul	Aug	Sep	Oct	Nov	Dec
PCP. Qune	20.12	18.66	64.20	87.76	83.65	64.73	102.0	197.1	116.8	42.27	17.68	17.88
PCP. Badesa	16.47	60.50	97.47	123.9	101.7	103.4	137.9	155.6	96.59	44.14	29.25	34.29

Figure 3-5 Monthly Rainfall data of the study area (2000-2022) (Source: National Meteorological Agency of Ethiopia)

3.2.5 Regional geological formation

Based on the geological map of Ethiopia, (Mengesha, Tadiwos, Workineh, Negusssie, & Kebede, 1996), and field observation of the route corridor, the project area is covered by Tertiary volcanic and Mesozoic sedimentary rocks (Figure 3-6, Geological map of the area). According to (Mengesha, Tadiwos, Workineh, Negusssie, & Kebede, 1996) the volcanic rock that predominates in the project area are two types. These are from the youngest to the oldest, the Tarmaber – Megezez Formation (Ntb) and the Alage Formation (PNa). Tarmaber Megezez formation (Ntb) is represented mainly by central type and fissural basaltic flows typical of the rift escarp while the Alage Formation (PNa) by transitional and sub alkaline basalts with minor rhyolite and trachyte eruption. The Alagi Formations are found around the beginning and end of the project alignment. They are found from fresh and sound rock to highly weathered gravelly and decomposed material or capping material. Thick succession of Mesozoic sedimentary rocks that belongs to Hamaneli (Jh), Urandab (Ju) / Antalo (Jt) Formation and Ambaradom (Ka) Formation are the other predominant rock along the project route. Rocks included under these formations are mostly thickly bedded limestone, shale and sandstone.

The geology of the route corridor was assessed in conjunction with 1:200,000 scale Geological map of Ethiopia (Mengesha, Tadiwos, Workineh, Negusssie, & Kebede, 1996). The geological units that are crossed by the route corridor have been identified and their potential use as sources of construction material is evaluated. Based on the geological map and field observation, the project route corridor is dominantly covered by basalt, sandstone and limestone with minor alluvial sediment.

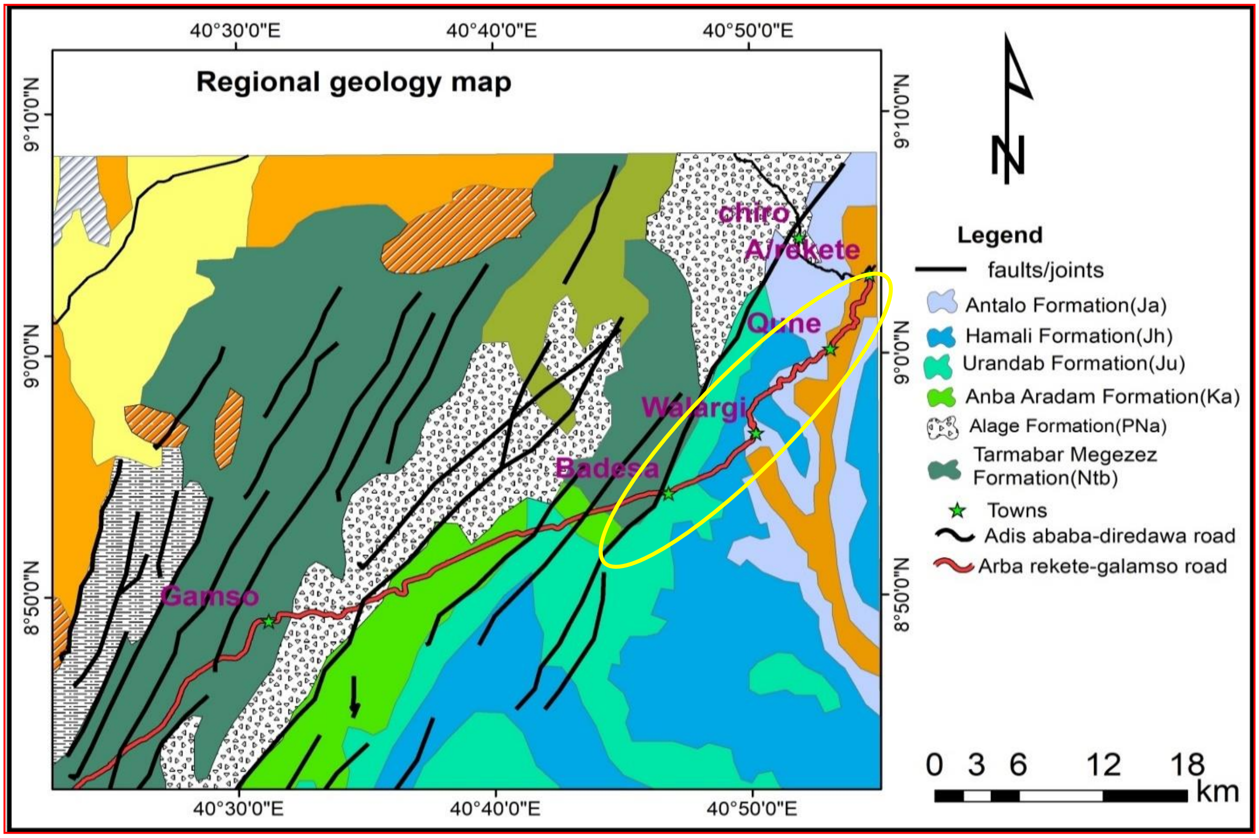

Figure 3-6 Regional geological map of the project area (after Mengesha et. al. 1996)

3.3 Secondary Data Collection and Field Survey

As part of this phase, important and relevant data that are used for slope stability analysis was able to be gathered from various reputable institutions, such as the National Metrological Agency. The investigation included a reconnaissance study and a thorough literature review on various causes and mechanisms of slope failure. A slope failure is most frequently caused by heavy rainfall (Abebe et al., 2010). The graphs of average monthly precipitation data from 2000 up to 2022 at Kune and Bedesa stations were drawn using Microsoft Excel (Fig.3.5). Similarly, the temperature data for the same period of time at Kune and Bedesa stations were presented using Microsoft Excel (Fig.3.4)

3.4 Detailed Field Work and Sampling

Based on the detailed field investigation, it was found that the slope was in an unstable state and required further stability analysis. During the fieldwork, the primary data was collected from the study area and information on geological structures, discontinuity characteristics, rock mass characteristics, and drainage conditions were identified. Primary data was also collected from the study area through discontinuity surveying, and sampling for laboratory tests. A critical slope section was identified based on field failure manifestations such as removal of slope toe, development of tension crack, tilting of slope face, existences of some springs and orientation of discontinuity. These critical slope sections were then further observed to identify possible failure phenomena such as slope inclination, drainage status, types of slope material, weathering conditions, and orientation of discontinuity. Further field observations were conducted to analyze the slope stability after identifying critical slope sections.

Table 3.1 location of critical slope sections studied along road sections

SN	Slope location	Side	Slope height(M)	Slope width(M)
SS1	11+820	RHS	18	60
SS2	12+078	RHS	20	50
SS3	12+420	RHS	25	40
SS4	13+507	RHS	16	55

Figure 3-7 Some of visible sign of slope failures during field survey.

3.5 Data collection

During the field work all relevant information and data pertaining to the stability condition of the slopes were collected. Information was collected through visual observations pertaining to aspects related to slope stability. Four soil samples were taken for laboratory determination of index and strength parameters. The sampling of soils was taken 1m horizontally from the face of the slope. The amount, as well as sample location, is decided based on the standards (ASTM, 2014 and EBCS, 2015).

Table 3.2 location samples taken for studied along road sections

SN	Slope location	Latitude(N)	Longitude(E)	Altitude(m)
SS1	11+820	8^{o}58’55.13’’	40^{o}51’09.15’’	2236
SS2	12+078	8^{o}58’55.62’’	40^{o}51’31.89’’	2287
SS3	12+420	8^{o}58’55.37’’	40^{o}51’31.40’’	2485
SS4	13+507	8^{o}58’55.62’’	40^{o}51’31.74’’	2260

Figure 3-8 Pit Depth 1m for sample taken to Laboratory tests at 11+820

.

Figure 3-9 Pit Excavation sample taking at 12+078 for Laboratory Tests.

3.6 Sampling of Soil for Laboratory Test

In order to better understand the engineering properties of the soils in the study area, representative samples were collected from the field for laboratory testing. Soil samples were collected for index and strength tests, ensuring a comprehensive understanding of the materials. To account for the variability of weathering degrees, rock samples were also taken from selected locations for the determination of unit weight using the buoyancy technique. These methods allowed for a thorough characterization of the materials and will inform future decision-making in the study area.

To properly analyze the stability of the slopes, disturbed soil samples were collected from selected critical sections as shown in Fig. 3.5. Four representative soil samples were taken for index and strength tests. To achieve this, four soil test pits were dug with a maximum depth of one meter, and collected the soil samples. The soil samples were placed in plastic bags to preserve their natural moisture content. The purpose of soil sampling was to obtain samples for laboratory testing. These soil investigations were conducted to characterize the materials and determine related parameters to better analysis slope stability.

3.7 Laboratory Testing of Soils

After conducting field sampling, various geotechnical laboratory tests were performed on representative soil samples. These laboratory tests were carried out on soil samples to determine particle size analysis using sieve and hydrometer analysis, specific gravity, natural moisture content, Atterberg limit (liquid and plastic limit), compaction, and shear strength. The types of tests that were carried out on these soils along with the standards used for testing, were discussed in great detail in the following sections.

3.7.1 Soil Laboratory Tests

The laboratory tests were performed on soil samples to evaluate the strength and index properties of the soil in the study area. Tests performed in the laboratory on soil samples included grain size analyses (sieve and hydrometer analyses), specific gravity tests, natural moisture contents Atterberg limit (liquid and plastic limit), compaction and shear strength tests (cohesion and angle of internal friction).

3.7.1.1 Grain Sizes Analysis

Based on the grain size analysis of the four soil samples taken from the critical slope's sections of the study area, it was found that there are both large and fine particles present. The analysis was conducted using both sieves and hydrometers. This data is crucial in understanding the characteristics of the soil and can be used to inform decisions regarding construction or other land use activities in the area.

A) Sieve Analysis: The sieve analysis was conducted following ASTM D422 (1998), which is a standard test procedure for determining soil particle size (Fig.3.7a). The purpose of the test was to determine the distribution of coarser grain sizes that are greater than 75 µm in diameter. To conduct the test in the laboratory, dry soil samples were first prepared and crushed into appropriate small sizes using a hammer and pestle grinder. Once the samples were ready, a stack of sieves was cleaned with a brush and a set of sieves were placed with progressively smaller openings from top to bottom, with the pan at the bottom of the finest sieve. After 15 minutes, the soil retained on each sieve and pan was measured using a digital balance. The dry mass of soil grains from individual sieving was used to find the percent passing and accordingly, the percent retained in each sieve size. The recorded data was then analyzed on a Microsoft Excel datasheet and the grain size distribution curve was drawn from the diameter versus percent finer using the sieve analysis result.

B) Hydrometer Analysis: In order to determine the distribution of fine particle sizes smaller than 75 µm in diameter, a hydrometer analysis was conducted following ASTM D422 (1998) standard test. The test was performed in the laboratory by first weighing 50 g of fine-grain soil retained on the pan and placing it in a beaker with water, into which 125 ml of dispersing agent (sodium hexametaphosphate) mixture with the soil was added. The soil slurry was then transferred into an empty sedimentation cylinder and distilled water was added up to the mark. The cylinder was covered and turned upside down for one minute, then observed for 24 hours by reading the top of the meniscus-formed suspension hydrometer (Hossain, Islam, Badhon, & Imtiaz, 2021). The cylinder was placed in a constant-temperature water bath during these tests. The grain diameter was computed by referring to the calibrated curves and the grain size distribution curve was drawn from the diameter versus percent finer using the analysis result.

3.7.1.2 Atterberg Limit Test

The Atterberg limit test is used to determine the liquid limit (LL) and plastic limit (PL) of soils. The liquid limit is the percentage (%) of moisture at which the soil changes from a liquid state to a plastic state, and the plastic limit is the percentage (%) of moisture at which the soil changes from plastic state to a semi-solid (El Jazouli, Barakat, & Khellouk, 2022)**.** The test was performed according to ASTM D 4318 (1998). The Atterberg limit test was determined on soil samples that passed the 40 sieve (0.425 mm) and distilled water was added to perform the Casagrande test. The laboratory test is carried out according to the following flow and yield test procedure.

A) Liquid limit test: The liquid limit (LL) is the point at which the soil changes from a liquid state to a plastic state. For this analysis, a portion of the soil sample that passed through the pore size of sieve #40 (0.425 mm) was placed in the evaporator dish. The soil sample is mixed with water and stirred with a spatula to create a smooth soil surface. The soil mixture is then divided into two parts using a grooving tool and rotating the handle at 2 rpm until it contacts the bottom of the trench at a distance of 13mm. The number of hits required to close two sections of a 13 mm soil sample was recorded. A representative sample was taken from the flow section and placed in wet boxes that were oven-dried for 24 h at 105°C. Next, moisten the can to determine the moisture content. Finally, the moisture content of each soil sample was recorded and analyzed.

B) Plastic limit test: The plastic limit (PL) is the percentage moisture content (%) at which the soil changes from a plastic state to a semi-solid state. This test is made from sample for liquidity limit test. The soil sample is placed on a glass dish and rolled with a finger to form a thread of uniform diameter. The wire is then rolled up until its diameter reaches 3 mm and crumbles. Debris samples were collected in containers and digitally weighed then placed in the oven for 24 h and the oven temperature was set at 105°C. Finally, the humidity boxes are removed from the oven and the results of each sample are recorded and analyzed. Finally, from the yield and plastic limit tests, the plastic index (PI) of the soil is determined according to Equation 3.2 as follows.

$$PI = LL - PL \qquad (3.2)$$

Figure 3-10 Sieve analyses and Atterberg limit tests of soils

3.7.1.3. Natural Moisture Contents Tests

The natural moisture content of the soil is an important factor in determining its condition in the field. According to (Arezo et al. 2020), cohesive soils are particularly affected by moisture content, which can impact their engineering behavior. To test the moisture content, fresh soil samples were taken and subjected to the ASTM D 2216 (1998) standard using the oven drying technique. In addition, representative soil samples were also collected from two critical slope sections and preserved in plastic bags to maintain their in-situ natural moisture content. The wet mass of the samples (Mw) was determined using a digital balance, and the dry mass was obtained by oven-drying the samples (Md) for 24 hours at 105°C. Using equation 3.3, the natural moisture content of the soil was able to be calculated.

$\mathrm{W}\ (\%) = (\mathrm{Mw} - \mathrm{Md})/\mathrm{Md} * 100$ -- (3.3)

Where: W is the natural moisture content in (%), Mw is the mass of wet soil samples in (g), and Md is the mass of oven-dried soil samples in (g).

3.7.1.4 Specific Gravity

The specific gravity of soil at the selected slope section was determined using a pycnometer with distilled water at a specific temperature (Diro, Kabeta, & Teshager, 2020). This test was performed according to the ASTM D 854 (1998) standard procedure to determine the specific gravity of soil using oven-dry techniques. To begin, the weight of the empty, clean, and dry pycnometer was determined and recorded. Then, the dry soil sample that passed through sieve No. 10 was placed in the pycnometer and its weight was determined (Md). Distilled water was then added to the pycnometer to fill just above the soil level and soaked for 10 minutes. Any entrapped air was removed through boiling. Finally, the pycnometer was filled with distilled water up to the calibration mark and its corresponding mass was measured (Mc). After emptying and cleaning the pycnometer, it was filled with distilled water up to the calibration mark to obtain the mass of the pycnometer filled with water (Ma).

$\mathrm{G} = \mathrm{Md}/(\mathrm{Md} + (\mathrm{Ma} - \mathrm{Mc}))$ --- (3.4)

Where G is specific gravity, Md is mass of dry soil+ pycnometer, Ma is mass of pycnometer filled with water, Mc is mass of pycnometer filled with soil and water.

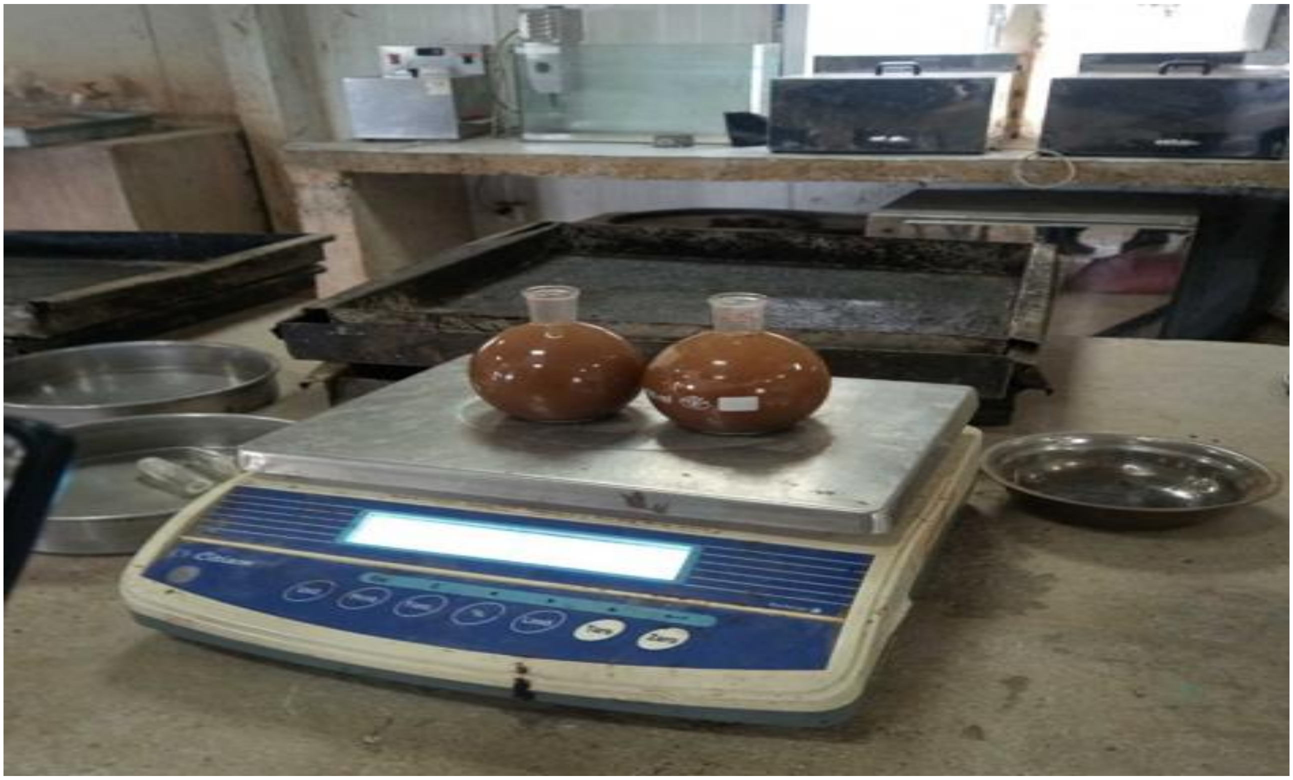

Figure 3-11 Specific gravity test of soils

3.7.1.5 Compaction Tests

The compaction tests determine the maximum dry density and optimal moisture content of the soil used in the shear strength test. Proctor tests are used to determine how soil compaction changes with moisture content. Tests were conducted in accordance with ASTM D698-07 (1998) on four soil samples taken along the critical slope section of the study area. To conduct the test, 5kg of the soil sample passing through the No. # 4 sieve was taken and mixed thoroughly with a measured amount of water. Determine the weight of compaction molds within the base (M1). The soil sample was then filled in the cylinder mold in three layers within 25 blows for each layer. Remove the collar, trim, and level of excess compacted soil beyond the rim of the mold. The weight of the compacted soil within its molds and base was recorded (M2) and the soil compacted from the molds was removed using a mechanical extrude. A sample from the bottom and top of the moisture cans was taken and put in the oven at 105 ° C for 24 hours. The bulk density and dry density of the soil were then determined using equations 3.5 and 3.6 respectively.

$\gamma b = (M2 - M1)/V$ --(3.5)

$\gamma d = \gamma b/((1 + w/100))$ --(3.6)

Where: γd is dry unit weight, γ_b is the bulk unit weight, M2- the mass of soil after being compacted with mold, M1- the mass of the mold, V is the volume of the mold and W is the moisture contents of soils. Finally, the results of the recorded data were analyzed on Microsoft Excel datasheet and plotted the graph of the dry density versus moisture contents for analysis result.

3.7.1.6 Unit Weight of Soils

When evaluating soil slope stability, one of the important input parameters is the unit weight of soil. To obtain this value, both the bulk (γb) and dry (γd) unit weights of soil were calculated. The laboratory test results of the soil are used to determine the saturated and dry unit weights of the soil, which were derived from the corresponding density and the acceleration of gravity (g). In this study, the unit weight of soil used for slope stability analysis is acquired through laboratory tests conducted on soil samples collected from a critical location where the slope has been cut and remolded for the shear strength test. First, the bulk and dry density are determined through laboratory tests. Then, using the bulk and dry density results, the unit weight of the soil is calculated using the formula provided bellow.

Bulk unit weight = Bulk density*g and Dry unit weight = Dry density*g----------------------(3.7).

3.7.1.7 Shear Strength Tests of soils

Shear strength is the maximum soil resistance to shear stresses just before failure. The shear strength is one of the most important engineering properties of soil. In this study, shear strength parameters such as cohesion and angle of internal friction in the selected failed slope sections have been determined from the direct shear strength test. The test was performed on soil samples measuring 60 x 60 x 25 mm that was compacted and remolded at their compaction tests moisture contents using ASTM D3080 (2002) standards at Addis Ababa Science and Technology University Geotechnical laboratory. The apparatus consists of a square brass box split horizontally at the level of the center of the soil sample which is held between metal grilles and porous stones as shown in. The vertical load is applied to the sample as shown in the figure and is held constant during a test. A gradually increasing horizontal load is applied to the bottom of the box until the sample fails in shear. For each normal load applied at regular intervals, the horizontal and vertical shear displacements were recorded. Shear stress and normal stress were calculated and plotted in the graph based on the test results. Finally, the Mohr-Coulomb failure criterion described the relationship between soil shear strength at a point on a particular plane and its normal stress as follows in equation 3.7.

$\tau = c + \partial\ tan(\phi)$---(3.7)

Where: C is the cohesion and ϕ is internal angle friction of the soil particles

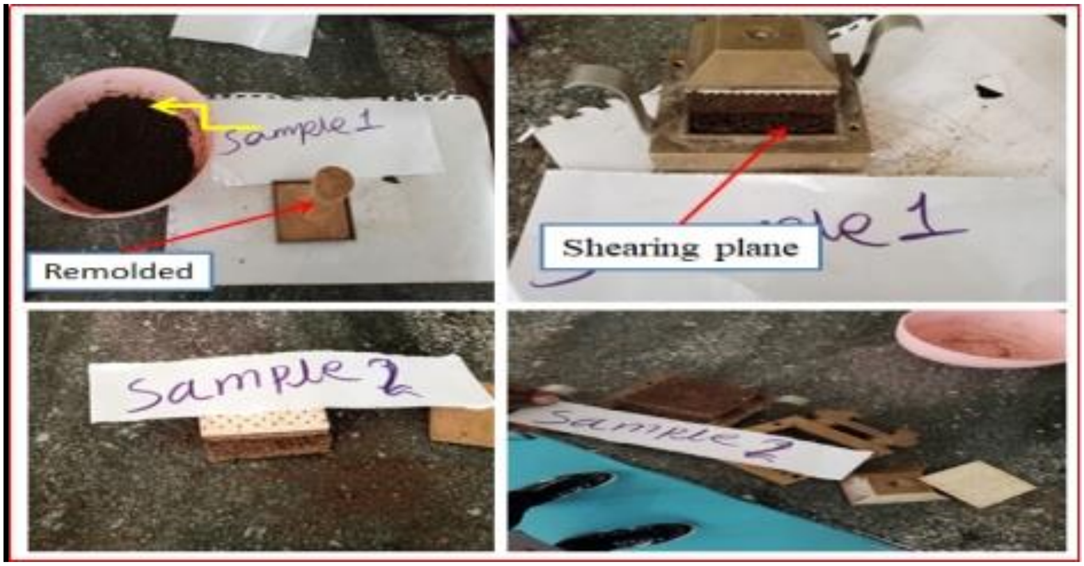

Figure 3-12 Direct shear tests of soil slope sections in the study area

3.8 Slope stability Analysis Method

The slope stability analysis for this present study was performed using limit equilibrium and finite element methods. The slope models were developed by compiling various geotechnical data gathered from field surveys and laboratory tests. This section provides a brief overview of each method for ensuring slope stability analysis

3.8.1 Limit Equilibrium Method

The safety factor of soil slope failures was analyzed using various methods. The limiting equilibrium approach was used to compare the shear strength adjacent to the sliding surface and the force needed to maintain the slope's equilibrium (Ullah et al., 2020). A limiting equilibrium method was used to analyze the stability of soil slope failures using Rocscience slide software. For this study, the limit equilibrium method of the slide 6.0 software was used to model and compute the factor safety for soil-selected slope sections (Rocscience, 2004). The input parameters for slide software include the shear strength parameter of soil, slope geometry, and external force. Finally, the General Limit Equilibrium (GLEM)/Morgenstern Price approach was used to compute the factor of safety of the limit equilibrium method under static dry, static saturated, dynamic dry, and dynamic saturated conditions.

3.8.2 Finite Element Method

The finite element method is a numerical method that is used to evaluate the stability of both natural and manmade slopes. Finite element analysis can be performed using PLAXIS 2D software, which uses a shear strength reduction technique to determine slope stability (Sato & Kanamori, 1999), (Griffiths & Lane, 2001). This study used the Plaxis 2D software (Rocscience, 2004) to determine slope stability, which is a strong finite element tool that can be used in a variety of situations (You et al., 2018). The data preparation and Plaxis 2D software analyses are obtained from laboratory tests. The slope width, angle and height were determined in the field. The material. Cohesive soils (such as Clay soils) are characterized by a very low number of dilatancy angles ($\psi \approx 0$). The formula $\psi = \varphi - 30°$ can be used to estimate the dilatancy angle for non-cohesive soils (sand, gravel) with the angle of internal friction $\varphi > 30°$.

Furthermore, soil's elasticity modulus (E) and Poisson's ratio (v) are used to analyze deformation in numerical modeling. Accordingly, suitable values of these parameters were derived from numerical correlations and literature review. The standard penetration test (SPT) has been used to correlate different soil parameters such as unit weight (γ), angle of internal friction (φ) and undrained compressive strength (qu) for estimating the stress-strain modulus elasticity of soils (Peck et. al., 1974; Bowles, 1977). For this study the SPT N, values were correlated with the saturated unit weight of soils (Bowles, 1977). The drained poisons ratio of granular soils can be calculated by using equation 3.14 as suggested by (Bowles, 1996). This study calculated the corrected standard penetration test N value to an average energy ratio of N60 using equation (Eq.3.15) proposed by Terzaghi and Pecks, (1967). The modulus of elasticity of the soil was calculated from the SPT N60 value as suggested by Das (1995) and (Ameratunga, J., Sivakugan, N., & Das, B. M., 2016) using equation 3.16 as follows:

$$V_d = 0.1 + 0.3\left(\frac{\phi - 25}{20}\right) \quad \text{For } \phi < 45^{\circ} \quad \text{--(3.14)}$$

$$\phi\,(\text{Deg}) = 27.1 + 0.3N_{60} - 0.00054N^2_{60} \text{--(3.15)}$$

$$E = 1200(N+6)\ \text{KN/m}^2 \qquad \text{for } N<15 \text{----------------------------------(3.16)}$$

$$E = 4000 + 1200(N - 6)\ \text{KN/m}^2 \qquad \text{for } N>15 \text{----------------------------------(3.17)}$$

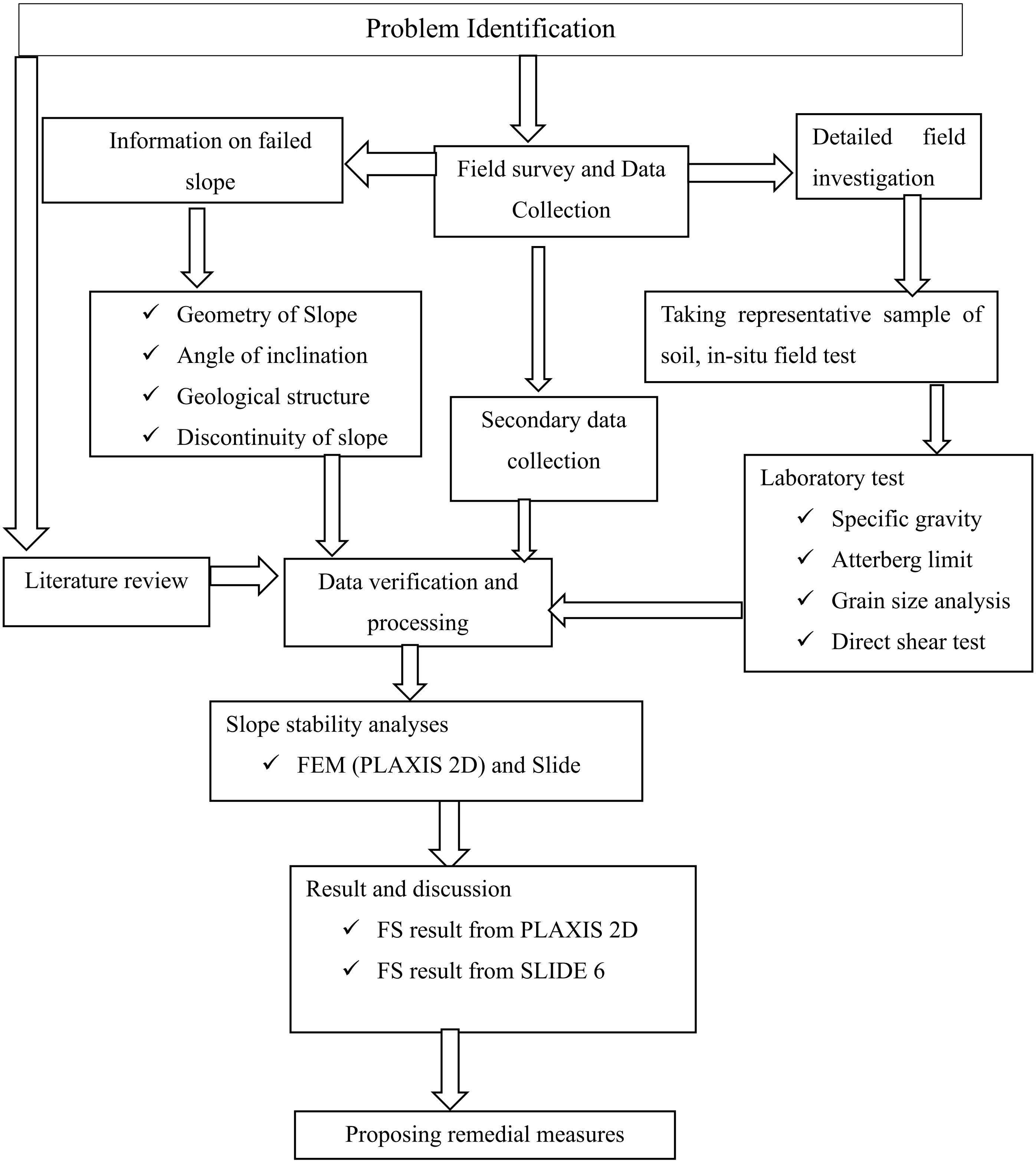

Figure 3-13 General methodology flow chart

3.9 Materials

The material and equipment that were used for this research work include both laboratory and field equipment. The field equipment that was used for field data collection, measurement and testing include GPS, tape meter and Ropes were used to determine the slope geometry. Soil mechanics laboratory equipment's were used for shear strength, sieve analysis, specific gravity; natural moisture content and Atterberg limit tests. A cylinder with known volume was used to determine the unit weight of the soil. For data analysis, different software such as Arc GIS 10.8, Microsoft excel, Slide 2D and plaxis 2D were utilized.

CHAPTER 4. LABORATORY TESTS AND DATA PROCESSING

4.1 INTRODUCTION

The data obtained from primary and secondary sources via desk-reconnaissance study, compressive field work, laboratory test and literature review were structured and processed in such a way that it could be suitably accessed during successive slope stability evaluations.

4.2. Geotechnical Characterization of slope materials

A detailed field assessment was conducted to identify the critical slope stability along the Quni-Bedesa road section and to describe the geological materials of soils. Based on the detailed field assessment conducted, it was found that there are Four critical soil slope sections failures identified along the road section. These findings are crucial in determining the critical slope stability along the road section and will be helpful in developing appropriate measures to ensure the safety of road section.

4.3. Engineering Properties of Soils

The engineering properties of soils are used as input parameters for slope stability analysis of soils at critical slope section of the study area and also to correlate, classify and characterize the soils. The Soil samples collected from the field survey were tested in the laboratory to determine the physical properties of soil such as grain size analysis, Atterberg limit tests, natural moisture contents, specific gravity tests, density and unit weight, compaction test and the shear strength tests were performed on the representative soil sample collected from the study area along the road section. Each parameter was discussed as follows.

4.3.1. Grain Size Analysis

Grain size analysis was performed to identify the percentage of different particle sizes in the soil from composes of critical soil slope located along the road. The laboratory test was conducted on the two disturbed soil samples collected from the test pits in the field. This test was carried out utilizing the mechanical sieve analysis and hydrometer analysis depending on the particle size soils. The mechanical sieve analysis was used for particle size larger than 0.075mm diameter (No.200 Sieve) and hydrometer analyses were employed for particle size smaller than 0.075mm diameter, (No.200 Sieve). Based on the particle size analysis results, the particle size diameter vs percent finer (particle size distribution curve) was plotted for each soil sample as shows on Fig.4.1. The grain size analysis results showed that the soil samples contained 10.07-30.86% of gravel, 67.25-86.47% of sand and 1.89-3.46% silt and clay. According to the results of grain size analysis, the soil of critical slope sections was classified as sand soil at both SS1 and SS2 of study area. The summary percentage of soil particles of each sample was shown in Table 4.1 below.

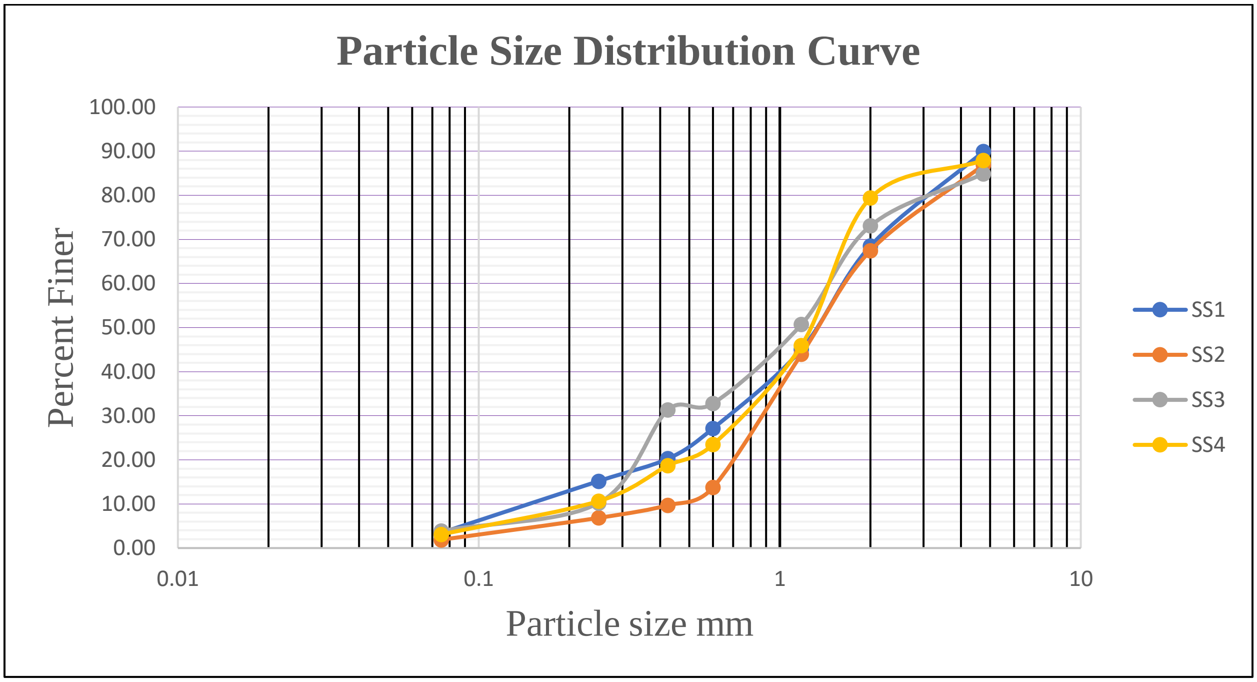

Figure 4-1 Particle size distribution curve from sieve analyses

Table 4.1 Particle size distribution curve from sieve analyses Grain size Analysis result of the soil slope sections of the study area.

Slope section	Depth (m)	The percentage of the soil particles.			CU	CC
		% Gravel	% Sand	% Fine		
SS1	1	10.07	86.47	3.46	9	4.6
SS2	1	30.86	64.19	4.95	3.6	2.92
SS3	1	39.25	50.36	10.39	4.6	1.74
SS4	1	12.6	71.3	16.1	4.83	2.72
SS = slope section						

4.3.2. Atterberg Limit Test

The Atterberg limit test was conducted on soil samples from the critical slope sections using the (ASTM D 4318, 1998) standard procedure and the Casagrande technique. This test is used to evaluate the liquid limit, plastic limit, and plasticity index of fine-grained soil and to classify soil using the Unified Soil Classification System (Moreno-Maroto & Alonso-Azcarate, 2022). The Liquid limit test was performed to determine the amount of water required for the soils to lose their cohesion and flow like a liquid. From the liquid limit determination chart (Fig.4.2) this test corresponds to 25 numbers of blows. A plastic limit test was conducted to determine the amount of water required for the soil to crumble. Furthermore, the plasticity index was determined from liquid and plastic limits (Table 4.2) to give the range over which the soils in the study area. The plasticity index of the soils in the study area ranges from 13.02 % to 34.29 % which indicates a medium to high plasticity soils and the liquid limit values are range from 38.42% to 63.24 % as shown in Fig.4.2. In addition, the minimum and maximum plasticity limits of the soil study area are 25.63% and 29.95 % respectively as shows in Table 5.2 below.

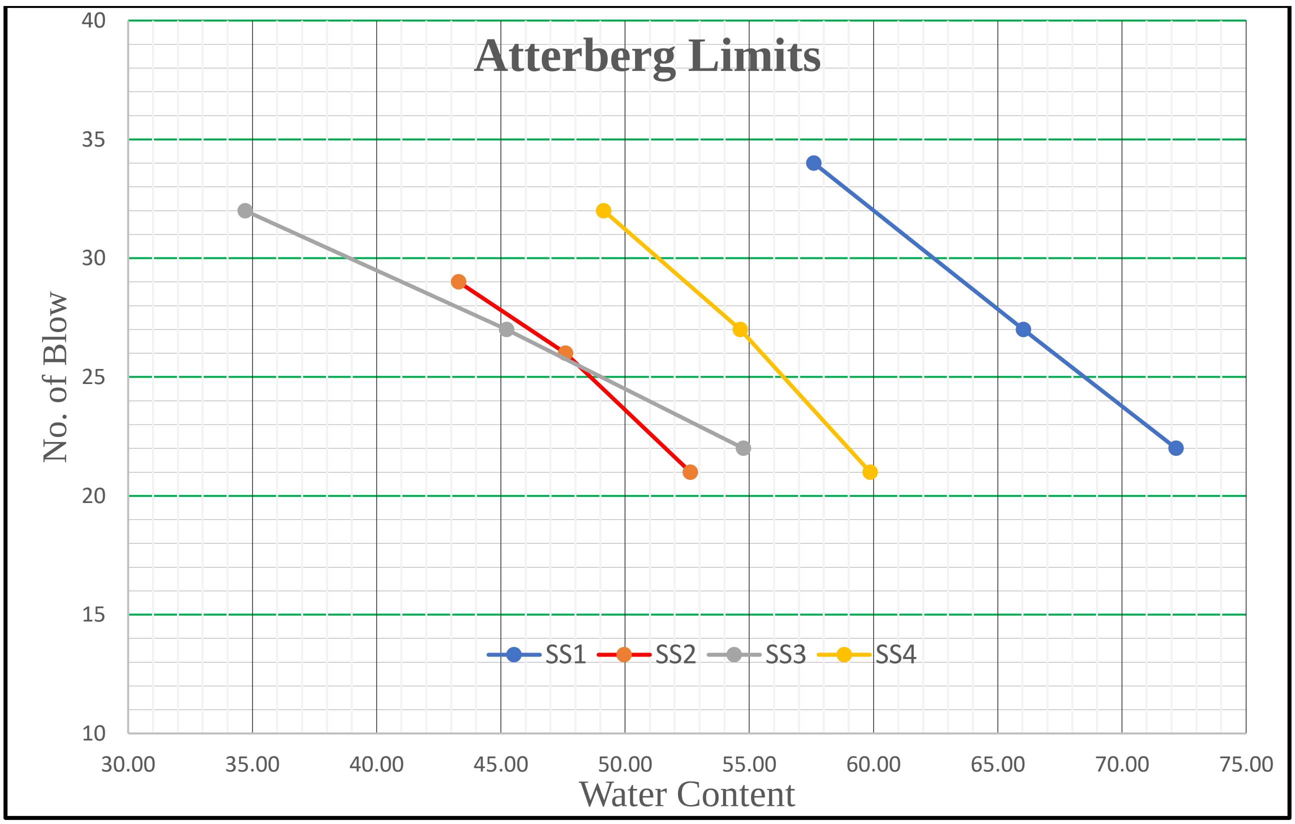

Figure 4-2 Liquid limit charts of critical soil slope sections.

Table 4.2 Atterberg limit tests and plasticity index result of soil at critical slope sections

Slope sections	Depth(m)	Sample types	Atterberg limit tests			Plasticity Class according to EN ISO 14688-2
			LL%	PL%	PI%	
SS1	1	Disturbed	63.4	29.3	34.1	High plasticity
SS2	1	Disturbed	44.4	28.03	16.37	Intermediate plasticity
SS3	1	Disturbed	38.65	25.63	13.02	Intermediate plasticity
SS4	1	Disturbed	52.3	27.5	24.8	High plasticity
SS = Soil slope section, LL = Liquid limit, PL = plastic limits, PI= Plasticity index						

According to Plasticity diagram of EN ISO 14688-2:2018 soil classification, the soil of the study area falls into medium to high plasticity classes. As a result, soil slope of SS2 and SS3 was assigned as a low plasticity index and soil slope of SS1 and SS4 was high plasticity index. The plasticity chart is one of the most significant measures of plasticity index and liquid limit according to (Casagrande, 1932). This plasticity chart can be used to differentiate silt soil from clay soil using the A-line equation (PI = 0.73(LL-20)). When the plasticity and liquid limits across below A-line the soil is inorganic silt with low, intermediate, high and very high plasticity and when each other across above A-line, the soil is inorganic clay soil with low, intermediate, high and very high plasticity. In addition, when the LL>50%, the soil has high plasticity and when the LL<50%, the soil has low plasticity.

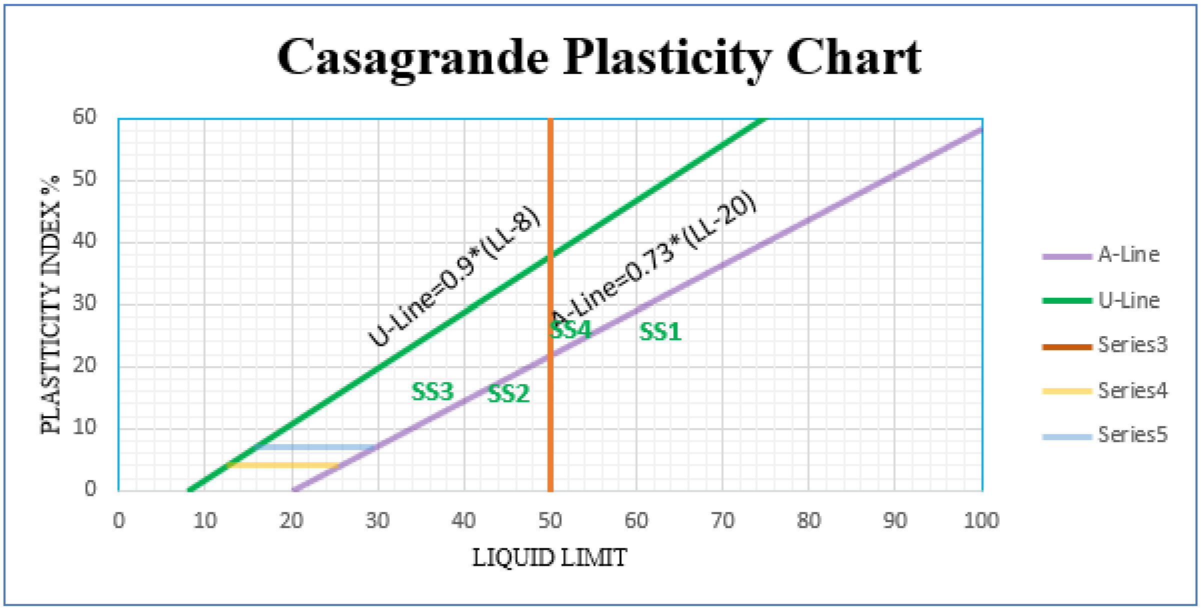

Figure 4-3 Plasticity chart of the critical soil slope section of the study area

4.3.3. Natural Moisture Contents

Natural moisture content (w) is the in-situ water content of soils determined using freshly excavated soil samples before exposing them to air. The test was conducted using fresh soil samples collected from two critical slope sections in accordance with (ASTM D2216, 1998). In the study area, the natural moisture content of the soils of critical slope section ranged from 12% to 25.6 % as shown in (Table 4.3). This demonstrates that the majority of soils are in dry state and the moisture holding capacity of the soils in the study area is low.

5.3.4. Specific Gravity of Soils

The specific gravity of soils in a selected slope section of the study area was evaluated using a pycnometer and distilled water at a specific temperature. For each sample, the specific gravity of the soil can be analyzed using the (ASTM D 854, 1998) standard. The specific gravity of soils at selected slope sections in the study area ranges from 2.68-2.7 as shown in (Table 4.3).

Table 4.3 Specific gravity and Natural moisture content of the soil slope sections

Slope section	Depth of sample (m)	Natural moisture contents	Specific gravity (Gs)
SS1	1	26.25	2.68
SS2	1	12.79	2.71
SS3	1	15.81	2.70
SS4	1	24.34	2.69

4.3.5. Unit Weight of Soils

The unit weight of the soil, both saturated and dry unit weight at critical slope section was determined from the laboratory test result of the collected soil samples from the fields. This test is performed for four soil samples that have been taken at different depth intervals of the study area. The result of the tests has been presented in Table 4.4. For this study, the unit weight utilized as an input parameter in slope stability analysis of the soil slope sections.

Table 4.4 Unit weight of soils for the soil slope section at SS1, SS2, SS3 and SS4

Slope sections	Unit weight of soils	
	γ_d(KN/m^3)	γ_{sat} **(**KN/m^3)
SS1	14.27	19.39
SS2	17.4	21.6
SS3	18.5	20.32
SS4	16.59	18.5

4.3.6. Standard Compaction Tests

The Standard proctor compaction test is performed to determine the relationship between the moisture content and the dry density of a specific soil sample at a specified compacting effort. This test was performed on four soil samples collected from the critical slope sections of the study area using a standard proctor test. The maximum dry density (MDD) and optimum moisture content (OMC) of the soil is used to remold the soil for the shear strength test were analyzed based on the results of the compaction test. The laboratory test results and the corresponding compaction curves of the four critical soil slope sections are shows in Fig.4.3. The result of maximum dry density (MDD) and optimum moisture content (OMC) are presented in Table 4.5.

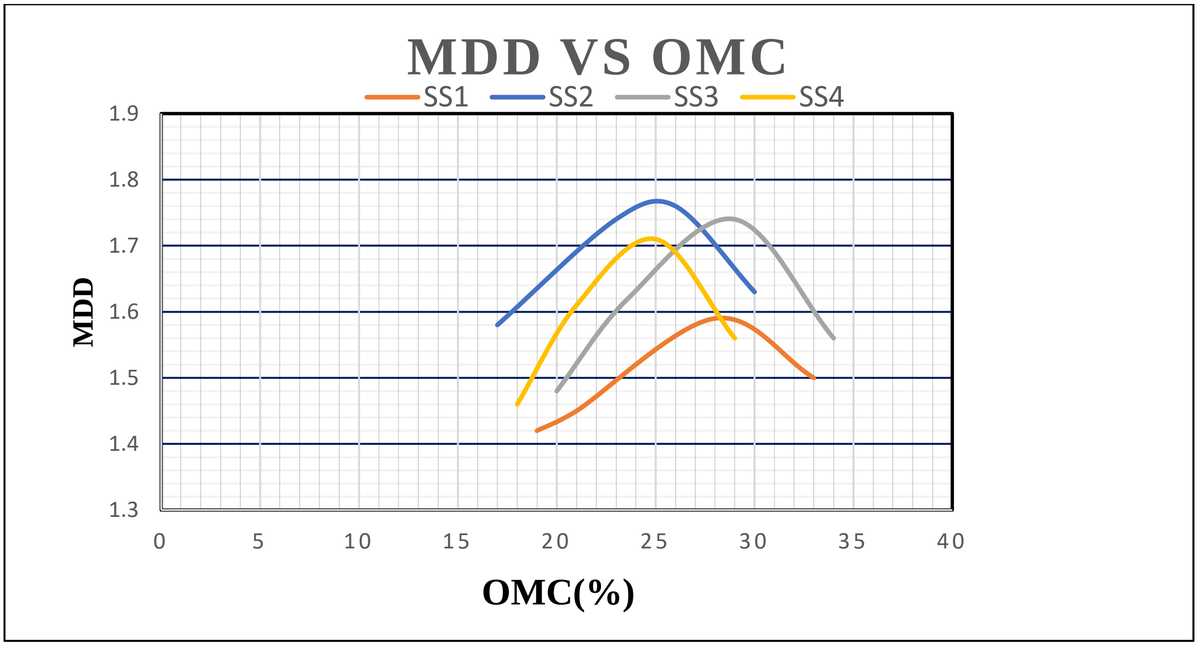

Figure 4-4 Compaction curves of the soil critical soil slope section of the study area SS1, SS2, SS3 and SS4.

Table 4.5 Maximum dry density and optimum moisture content of the soil slope section at SS1 and SS2

Slope sections	MDD, (g/cm3)	OMC (%)
SS1	1.45	35.89
SS2	1.74	24.38
SS3	1.72	26.51
SS4	1.53	31.54

4.3.7. Direct Shear Strength Tests

The direct shear test is one of the common strength tests for soils in which the shear strength parameters are determined to be used for slope stability analysis. In this study the shear strength parameter such as cohesion and angle of internal friction of the selected critical soil slope section has been determined from the direct shear tests as shown in Table 4.6. The result from direct shear test (Table 4.6) indicates that the Min and maximum cohesion of soil slope section three (SS3) and the soil slope section one (SS1) are 9.65 KN/m2 and 21.4 KN/m2, respectively. While the internal friction angle of the soils from slope section one (SS1) and the slope section three (SS3) were found to have 28.69 and 34.68 respectively (Fig.4.4).

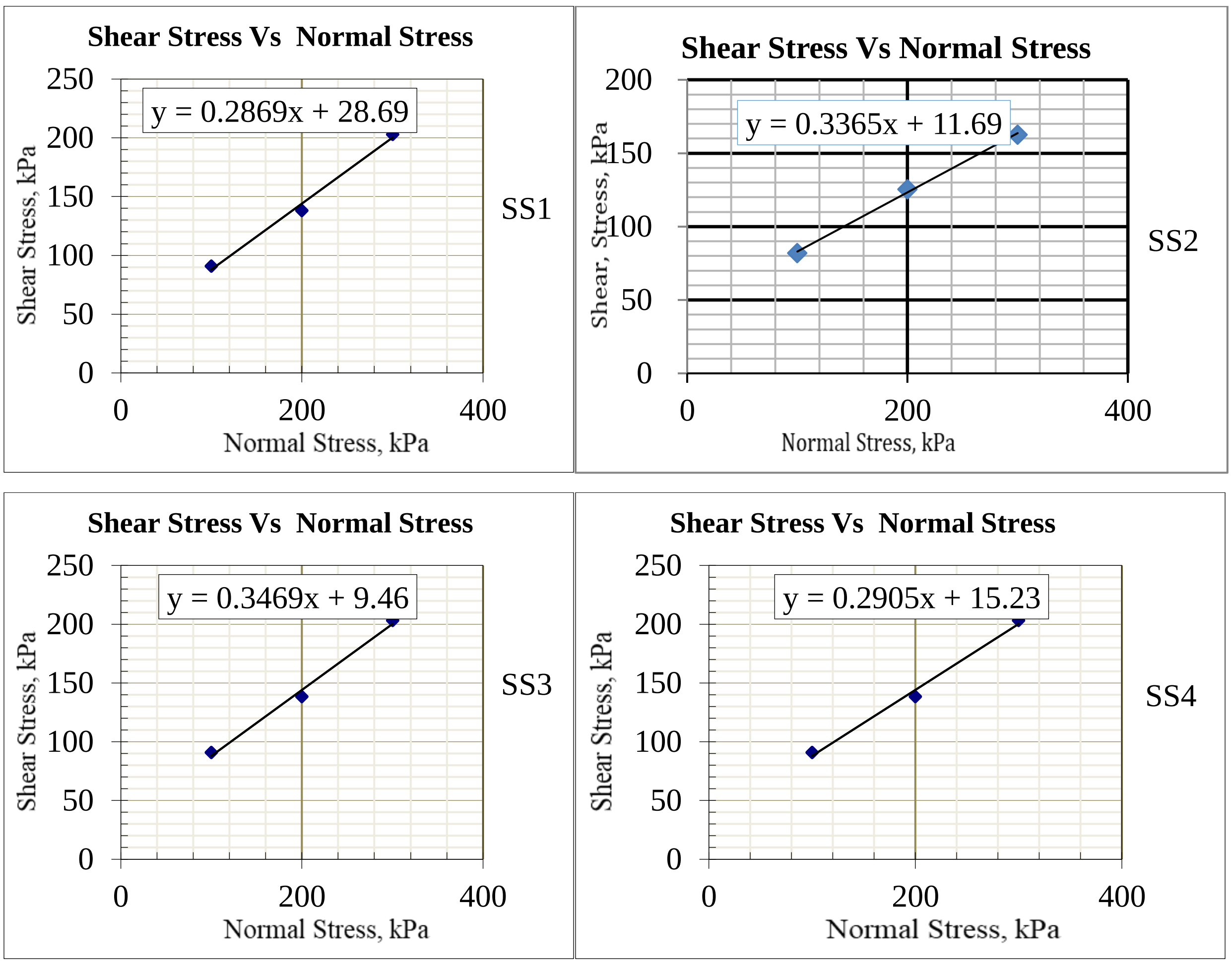

Figure 4-5 Shear stress vs Normal stress of soil at a) SS1, SS2, SS3 and SS4

Table 4.6 Shear strength parameters of soils for the soil slope section.

Slope section	Shear strength parameter	
	Cohesion, (C) Kpa	Angle of internal friction (ϕ)
SS1	21.36	28.69
SS2	11.65	33.65
SS3	9.65	34.68
SS4	15.23	29.05

4.4. Classification of Soils Based on Unified Soil Classification System (USCS)

The soils from selected critical slope section along the road section of the study area were classified by USCS system using gradation analyses and Atterberg limit test results (Table 4.7). According to the USCS system, soil samples from SS1 of the critical slope section along the road fall into SC (Clayey sand), while SS2 and SS3 of the critical slope section fall into the SW-SM (sand with silt and gravel) soil types and SS4 fall into SM (silty sand). The detailed result and the USCS classification of the soils for the study area are presented in Table 4.7

Table 4.7 Classifications of Soils based on USCS Classification System

S.ID	Atterberg limit			Grain size analysis					Soil Classification System
	LL	PL	PI	% Gravel	% Sand	% Fine	Cc	Cu	USCS
SS1	63.4	29.3	34.1	10.07	86.47	3.46	4.6	9	SC (Clayey sand)
SS2	44.4	28.03	16.37	30.86	64.19	4.95	2.92	3.6	SW-SM (sand with silt and gravel)
SS3	38.65	25.63	13.02	39.25	50.36	10.39	1.74	4.6	SW-SM (sand with silt and gravel)
SS4	52.3	27.5	24.8	12.6	71.3	16.1	2.72	4.83	SM (Silty Sand)

4.6. Soil stiffness parameters

The stiffness parameters for soil (Es and v) are used for deformation analysis in numerical modeling. Hence, suitable values of these parameters were obtained from numerical correlations and Literature. The drained poisons ratio of granular soils is obtained from equation 4.6 as suggested by Kulhawik and Mayne (1990) and Bowles's (1996) recommendation and the modulus of elasticity of the soil was calculated from the SPT N60 value as suggested by (Ameratunga, J., Sivakugan, N., & Das, B. M., 2016). using equation 4.17 (see chapter 3).

Cohesive soils (such as Clay soils) are characterized by a very low number of dilatancy angles ($\psi \approx 0$). The formula $\psi = \varphi - 30°$ can be used to estimate the dilatancy angle for non-cohesive soils (sand, gravel) with the angle of internal friction $\varphi > 30°$.

In addition, horizontal earthquake coefficient was taken from EBCS 8 (1995).

Table 4.8 Soil parameters summery used in numerical modeling

Slope section	Description of soil and rock	Strength Model	C (Mpa)	ϕ, (º)	E (KN/m2)	Unit weight (KN/m3)		V	α (g)
						γdry	γsat		
SS1	SC	Mohr-coulomb	21.36	28.69	12	14.27	19.39	0.3	0.07
SS2	SW-SM	Mohr-coulomb	11.65	33.65	18	17.4	21.6	0.25	0.07
SS3	SW-SM	Mohr-coulomb	9.65	34.68	17	18.5	20.32	0.25	0.07
SS4	SM	Mohr-coulomb	15.23	29.05	13	16.59	18.5	0.3	0.07

SS = slope section, C = cohesion, ϕ = angle of internal friction, γ = Unit weight of Soil, V = Poisson ratio and α = seismic horizontal acceleration,

CHAPTER 5. NUMERICAL MODELING AND VALIDATION

5.1 Introduction

Numerical models allow geotechnical engineers to simulate the real and actual situations of the geotechnical problem such as construction stages, various loading conditions, excavation conditions, and boundary conditions. The result allows to get a better understanding of the mechanisms of failure, deformation, and safety of structures. The finite element method is a common and power full advanced numerical modeling tool in geotechnical engineering. For the same reason, the method was selected for this work to predict the stability of the road cut slope and to investigate the performance of slope profiles. Plaxis-2D was used to determine the deformation and safety factor under static and dynamic loading conditions. The limit equilibrium method also included in this evaluation using a LE based slide software. In this section, the procedures required to model and analysis of slopes in FEM (plaxis) and LEM (slide) are included. The numerical evaluation in the performance of slope profiles also addressed in this chapter. Finally, validation of the model was carried out using previous case studies obtained from the literature and hand calculation.

5.2 Formulation of finite element method

Finite element modeling is a method of discretizing a continuum into small pieces or elements to describe the behavior or actions of individual pieces and reconnecting them to represent the behavior of the continuum as a whole (Meko, 2023). Each element has some nodes and each node have some degrees of freedom corresponding to displacement components in deformation analysis. Defining the problem domain is the 1st step in FEM which includes defining the geometrical model, material model, and applying boundary conditions. The domain can be later discretized into a series of continuum elements to form a mesh that connects with nodes to transfer forces and displacements between them. Triangular areal elements were used to discretize soils in plaxis 2D software. Once the problem domain is defined and discretized into finite elements the element stiffness functions are formed (Plaxis, 2013). Equation 5.1 shows the relationship of element stiffness matrix (K), a vector of an unknown degree of freedom or nodal displacement (d), and a resultant vector of element nodal forces (f). The elastic element stiffness matrix is also expressed as a function of strain interpolation matrix (B) and an elastic material matrix (De) as shown in Eqn 5.2.

$[K]\{d\} = \{f\}$---(5.1)

$K = \int B\ TD\ e\ BdV$ ---(5.2)

The element stiffness matrix is gathered and assembled to form a global continuum equation containing the material and geometric data. The unknown nodal displacements are solved from the global equations by applying known boundary conditions and the values between nodes are obtained from interpolated shape functions (Meko, 2023). The remaining parameter forces, stresses, and strains are obtained by post-processing using determined nodal displacements in the element and global equations (Plaxis, 2013). In numerical modeling proper selection of parameters such as element type, mesh size, boundary conditions, constitutive models increase the accuracy of results. Hence, emphasis was given in the selection of these parameters. The selection and modeling of these parameters are discussed in the following sections.

5.3 Modeling with plaxis 2D

5.3.1 Geometric modeling

Two critical sections of the cut slope were used for plaxis modeling as shown in figure 5.1. During FE geometric modeling the selection of model extent influences the accuracy of the result. To minimize this effect the selection of domain extent was made by performing sensitivity analysis for vertical and lateral boundaries under constant loading condition. From the result, the boundary with a negligible effect on deformation (displacement) was selected as shown in Figure 5.2. Then the selected domain of slope geometry was modeled using both plaxis 2D. As the slope have a constant cross-section with a larger thickness plane strain model was used during modeling.

5.3.2 Material modeling

The mechanical behavior of soils and rocks can be modeled with various digress of accuracy. For this study, the elastic perfectly plastic Mohr-Coulomb model was used. Rock layers were modeled using Hoek's -Brown equivalent Mohr-Coulomb model. The model uses E and v as soil elasticity, φ, and c as soil plasticity and ψ as angle of dilatancy. The model does not include stiffness varying with stress and strain. The effective soil and rock parameters determined in chapter 3 were used for this modeling.

5.3.4 Mesh generation

The finite element numerical method is based on the discretization of a continuum into finite elements, describing the behavior or actions of each element and reconnecting them to represent the continuum. Different types of elements like a beam, shell, solid and different types of shapes like triangular, quadrilateral, tetrahedral with various order of equations can be used in FE discretization based on the nature of the project. In this work, the 4th order 15-node triangular element was used. Generally, the accuracy of the solution is increased with decreasing element size and increasing the order of interpolation (i.e., quadratic is more accurate than linear). But the computation time increases with decreasing element size and increasing order of interpolation (Plaxis 2013). To avoid such disadvantages optimal mesh size was selected by conducting sensitivity analysis. It was carried by evaluating the effect of different mesh sizes on total and horizontal displacement with constant loading conditions as shown in Figure 5.4. From Figure 5.4 reducing element, size increases horizontal displacement and its effect becomes negligible beyond element number 324 (fine mush size). Accordingly, fine mesh sizes were used for this modeling. Finally, mesh generation was made using automatic unstructured mesh as shown in Figure 5.5.

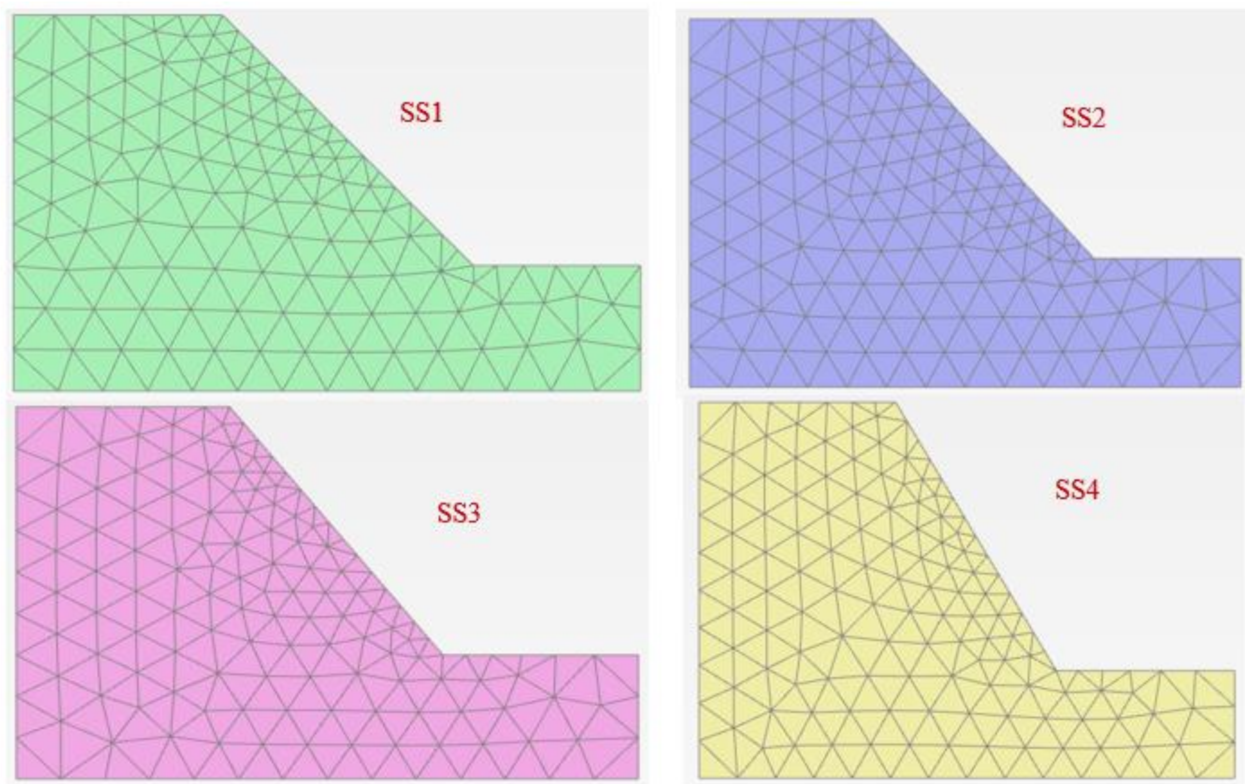

Figure 5-1 Mesh generated for slope section using PLAXIS 2D.

5.3.5 Calculations with plaxis

Plaxis allows various calculation options (i.e., plastic calculation, safety analysis, dynamic analysis, and fully coupled flow-deformation analysis) depending on loading and/or boundary conditions. The execution of these calculation needs a generation of initial stress and pore water pressure distribution. Hence, the initial stress distribution was generated by k_0 procedure in terms of $\sigma' v_0$ and $\sigma' x_0$. The horizontal initial stress values are related to the vertical one using K_0, x as shown in figure Eqn. 5.3. On the other hand, the initial pore water condition was generated using phreatic level from the global water level.

$$\sigma' x_0 = K_0,\ x * \sigma' v_0 \quad \text{.......} 5.3$$

Moreover, as the non-linear numerical analysis is an approximate method there is always some drift of result from the exact solution. To bound this error within safe and working limits plaxis allows the use of tolerated error. In this modeling, a tolerated error 0.01 or 1% was used in all calculations.

5.3.5.1 Deformation analysis

The deformation analysis was carried with plastic calculation i.e., used for an elastic-plastic deformation analysis using constant stiffness. The method is suitable when the change of pore water pressure with time is not necessary (i.e., the case). Two critical slope sections were analyzed in this method using static and dynamic loading conditions. In the static condition, the evaluation was made for its material weight using $\sum Mweight$ as a multiplier. The hard rock at the top of the slope is represented as a surcharge load ($q = \gamma * h$). Whereas the dynamic condition was carried by introducing the earthquake forces in terms of horizontal acceleration coefficient (α=0.12 and 0.15) which uses multiplier (ΣMaccel) in the calculation routine. In this analysis additional horizontal driving force ($\alpha * \sum Mweight$) was applied from the previous step as discussed in chapter 2. Table 5.2 shows the calculation phases and corresponding loading types.

Table 5.1 Deformation for slope section using PLAXIS 2D.

Deformation			
	Total displacements(m)	element	Node
SS1	0.437 *10-3	444	2907
SS2	0.6784 *10-3	217	816
SS3	$0.327*10^{-3}$	210	987
SS4	$4.14*10^{-3}$	241	788

5.3.5.2 Safety analysis

To evaluate the stability of the slope factor of safety was determined for each critical section using plaxis 2D. In plaxis safety analysis was carried using a phi-c reduction method i.e., a method where the shear strength parameters (c & $\tan\emptyset$) are successively reduced until the failure occurs. During the prosses the strength reduction factor ($\sum Msf$) is increased start from 1. The global safety factor is equal to the total multipliers $\sum Msf$ at the point of failure which is expressed as the ratio of initial and reduced strength parameters as shown in Eqn. 5.4.

FS = $\sum$ Msf = tan$\emptyset input/$ tan$\emptyset$reduced = Cinput /Creduced = Su input /Sureduced ----------(5.4)

Table 5.2 Soil conditions and its calculation phase in plaxis software.

Sample	ɣsat (KN/M³)	ɣdry	C (KN/M²)	Ø°	E (Mpa)	V	Soil State
SS1	19.39	14.27	21.36	28.69	12000	0.3	Dry state
							Wet State
SS2	21.6	17.4	11.65	33.65	18000	0.25	Dry state
							Wet State
SS3	20.32	18.5	9.65	34.68	17000	0.25	Dry state
							Wet State
SS4	18.5	16.59	15.23	29.05	13000	0.3	Dry state
							Wet State

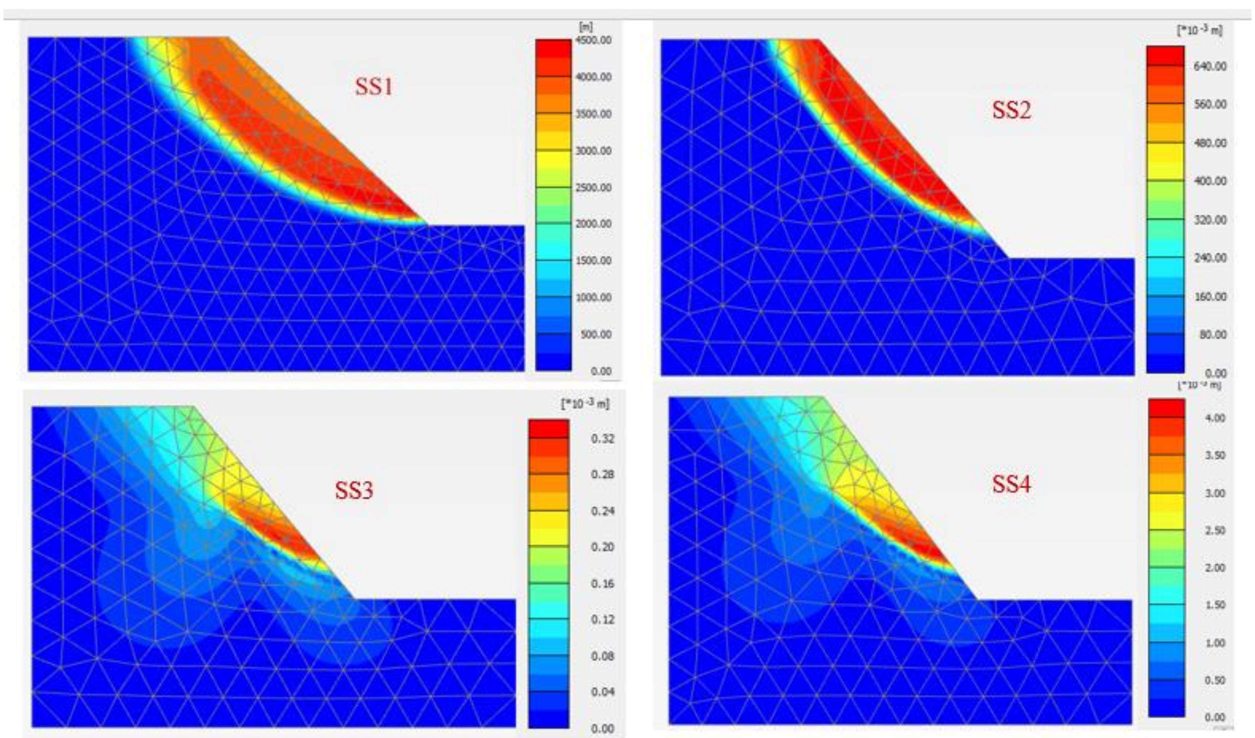

Figure 5-2 Deformation of SS2 in plaxis 2D

5.4 Modeling with slide

Modeling was also made in slide software to evaluate the FS of the slope using LEM to compare the result with FEM. The first step in slide modeling is the project setting where various important modeling and analysis options of the problem i.e., failure direction, units, analysis methods, and groundwater conditions are set. Two critical sections of the cut slope were modeled with similar geometric boundaries used in plaxis software. Mohr-Coulomb strength criterion was used to define the material properties of the slope. The criterion uses unit weight, cohesion, and angle of internal friction as the input parameter. In the analysis factor of safety and slip surface were evaluated for both static and dynamic loading conditions using bishop, Jambu, and GLE method. During modeling, most slope failures occur in a circular slip surface with little inaccuracy unless there are geological layers that favor the failure in a non-circular slip surface. Hence, a circular failure surface was used to define the type of slip surface and grid search is used to locate the critical slip surface (slip surface with the lowest safety factor). Figure 4.8 shows the slice, depth of slip surface, and grid search for FS using the GLE method.

5.5 Numerical validation

The software and procedures used to model critical slope sections in this study should be validated before the results of the analysis are accepted. As it is difficult to measure or/and monitor the deformation and FS in the field, existing literature of previous case studies and hand calculations were used to validate this numerical modeling.

5.5.1 Validation with hand Calculation

To validate the numerical modeling with hand calculation the critical slope section 1 was evaluated using the ordinary method of a slice (Fellenies method) as shown in Figure 5.11. FS were determined for circular trial slip surface AC by considering the location of slip surface on LE based slide software.

For equilibrium of trial wedge ABC, the moment of driving force about "o" equals the moment of resisting force about "o".

$$Fos = \frac{\sum_{i=1}^{i=n} (c * ln + W\cos\alpha n * \tan\Phi)}{\sum_{i=1}^{i=n} W\sin\alpha n} \quad \ldots\ldots\ldots\ldots\ldots\ldots 5.6$$

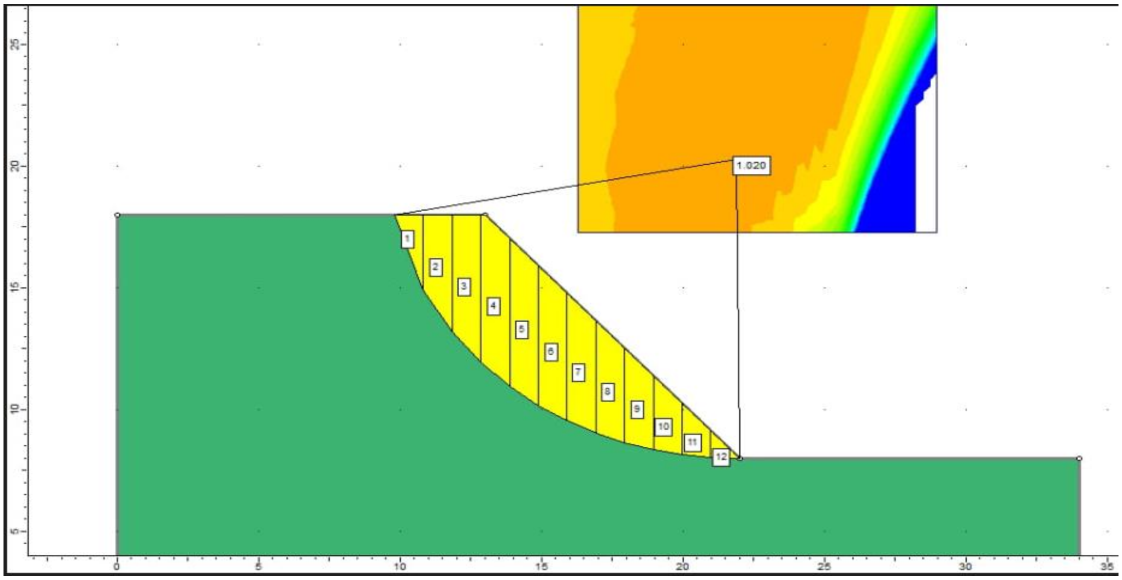

Figure 5-3 Slip surface for hand calculation on slope section 1

Table 5.3 Calculation of resisting and driving forces for each slice

Slice No	∅	C	α_n	W (KN)	b	Cosαn	Sinαn	ln	W*Cosαn	W*Sinαn
1.00	22.68	18.95	71.69	24.24	1.02	0.85	0.53	1.21	20.49	38.32
2.00	22.68	18.95	59.47	62.18	1.02	0.98	0.22	1.05	60.67	13.03
3.00	22.68	18.95	51.04	89.47	1.02	0.72	0.70	1.42	64.15	35.58
4.00	22.68	18.95	43.98	105.35	1.02	1.00	0.00	1.02	105.35	0.19
5.00	22.68	18.95	37.69	105.44	1.02	1.00	0.01	1.02	105.44	0.22
6.00	22.68	18.95	31.91	101.85	1.02	0.88	0.47	1.16	89.64	15.15
7.00	22.68	18.95	26.48	93.30	1.02	0.23	0.97	4.51	21.12	25.79
8.00	22.68	18.95	21.29	80.60	1.02	0.76	0.65	1.34	61.49	13.76
9.00	22.68	18.95	16.28	65.80	1.02	0.84	-0.54	1.21	55.33	8.81
10.00	22.68	18.95	11.40	49.08	1.02	0.39	-0.92	2.61	19.19	10.49
11.00	22.68	18.95	6.60	30.56	1.02	0.95	0.31	1.07	29.06	2.04
12.00	22.68	18.95	1.84	10.32	1.02	0.27	0.96	3.77	2.79	1.78
SUM								4.24	233.17	125.74

$$Fos = \sum_{(i=1)}^{(i=n)} ((4.24 * 18.95 + 233.17 \tan(22.68)) / (\sum_{(i=1)}^{(i=n)} 125.74) = 1.150$$

CHAPTER 6. RESULT AND DISCUSSION

6.1 Introduction

As discussed in chapter 5 different modeling was made to evaluate the stability conditions of the slope and performance of slope profiles on critical slope sections. In this section, the factor of safety (FOS) was analyzed and interpreted using the limit equilibrium and finite element methods for failure surface in soil slopes under static dry and static wet conditions. A comparison of results also conducted between FEM & LEM. Furthermore, performance evaluation results of slope profiles also presented (i.e., discussion was made on the performance, suitable condition, and advantages of one over another for a different point of view).

6.2 Discussion on the analysis results of the critical slope section

6.2.1. Slope Stability Analysis of Soils

For this study, the factor of safety for the four soil slope sections were estimated under limit equilibrium and finite element methods using the same material properties, slope angle, and slope geometry. The analysis was carried out to identify whether the slope is stable or unstable. The factor of safety (FOS) was analyzed and interpreted using the limit equilibrium and finite element methods for failure surface in soil slope under static dry and static wet conditions.

6.2.1.1 Slope Stability Analysis of Soils Using Limit Equilibrium Method

Slope stability analyses of four soil slope sections were conducted using four limit equilibrium methods: Morgenstern-Price method (GLE), Spencer, Bishop simplified and Ordinary/Fellenous methods. In slope stability analysis using limit equilibrium method, determining the critical potential slip surface is an essential measure on obtaining a minimum factor of safety in each slope section utilizing slide software (Abramson, Lee, Sharma, & Boyce, 2002). In addition, in the Rocscience Slide software, the general limit equilibrium approaches satisfy all the equilibrium conditions (Amir & Beyabanaki, 2020). Soil slope section one (SS1) has 18 meters of height, 60 meters of length, and approaches the road at nearly a 60-degree angle. Similarly, the Soil slope section two (SS2) has approximately 20 m height, 50m length and nearly dips at 48 degrees towards to the road. All soil slope sections have a circular mode of failure as identified in the field. The critical SS1 and SS2 were composed of homogeneous material as determined by field observations based on physical characteristics and laboratory analysis such as grain size and Atterberg limit test results. According to the results of the laboratory test the SS1 is clayey sand

and SS2 is sand with Clay and gravel. It shows that the two soil slope sections were composed of sandy soil. The determination of slope geometry, shear strength parameters (angle of internal friction and cohesion) and soil unit weight is very important, because they are the input parameters of soil slope stability analysis. The internal friction angle, cohesion, and unit weight of SS1, SS2, SS3 and SS2 are determined from laboratory test and summarized in Table 4.14. The study area is found in a high seismic zone and the horizontal acceleration from seismic loading with a magnitude average (α) of 0.07g taken from EBCS 8 (1995). In this study four limit equilibrium methods (Morgenstern-Price method (GLE), Spencer, Bishop simplified and Ordinary/Fellenous methods) were used to determine the factor of safety for different soil slope sections with varying geometry under static dry, and static saturated slope conditions. The summary of input parameters for selected soil slope sections is shown in (Table 6.1).

Table 6.1 The input parameter for soil slope stability analysis in slide software

Soil Sample	ɣsat (KN/M3)	ɣdry	C(KN/m2)	Ø˚	Soil state
SS1	19.39	14.27	21.36	28.69	Dry State
					Wet State
SS2	21.6	17.4	11.65	33.65	Dry State
					Wet State
SS3	20.32	18.5	9.65	34.68	Dry State
					Wet State
SS4	18.5	16.59	15.23	29.05	Dry State
					Wet State

For this study during analysis using the above input parameters in Table 6.1 the factor of safety (FOS) and slip surface were determined and interpreted for static dry and static saturated conditions using four limit equilibrium methods (Morgenstern-Price method (GLE), Spencer, Bishop simplified and Ordinary/Fellenous methods). The safety factor evaluation was performed under static dry conditions, representing the stability status and presumed to be dry during the dry season in the study area. In addition, the safety factor evaluation was performed under dynamic wet conditions, which means the slope was subjected to seismic horizontal acceleration (α=0.07g) of the study area and presumed to be saturated during heavy rainfall in the study area (Lamesa & Meten, 2021b).

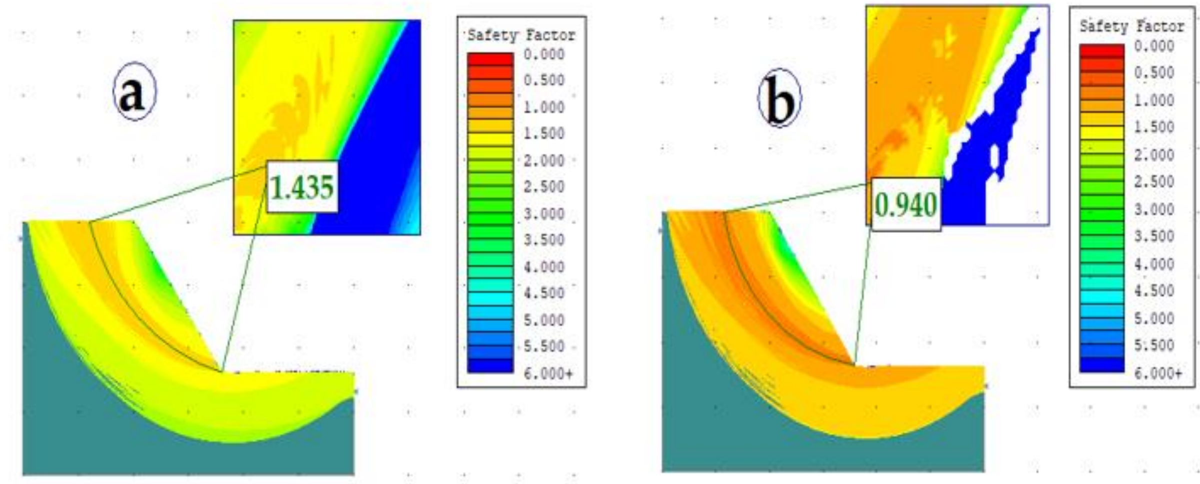

Figure 6-1 Slope stability analysis by Limit equilibrium method for SS1 under a) static dry and b) static wet conditions.

According to the above analysis results, the factor of safety for SS1 using limit equilibrium analysis is 1.435 and 0.940 under static dry and static wet conditions respectively, as illustrated in Figs 6.1 (a) and (b) respectively. This demonstrates that under dry conditions the slope at critical SS1 is stable as the result of the factor of safety greater one. However, the factor of safety that was determined under static wet condition is 0.940 as shown in Fig.6.1 (b). This implies that the soil slope section one is unstable under wet conditions. In addition, when the static dry condition is compared with the static saturated condition, the factor of safety is very low for SS1 (Fig.6.1). This implies the effect of Rainfall on slope stability is very high. This was due to the Rainfall can affect slope stability by increasing pore water pressure and weight on a slope when the soil mass is got wet, decreasing effective stress and result in loss of shear strength parameter.

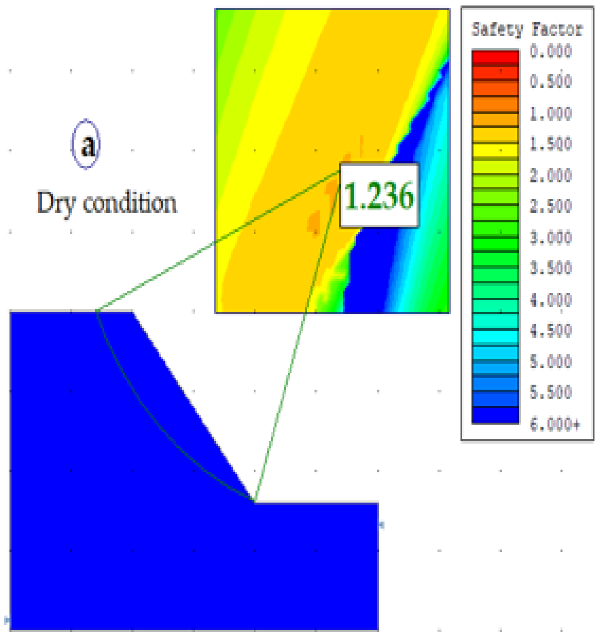

Figure 6-2 Slope stability analysis by Limit equilibrium method for SS2 under a) static dry and b) static wet conditions

According to the above analysis results, the factory of safety for SS2 using limit equilibrium analysis is 1.236 and 0.975 under static dry and static saturated conditions respectively, as illustrated in Figs 6.2 (a) and (b) respectively. This demonstrates that under dry conditions the slope at critical SS2 is stable as the result of the factor of safety greater one. However, the factor of safety that was determined under static wet condition is 0.975 as shown in Fig.6.2 (b). This implies that the soil slope section two is unstable under static saturated conditions. In addition, when the static dry condition is compared with the static saturated condition, the factor of safety is very low for soil slope section two (Fig.6.2). This indicates that the rise in the groundwater table during the high rainfall season has more significant impact on the slope instability.

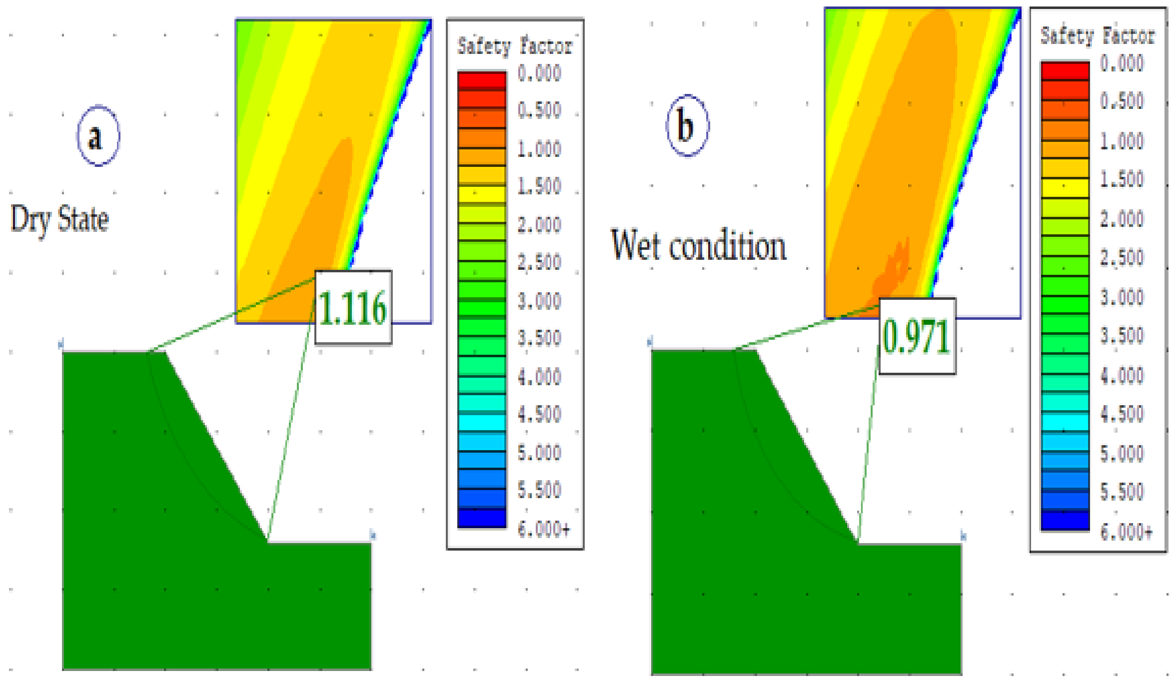

Figure 6-3 Slope stability analysis results using Limit equilibrium method for slope section SS3 under a) static dry condition and b) Static saturated condition

The minimum factor of safety and critical slip surface of the soil at critical slope section SS3 is determined using the General limit equilibrium methods/spencer by considering various conditions as indicated in Figures 6.5. Accordingly, the analyses result at the critical soil slope section SS3 revealed that the factor of safety under static dry condition factor of safety is 1.116 as shown in (fig.6.5 (a); while under static saturated condition FOS is 0.971 as shown in (Figs.6.5b). This indicated that the soil at critical slope section SS3 was stable under static dry; whereas, it was unstable under static saturated conditions. In addition, a factor of safety analyzed under saturated slope conditions is relatively small compared to static dry slope conditions. This clearly shows the impact of Rainfall on slope stability.

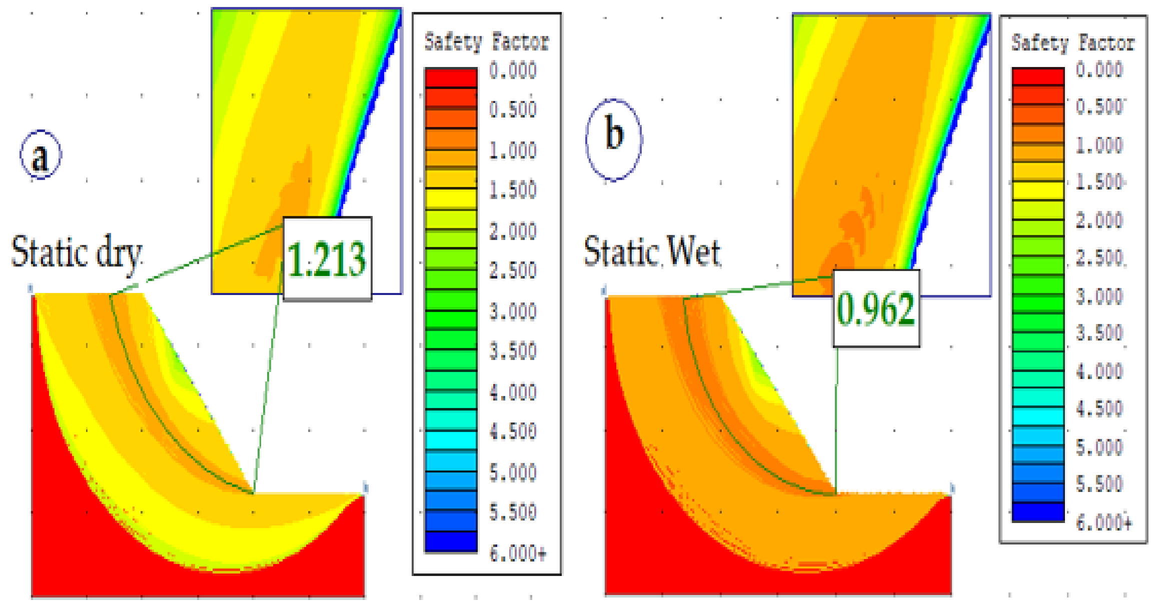

Figure 6-4 Slope stability analysis result using Limit equilibrium method for slope section SS4 under a) static dry condition and d) static saturated conditions.

Based on the above analysis results, the minimum factor of safety and critical slip surface of the soil at critical slope section SS4 is determined using the General limit equilibrium methods/spencer by considering various conditions as indicated in Figures 6.6. Accordingly, the analyses result at the critical soil slope section SS4 revealed that the factor of safety under static dry was 1.213 as shown in (figs.6.6 (a); while under static saturated condition FOS is 0.962 as shown in (Figs.6.6b). This indicated that the soil at critical slope section SS4 was stable under static dry whereas, it was unstable under static saturated conditions. In addition, a factor of safety analyzed under saturated slope conditions is relatively small compared to dry slope conditions. This clearly shows the impact of groundwater on slope stability.

The summary of factor of safety determined using the general limit equilibrium method (GLEM), spencer, Ordinary/Fellenies and Bishop simplified methods under static dry and static saturated slope conditions was presented in table 6-2.

Table 6.2 Factor of safety and slope status under different anticipated condition of soil slope sections

Slope Section	Soil Condition	FOS SLIDE				Slope stability conditions
		Ordinary/ Fellenius	Bishop simplified	Spencer	GLE/Mongster price	
SS1	Dry	1.435	1.453	1.456	1.452	Stable
	Wet	1.085	0.908	0.943	0.904	Unstable
SS2	Dry	1.192	1.234	1.243	1.236	Stable
	Wet	1.018	0.976	0.981	0.975	Unstable
SS3	Dry	1.116	1.108	1.168	1.163	Stable
	Wet	0.971	0.856	0.931	0.982	Unstable
SS4	Dry	1.213	1.207	1.252	1.248	Stable
	Wet	1.027	0.912	0.964	0.965	Unstable

6.2.1.2. Slope Stability Analysis of Soil Using Finite Element Method

The factor of safety (FOS) was analyzed and interpreted using the finite element method for failure surface in soil slope under static dry and static saturated conditions. The input parameters for the four soil slope sections which are used in finite element modeling include cohesion, internal friction angle, the unit weight of soil, Poisson's ratio (ν), dilatancy angles (ψ) and elastic modulus. The internal friction angle, cohesion, and unit weight of the soils slope sections are determined from laboratory tests. The elastic modulus of a soil (Es) and Poisson's ration (v) that is used for numerical modeling were determined from the correlation and recommendation of literature (TESHAGER, 2019). The Poisson's ration (v) was calculated using equation 3.15 (Bowles, 1996) and the deformation modulus was calculated from equation 3.17 (Das, 2002).

The safety factors for the selected critical soil slope sections were determined in PLAXIS 2D version 21.01.00.479 software using the Mohr-Coulomb model and discussed as stated bellows.

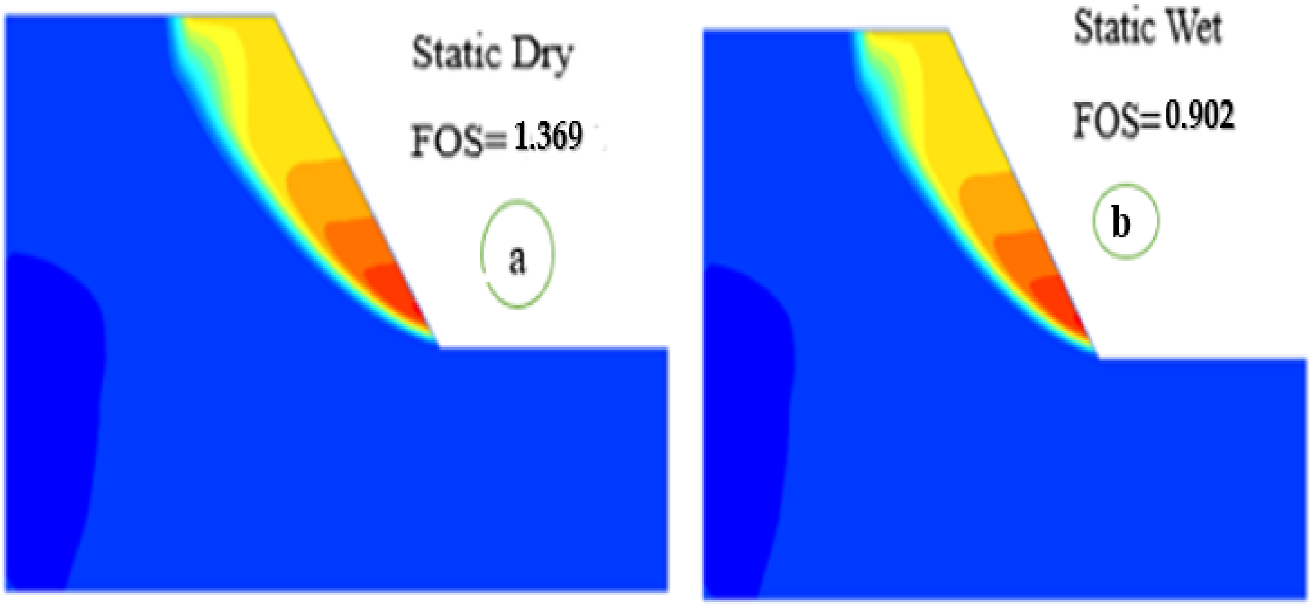

Figure 6-5 Factor of safety for SS1 using plaxis 2D software under a) static dry and b) static saturated conditions.

According to the above analysis results, the strength reduction factor for SS1 using limit equilibrium analysis is 1.369 and 0.902 under static dry and static saturated conditions respectively, as illustrated in Figs 6.3 (a) and (b) respectively. This demonstrates that under the static dry conditions the slope at critical SS1 is stable as the result of the factor of safety greater one. However, the strength reduction factor that was determined under static saturated condition is 0.0.902 as shown in Fig.6.3 (b). This implies that the SS1 is unstable under static saturated conditions. In addition, when the static dry condition is compared with the static saturated condition, the factor of safety is very low for SS1 (Fig.6.3). This indicates that the rise in the groundwater table during the high rainfall season has more significant impact on the slope instability. The ground water can affect slope stability by increasing pore water pressure and weight on a slope when the soil mass is fully saturated, decreasing effective stress and result in loss of shear strength parameter. When we compare the result of the strength reduction factor at different conditions the strength reduction factor decreased 4.6% from static dry to static saturated conditions. This demonstrating that pore water pressure has a greater effect on destabilizing these slope sections.

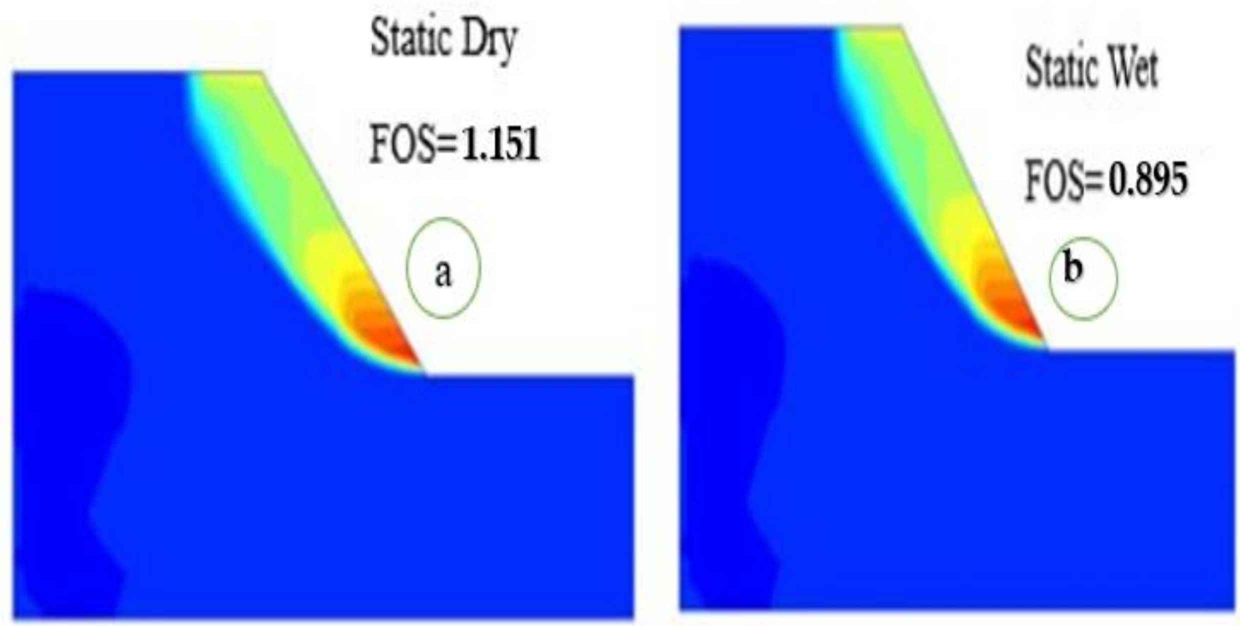

Figure 6-6 Factor of safety for SS2 using plaxis 2D software under a) static dry and b) static saturated conditions.

From the above analysis result, the minimum factors of safety or strength reduction factor determined from the FEM analyses of the SS2 is 1.151 and 0.895 for static dry and static wet condition as shown in (Figs.6.4a and b). This indicates that the soil slope section SS2 was stable in static dry conditions. However, the strength reduction factor that was determined under static saturated conditions of the soil slope section SS2 is 0.895 as shown in (Figs6.4b). This revealed that when the slope is supposed to be static saturated the critical SRF or FOS is less than one, indicating that the slope was unstable (Shariati & Fereidooni, 2021). When we compare the result of the strength reduction factor under different anticipated conditions the strength reduction factor decreased by 2.56% from static dry to static saturated conditions. The factor of safety is decreasing that indicates pore water pressure has a significant impact on the slope stability since it affects the shear strength of the materials (Bekele & Meten, 2023).

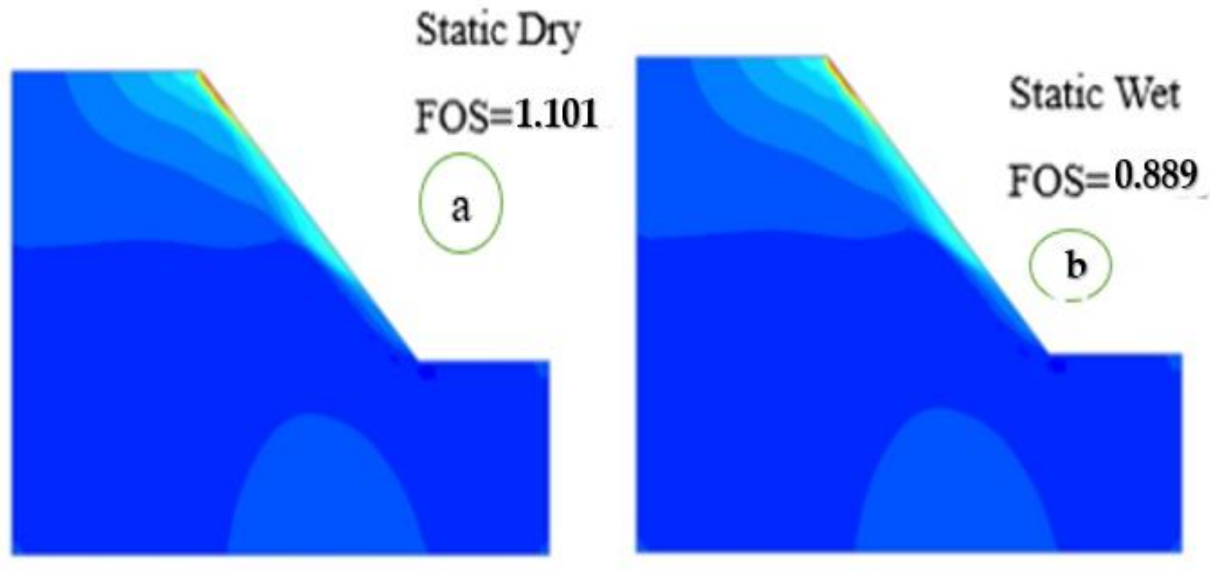

Figure 6-7 Slope stability analysis finite element method for rock slope section SS3 under a) static dry and b) Static saturated conditions.

According to the analysis results, the strength reduction factor of the soil slope section SS3 is 1.101 under static dry condition as shown in Figs.6.7 (a). This demonstrates that in static dry condition the soil at critical slope section SS3 is stable as the result of the factor of safety greater one (Christian, 2004); (Shariati, M. & Fereidooni, D, 2021). However, the strength reduction factor of soil slope section (SS3) was 0.889 under static saturated conditions as shown in Figs.6.7 (b). The results showed that the critical SRF or FOS static saturated conditions is less than one, indicating that the slope is unstable (Christian, 2004); (Shariati, M. & Fereidooni, D, 2021). Furthermore, when we compare the result of the strength reduction factor under different anticipated conditions for this slope section, the strength reduction was decreased by 2.12% when we move from static dry to static wet condition. This demonstrates that pore water pressure has a greater degree of influence on destabilizing these slope sections (Kabeta, W. F., Tamiru, M., Tsige, D., & Ware, H., 2023).

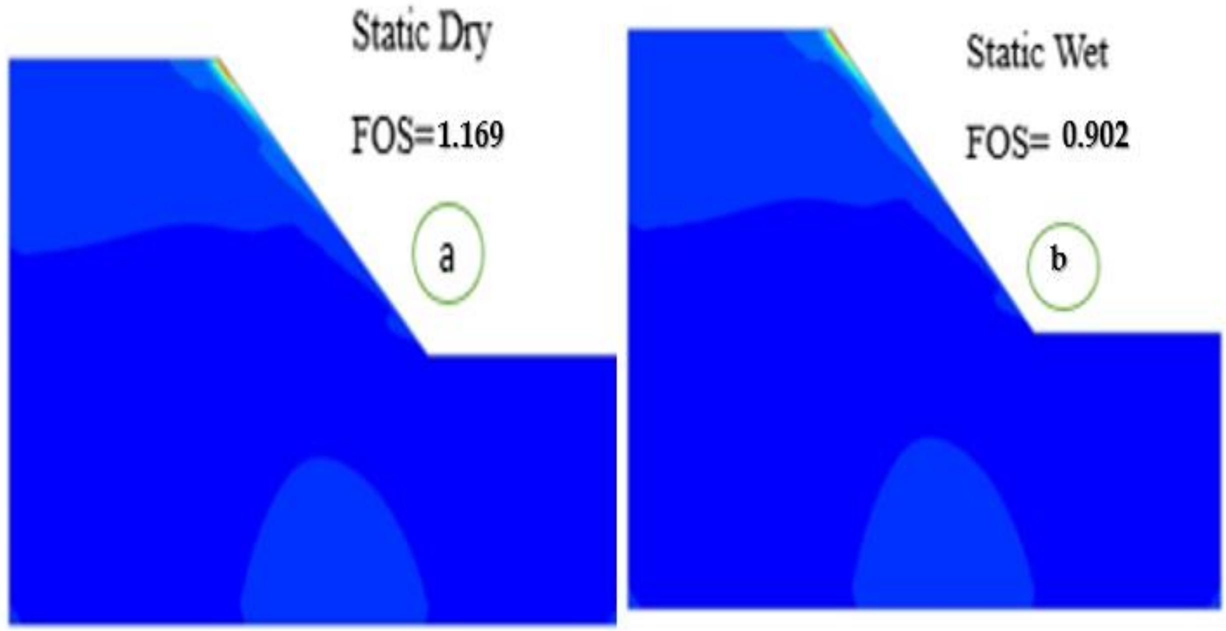

Figure 6-8 Slope stability analysis finite element method for soil slope section SS4 under a) static dry and b) Static saturated conditions.

According to the analysis results, the strength reduction factor of the soil slope section SS4 is 1.169 under static dry conditions as shown in Figs.6.8 (a). This demonstrates that in static dry condition the soil at critical slope section SS4 is stable as the result of the factor of safety greater one (Christian, 2004); (Shariati, M. & Fereidooni, D, 2021) However, the strength reduction factor of soil slope section (SS4) is 0.902 under static saturated conditions as shown in Figs.6.8 (b). The results showed that the critical SRF or FOS for static saturated condition is less than one, indicating that the slope is unstable (Christian, 2004); (Shariati, M. & Fereidooni, D, 2021). There is a possibility that the slope may fall under influence of triggering events such as excessive rain and seismic activity. The results indicated that pore water pressure plays a greater role in destabilizing slope sections. Furthermore, when we compare the result of the strength reduction factor under different anticipated conditions for this slope section, the strength reduction was decreased by 16.7 % when we move from static dry to static dry to static saturated condition.

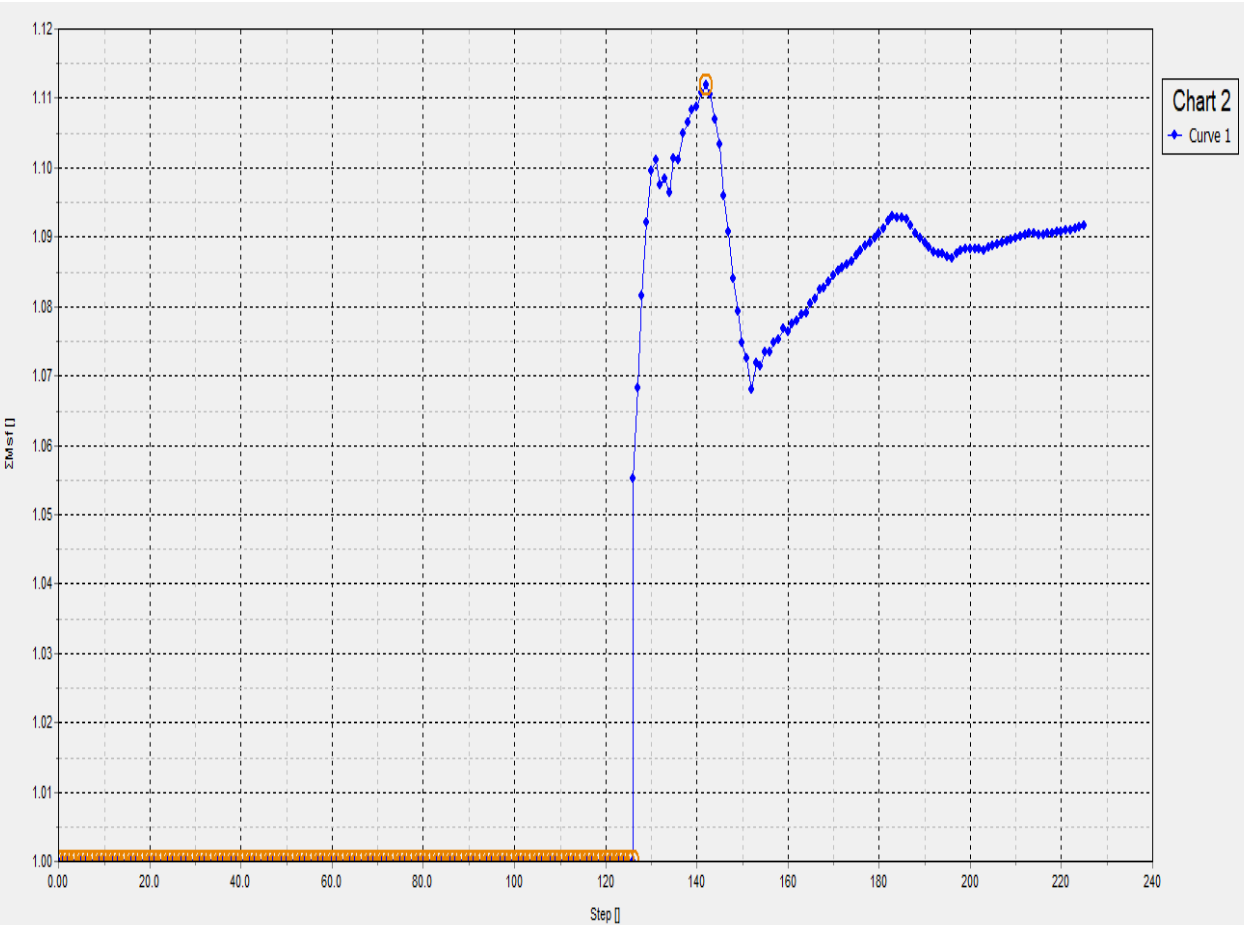

Figure 6-9 Plaxis Curve showing Fos generated for SS4 at dry state

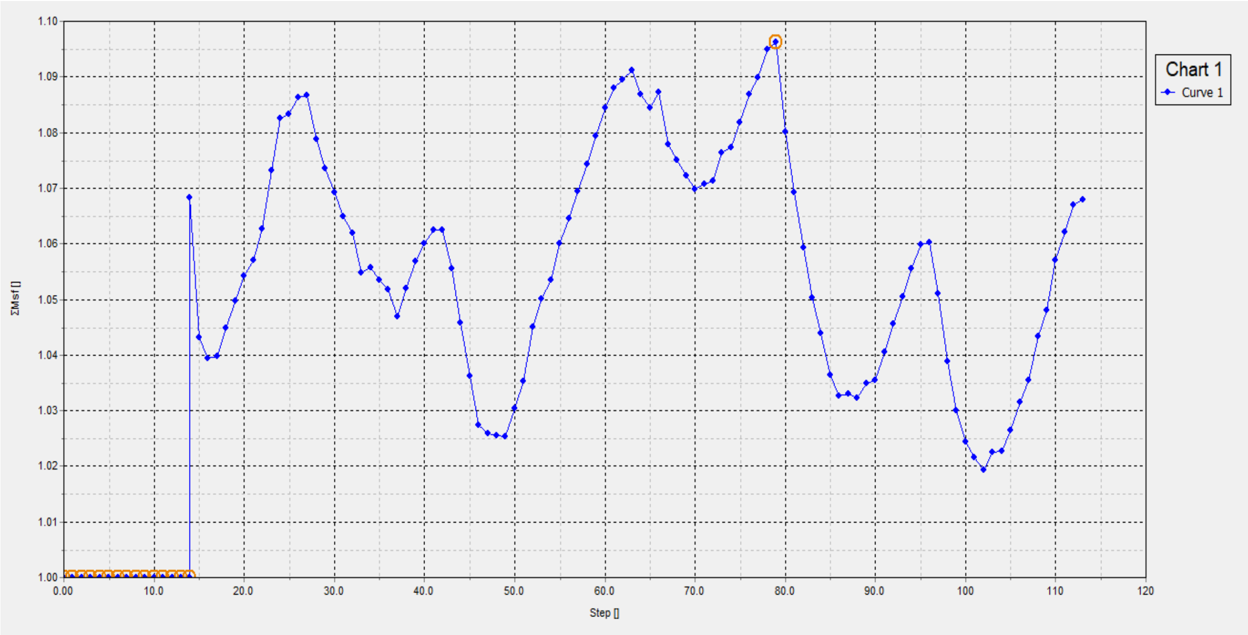

Figure 6-10 Plaxis Curve showing Fos generated for SS4 at Wet state

Table 6.3 Factor of safety and slope status under different anticipated condition of soil slope section SS1, SS2, SS3 and SS4.

Sample	ɣsat (KN/M^3)	ɣdry	C (KN/M^2)	Ø°	E (Mpa)	V	PLAXIS	Stability Condition
SS1	19.39	14.27	21.36	28.69	12000	0.3	1.369	Stable
							0.902	Unstable
SS2	21.6	17.4	11.65	33.65	18000	0.25	1.151	Stable
							0.895	Unstable
SS3	20.32	18.5	9.65	34.68	17000	0.25	1.101	Stable
							0.889	Unstable
SS4	18.5	16.59	15.23	29.05	13000	0.3	1.196	Stable
							0.902	Unstable

6.3 Comparison of LEM and FEM

The LEM and FEM are compered using results from the slide and plaxis software. Outputs show that a slightly higher FS is obtained in LEM than FEM. It has been seen that results from FEM (plaxis software) give more information about the failure surface i.e., the stress, strain, deformation, and displacements at any point in the slope section. Whereas the LEM (slide) gives only uniform FS along the failure surface. The deformation in FEM (plaxis) indicates that failure can occur in any shape and the movement can vary at each point of the slope section as shown in Figure 6.6. This disproves the assumptions of uniform FS along the slip surface and rigid movement above the failure surface in LEM. Besides, the strength reduction method provides a more realistic estimation of FS and slope failure (i.e., non-convergence of algorism in a specified iteration indicates failure as shown in Figure 6.4) compared with the LEM (i.e., searching of the minimum FS in the predefined shape of failure surface). Figures 6.6 and 6.7 show the total displacements at each finite element node and the relative shear stress (i.e., the proximity of the stress points to the Mohr-Coulomb failure envelop) from FEM which is not accessible in LEM. On the other hand, Figure 6.8 shows the FS and slip surface in LEM using different approaches. The result shows that the value of FS also varies within LEM depending on the method use

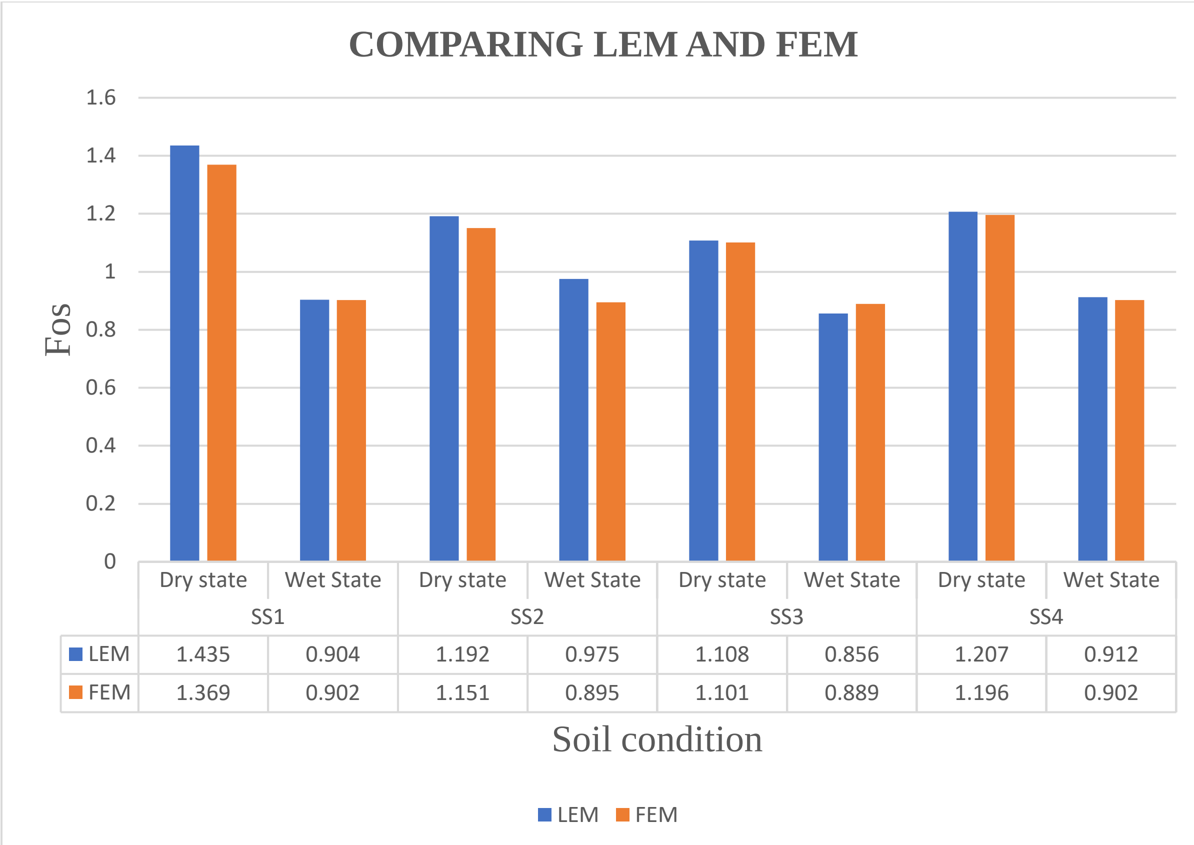

Figure 6-11 Factor of safety comparison with LEM and FEM at different conditions

6.4 Remedial Measures

According to (Popescu, 2001), Correction of an existing landslide or the prevention of a pending landslide is a function of a reduction in the driving forces or an increase in the available resisting forces. Any remedial measure used must involve one or both of the above parameters.

Selection of an appropriate remedial measure depends on: a) engineering feasibility, b) economic feasibility, c) legal/regulatory conformity, d) social acceptability, and e) environmental acceptability.

Engineering feasibility involves analysis of geologic and hydrologic conditions at the site to ensure the physical effectiveness of the remedial measure. An often-overlooked aspect is making sure the design will not merely divert the problem elsewhere. Economic feasibility takes into account the cost of the remedial action to the benefits it provides. These benefits include deferred maintenance, avoidance of damage including loss of life, and other tangible and intangible benefits. Legal-regulatory conformity provides for the measure meeting local building codes, avoiding liability to other property owners, and related factors. Social acceptability is the degree to which the remedial measure is acceptable to the community and neighbors. Some measures for a property owner may prevent further damage but be an ugly eyesore to neighbors. Environmental acceptability addresses the need for the remedial measure to not adversely affect the environment. De-watering a slope to the extent it no longer supports a unique plant community may not be environmentally acceptable solution. Engineering countermeasures for reducing landslide risk are observable; these generally involve the use of slope stabilization methods such as benching, improvement of subsurface drainage, construction of retaining structures, and reinforcement of slopes.

Modification of slope geometry: This can involve reshaping the slope by adjusting its angle or creating terraces to reduce the overall slope height and enhance stability.

Providing drainage: Effective drainage systems should be implemented to manage surface and subsurface water. This can include surface drainage channels, subsurface drains, and erosion control measures to prevent water accumulation and minimize the risk of slope failure.

Engineering retaining structures: Depending on the slope conditions, retaining structures such as retaining walls or gabion walls should be required to provide additional support and stability to the slope. Internal soil reinforcement: Measures such as soil nailing, ground anchors, or geosynthetic reinforcements can be employed to strengthen the soil within the slope and improve its stability. By implementing these recommended measures, the stability of the critical slope sections in the study area can be effectively maintained, reducing the risk of slope failure and ensuring the safety of the area.

In this study, appropriate remedial measures were recommended based on the actual stability condition of the slope, determined through numerical evaluation and field investigation.

6.4.1 Modification of Slope Geometry

The study area slope is moderately steep to very steep which causes an increase in tangential gravity force due to maximum value of shear stress there by favors slope instability. The geometry of the slope is one of the most important parameters which effects of its stability from the landslide of the study area (Raghuvanshi T. K., 2017); (Shiferaw, 2021)). For this study, according to the analysis results the slope height and slope angle are critical elements influencing the stability conditions of the studied slopes. Considering these factors, mitigation measures to reduce their instability were suggested. Slope stability assessment for remedial works was conducted using LEM method with the applications slide software (slide 6 Rocscience 2004). The slope was assessed for its stability in term of factor of safety (FOS). The remedial measures for slope modification geometry were proposed such as the effect of slope height, slope angle and benching slope was evaluated using slide 6 software (Popescu, 2001). The slope geometry can be changed by reducing a slope angle, slope height and removing material from the landslide of the study area (Raghuvanshi T. K., 2017); (Shiferaw, 2021).

6.4.1.1. Reducing of Slope Angle

The stability of slopes is affected by slope angle and height as discussed in various studies (Shiferaw, 2021); (Chatterjee, D., & Murali Krishna, A., 2019); (Anbalagan, 1992); (Raghuvanshi T. K., 2014). The numerical models were conducted for different slope heights and angles, and the results indicate that decreasing slope angle and height tend to increase the factor of safety. It is important to note that there is an inverse relationship between slope angle/height and factor of safety. The evaluation results were generated using slide 6 software (Rocscience, 2004) and presented in Figures 6.12

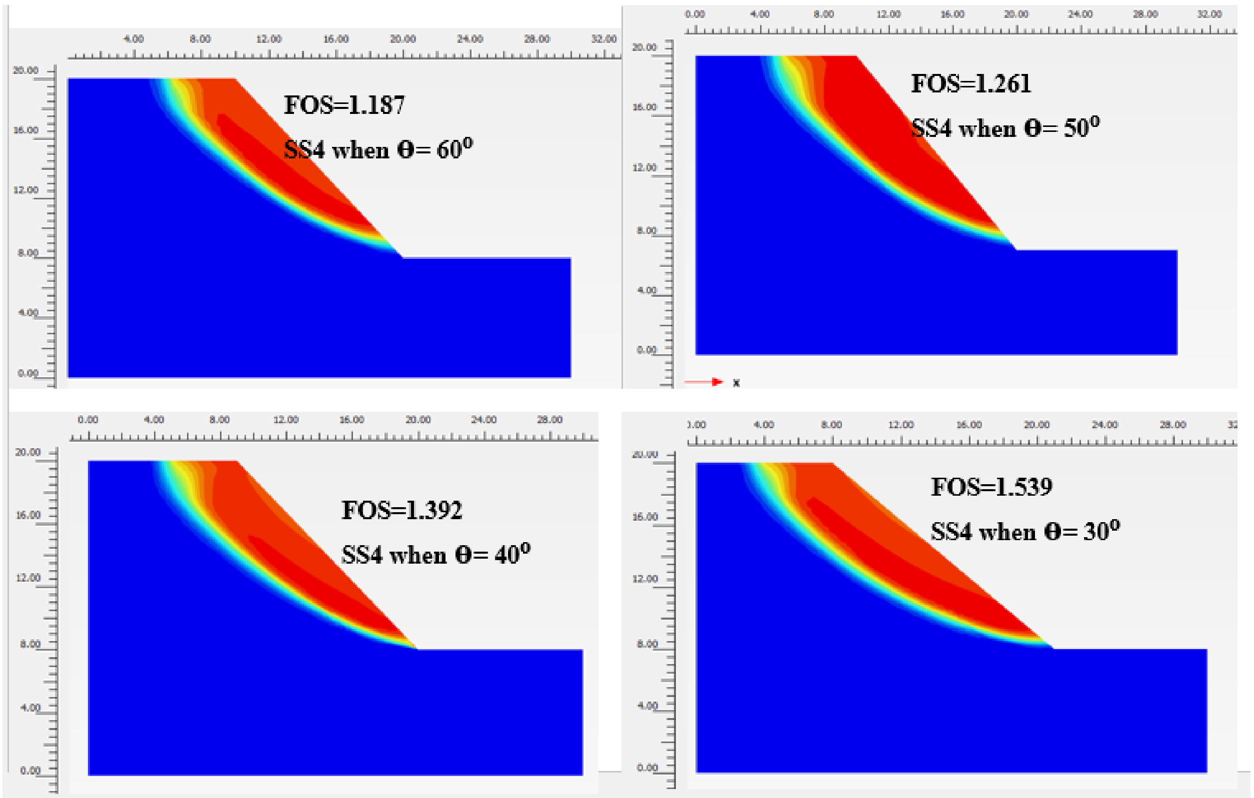

Figure 6-12 Effect of slope angle on factor of safety of slope analysis using slide software for SS1 at 60º, at 50º, 40 and 30º Respectively

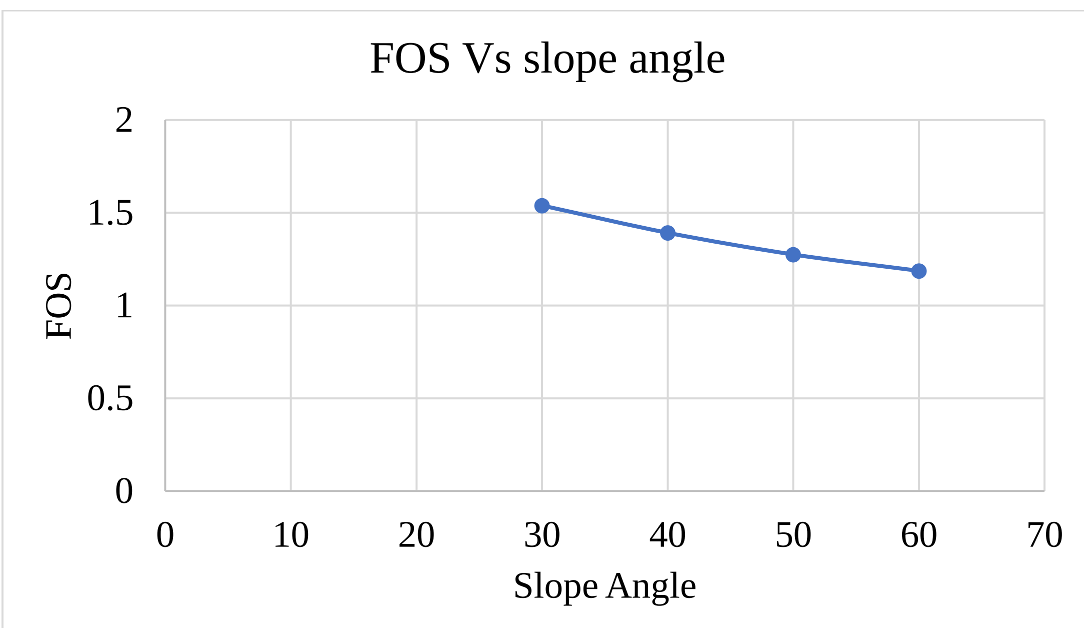

Figure 6-13 Graph of factor of safety Vs slope angle on of slope stability analysis using PLAXIS software for SS1.

6.4.1.2. Benching the Slope

Through the utilization of benching, a single steep slope can be transformed into multiple lower ones (Abramson, Lee, Sharma, & Boyce, 2002). This technique is especially useful in changing a very steep slope into a gentler one on a single slope profile. In this study, the focus was on unstable soil slope section 1 (SS1) and the effect of benching on slope cut, with the factor of safety analyzed using slide 6 software (Rocscience, 2004) under the static wet condition. As a result, the effect of slope bench on the safety factor was determined for one, two, and three bench numbers. Fig.6.12 demonstrates the slide software analysis results which was plotted and presented.

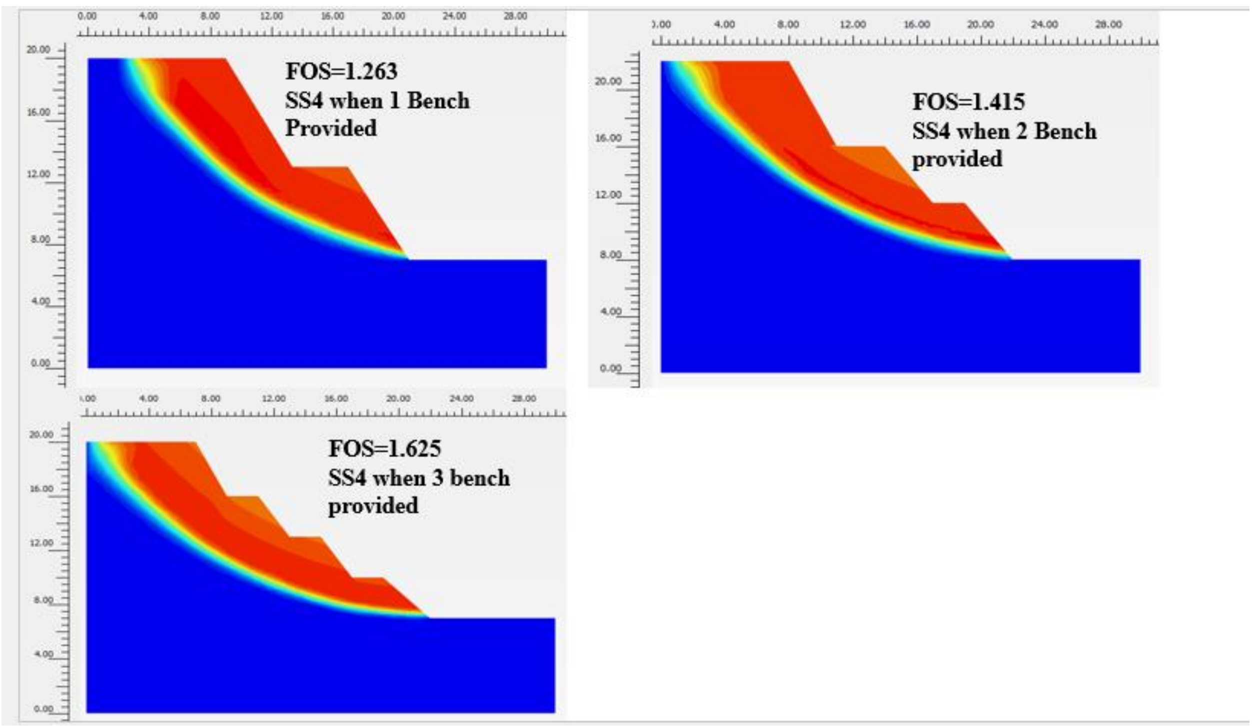

Figure 6-14 Effect of benching slope face on factor of safety for slope stabilization of SS1 using Plaxis software.

Table 6.4 : FOS Vs Bench number

No. of Bench	FOS
1	1.263
2	1.415
3	1.625

The results of this analysis, as shown in Fig.5.26, demonstrate that the factor of safety increases as the number of benches increases. This highlights the strong and direct relationship between the bench number in slope and the factor of safety, indicating that increasing benching can be important for slope stabilizations. Ultimately, the slope was found to be most stabilized when 2 and 3 benches were performed, with an increase in bench number leading to improved performance in stabilizations.

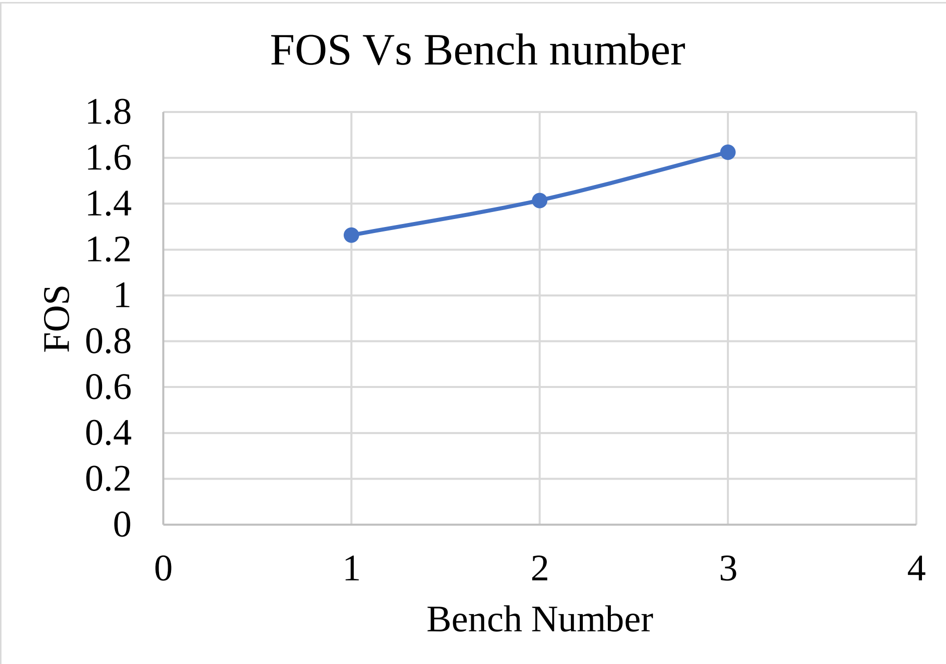

Figure 6-15 Graph of benching slope face on factor of safety for slope stabilization of SS1.

6.4.2 Soil nail

Soil nailing is a method of reinforcement that utilizes passive inclusions that will be mobilized if and when movement occurs. It is usually done to retain excavations and stabilize slopes by creating an in-situ, reinforced soil mass.

The design an application follows the procedures of (Lazarte & Helen Robinson, 2015)

Soil Nail Spacing: Soil nails are installed in a grid pattern. The horizontal nail spacing, SH, is often the same as the vertical nail spacing, SV. Nail spacing in both directions generally ranges from 4 to 6 ft and occasionally up to 6.5 ft, and is routinely selected at 5 ft. The spacing can be checked such that SH × SV is less than approximately 36 to 42 ft2. The first row of nails should not be installed deeper than approximately 2 to 3.5 ft from the top edge of the wall to reduce the potential for instability of the upper excavation lift and to reduce cantilever effects on the temporary facing. The lowermost row of nails should be installed about 2 to 3 ft above the base of the excavation. These requirements are the result of the limited ability of the facing to work as a cantilever at the top and bottom of the wall. However, these limits may be adjusted for project-specific conditions, and when based on suitable analysis. The engineer should consider adopting uniform nail spacing to simplify construction and quality control. However, nail spacing needs to be adjusted near the top and bottom of walls and where the grade changes. It may be difficult to obtain uniform nail spacing along the vertical edges of wall corners, where a wall ends and around existing utilities or underground structures. It is commonly more practical to install upper nails along one or two rows parallel or sub-parallel to the top of the wall, and install other nails in between, not exceeding a maximum spacing of approximately 6 ft. A minimum soil nail spacing of approximately 3.5 ft must also be specified so the potential for drilling into previously installed nails due to drilling deviations will be reduced. Further, close spacing of nails may result in stress overlap in the load transfer similar to closely spaced piles. Exceptions to this guidance may arise in areas where concentrated loads (such as those from existing foundations) are applied above or immediately behind the soil nail wall.

Soil Nail Inclination: Soil nails are installed at 10 to 20 degrees from the horizontal, and most commonly at 15 degrees. The grout can flow at these inclinations from the bottom of the drill hole to the head. Grout generally can fill the hole without leaving air pockets for typical drill-hole dimensions and grout mixes. Nail inclination angles less than 10 degrees should be avoided to prevent creating voids in the grout and an extended "bird's beak" at the nail head. Voids can reduce the pullout resistance and decrease corrosion protection.

Soil Nail Length: To develop a preliminary cross section for analysis, the soil nail length can be estimated to be approximately 0.7H, where H is the wall height. Longer nails will be needed: (i) in weak soils; (ii) where deep-seated critical slip surfaces exist; (iii) when large surcharge loads exist behind the wall; and/or (iv) when a rising backslope exists behind the wall. Battered walls typically result in slightly shorter nails. A batter of 10 percent reduces the soil length requirements by approximately 10 to 15 percent when compared to walls with vertical faces, with all other conditions equal. If it is determined with well-selected parameters and appropriate stability analysis that nail lengths would have to be greater than about 1.2H, this result may suggest that ground conditions are not favorable for soil nail walls. On the other end of the range, nail lengths less than 0.5H will not likely satisfy sliding stability requirements. Nail lengths less than approximately 0.6H are rare.

Distribution of Soil Nail Lengths in Elevation: All nails in a wall can have uniform length for simplicity. This pattern is common in many walls. However, design engineers must take into account other considerations related to a uniform versus a non-uniform soil nail length pattern.

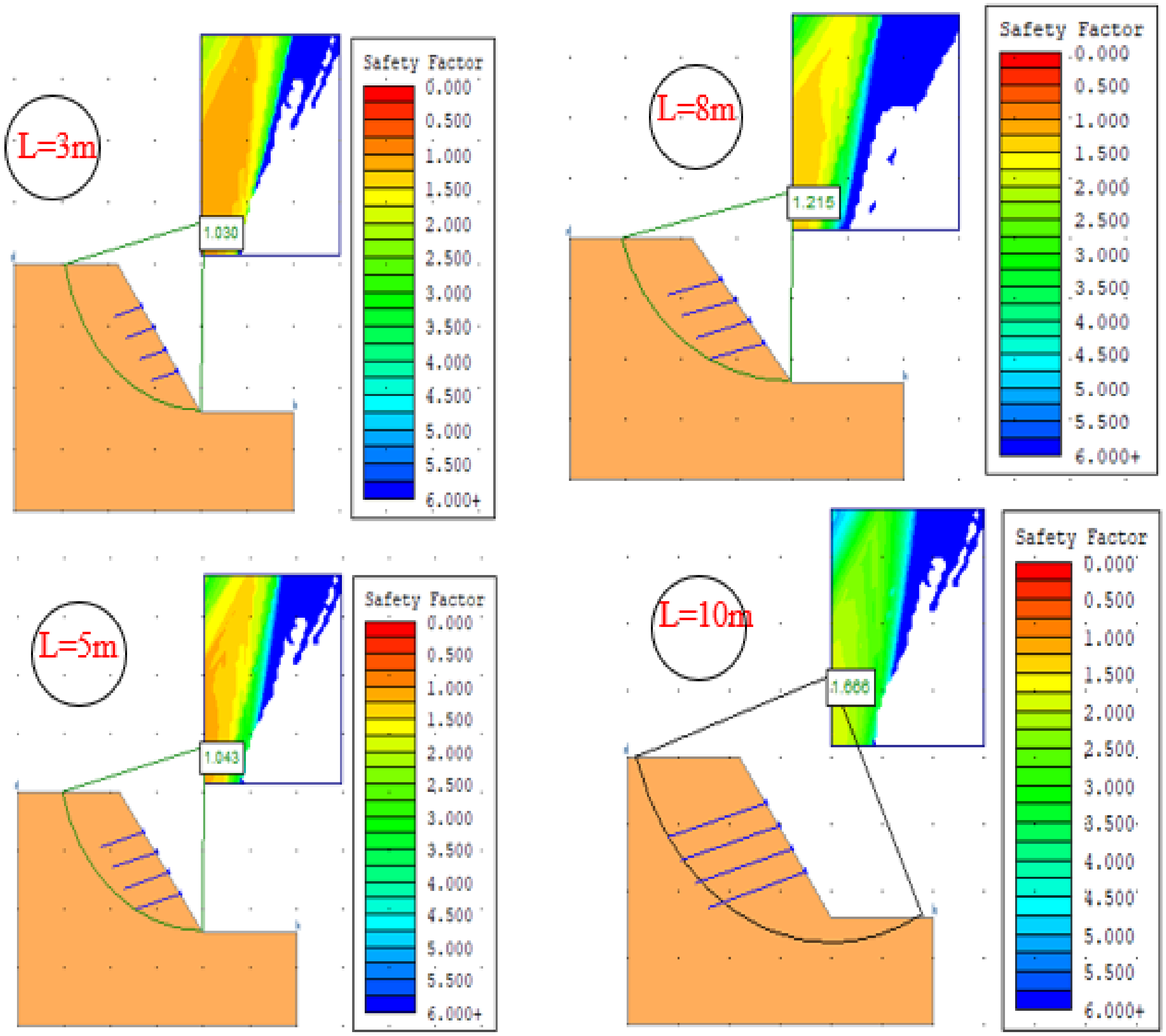

Figure 6-16 Effect of Soil nailing length face on factor of safety for slope stabilization using slide software.

Table 6.5: FOS Vs Soil nailing length

Nailing length (m)	Orientation	Spacing (m)	FOS
3	15°	2.2	1.03
5	15°	2.2	1.043
8	15°	2.2	1.241
10	15°	2.2	1.666

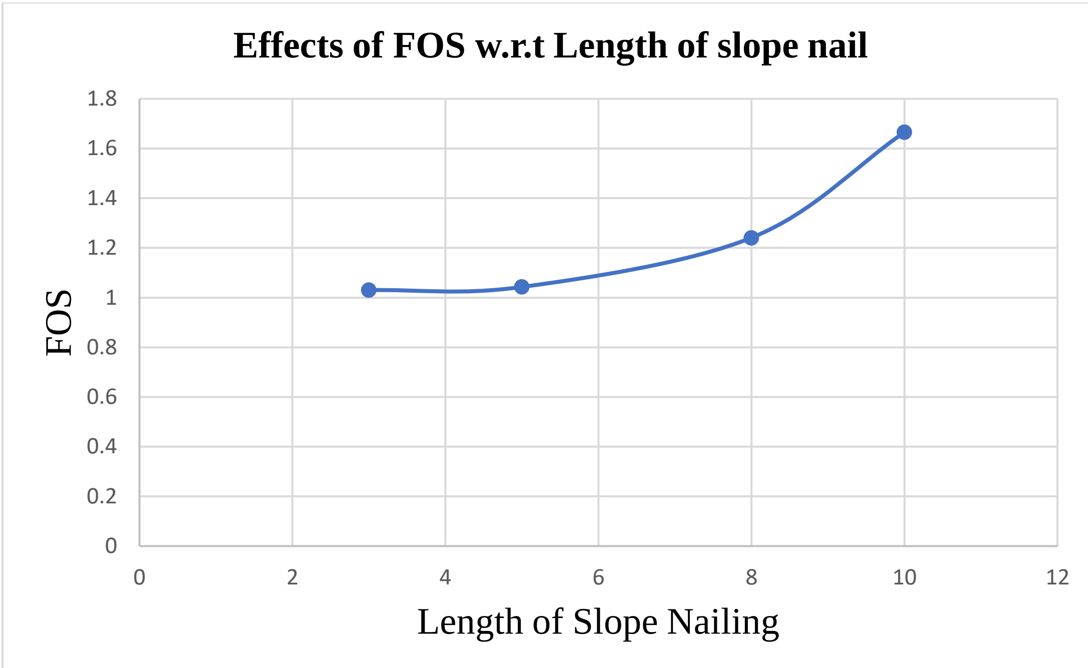

Figure 6-17 Relation of FOS Vs Slope nailing

SS4 Remedial Measures

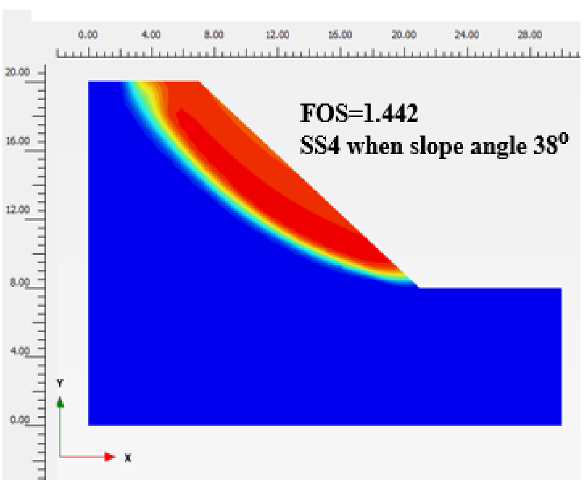

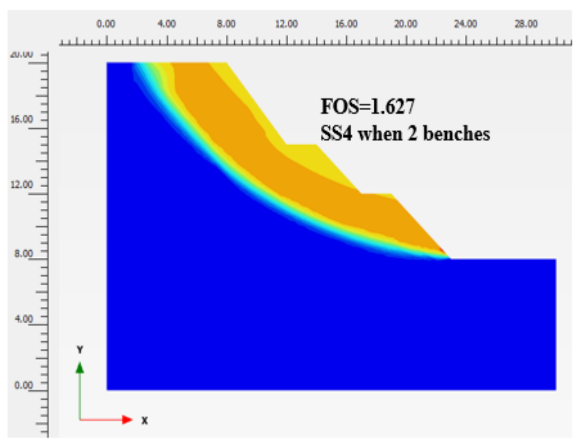

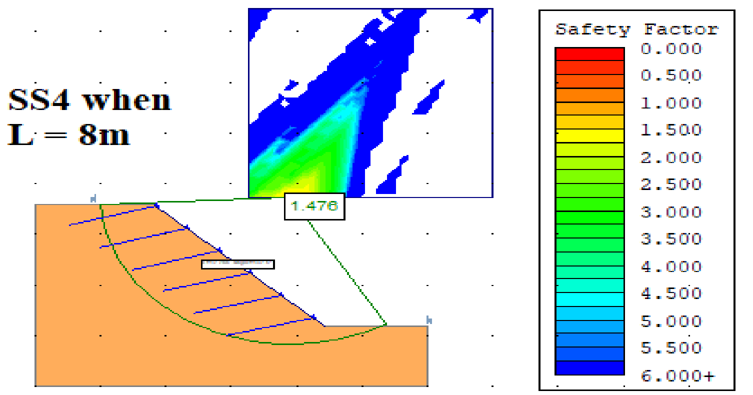

Figure 6-18 FOS of SS4 when slope angle 38o, 2 Benches, and soil nailing length is 8m are provided respectively.

SS2 Remedial Measures

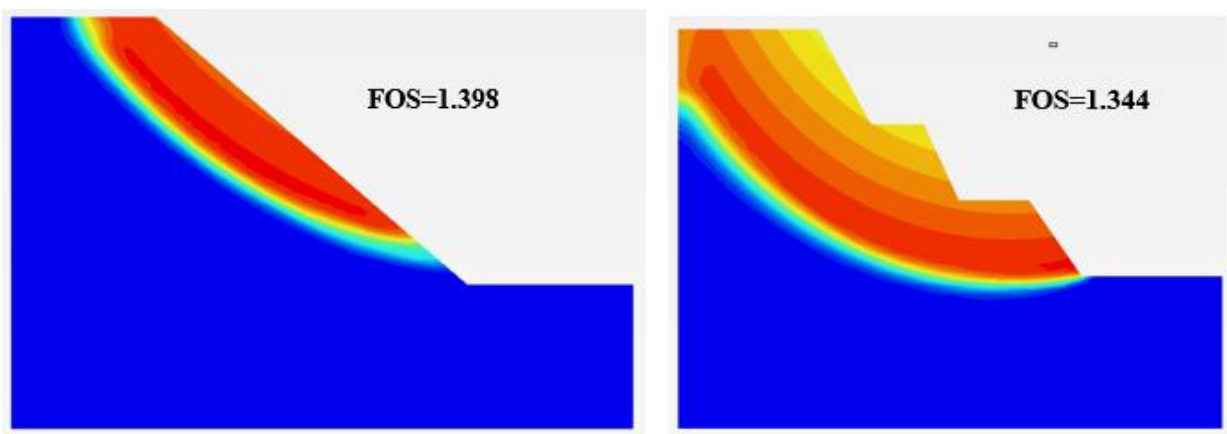

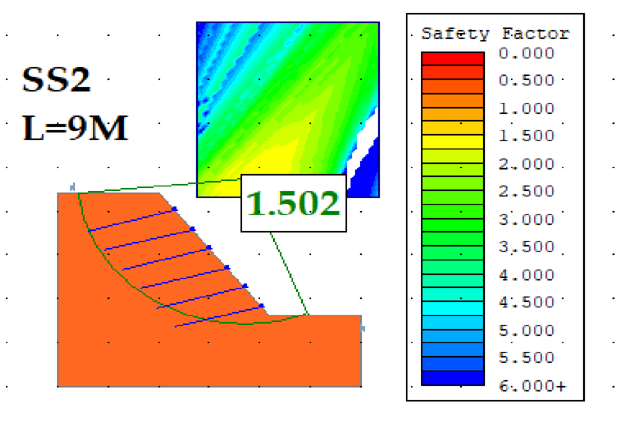

Figure 6-19 FOS of SS2 slope angle 43o, 2 Benches and when soil nailing length is 9m are provided respectively.

Table 6.6: Summery of FOS using 2 Bench for SS1, SS2, SS3 and SS4

Slope section	FOS before remedial	Bench Provided	FOS after Remedial
SS1	0.902	2	1.415
SS2	0.895	2	1.344
SS3	0.889	2	1.314
SS4	0.902	2	1.627

Table 6.7: Summery of FOS using slope angle reduction for SS1, SS2, SS3 and SS4

Slope section	FOS before remedial	Slope Angle	FOS after Remedial
SS1	0.902	30^o	1.539
SS2	0.895	43	1.398
SS3	0.889	40	1.382
SS4	0.902	38^o	1.442

Table 6.8: Summery of FOS using different Slope nailing length for SS1, SS2, SS3 and SS4

Slope section	FOS before remedial	Soil Nail length =0.7H	soil nail inclination	Soil Nail Spacing	FOS after Remedial
SS1	0.902	10	15^o	2.2	1.666
SS2	0.895	9	15^o	2.2	1.502
SS3	0.889	9	15^o	2.2	1.547
SS4	0.902	7	15^o	2.2	1.476

6.4.3. Providing Drainage

To address the active landslide problems, it is crucial to implement effective remedial measures, such as providing drainage for both surface and subsurface water (Panigrahi, 2021). The absence of drainage in the studied area makes it susceptible to erosion and instability during heavy rainfall. To mitigate these issues, it is recommended to install surface drainage along the top side of the slide area, running from east to west. This will help divert excess water away from the slope, reducing the potential for erosion and instability.

Additionally, limiting runoff is essential to reduce the continuity of slope failure in selected critical soil slope sections across the road. Implementing measures such as terracing, contour trenches, or retention ponds can help control and manage runoff, preventing it from accumulating and further destabilizing the slope. By providing effective drainage systems and managing runoff, the risk of erosion and slope failure can be significantly reduced, ensuring the stability and safety of the road and surrounding areas.

6.4.4. Providing Engineering Retaining Structures

It's important to manage soil movement along the slope for safety reasons. One way to do this is by building gabion on one side of the slope. Additionally, supplying embankments along the failed slope can help create a stable slope at critical soil slope sections. To further mitigate risks, several retaining structures such as gravity retaining walls, reinforced earth retaining structures, rock slope face retention nets, and rock fall stopping systems are recommended. Protective rock measures against erosion can also be applied to the slope rock to reduce the probability of rock failures onto the road. While some rock slope sections in the study area are stable, others may require the removal of loose blocks to prevent future rock falling or sliding. To prevent this from happening, retention measures such as engineered ditches, wide shoulders, berms, steel barriers, and net should be provided along with retaining walls.

6.4.5. Soil Bioengineering: Bioengineering is defined as the use of any form of vegetation, whether a single plant or a collection of plants, as an engineering material. Similarly, biotechnical engineering refers as techniques where vegetation is combined with inert structures which benefits of both the vegetative and non-vegetative components of the scheme. The vegetation is carefully selected for the function it can serve in stabilizing unstable slopes and for its suitability to the sites. Soil bioengineering uses living vegetation purposely arranged and imbedded in the ground to prevent shallow mass movement and surficial erosion. However, the use of soil bioengineering in itself is limited to stable slope masses. Combining this highly erosive system with geosynthetic reinforcement produces a very durable, low maintenance structure with exceptional aesthetic and environmental qualities (Berg, Christopher, & Samtani., 2009).

Appropriately applied, soil bioengineering offers a cost-effective and attractive approach for stabilizing slopes against erosion and shallow mass movement, capitalizing on the benefits and advantages that vegetation offers. The value of vegetation in civil engineering and the role woody vegetation plays in the stabilization of slopes has gained considerable recognition in recent years (Gray and Sotir, 1995). Woody vegetation improves the hydrology and mechanical stability of slopes through root reinforcement and surface protection. The use of deeply-installed and rooted woody plant materials, purposely arranged and imbedded during slope construction offers:

CHAPTER 7. CONCLUSION AND RECOMMENDATION

6.1 CONCLUSION

In conclusion, the present study successfully utilized various methods to assess the stability of slopes along the road corridor from Quni to Bedesa town in the southeastern plateau of Ethiopia. Through reconnaissance studies and extensive field surveys critical rock and soil slope sections prone to failure were identified. Extensive field work, laboratory tests, and in-situ measurements provided valuable data on the geological and slope conditions. The limit equilibrium, and finite element methods were employed to analyze slope stability under different loading conditions. The results indicated that the critical slope sections have been evaluated and their stability assessed. This information will play a crucial role in ensuring the safe and effective management of the road corridor.

Based on the comprehensive data acquisition and analysis methods used in this study, several key findings can be concluded.

- The study area exhibits heavily fractured and weathered rock masses, with two critical rock slopes and two critical soil slope sections identified.
- The rock qualities, determined by GSI values identified the two-rock slope section were poor. Based on the in-situ tests, it was determined that most of the rocks along the road sections have medium strength basalt rock units.
- Consequentially, finite element and limit equilibrium stability analyses methods were performed on two non-structural critical rock slope sections. From FEM analysis results SS3 were stable under static dry, dynamic dry, and static wet conditions but unstable under dynamic wet condition. In similar Manner SS4 were stable under static dry and static wet condition but unstable under dynamic dry and dynamic wet conditions.
- Additionally, the study conducted gradation analyses and Atterberg limit tests on the soils in the slope sections. The results indicated that the soils have medium to high plasticity index and a high liquid limit. The moisture content tests revealed a range of 11.5% to 20.7% for the soils in the study area.
- Furthermore, the analysis of soil slope sections using both the Limit Equilibrium Method (LEM) and Finite Element Method (FEM) showed that the soil slopes were stable under static dry and dynamic dry conditions and static wet, but unstable under dynamic wet

conditions. This implies the effect of rainfall factor in the study area is critical factor for slope instability along road sections.

- Comparing the factors of safety (FOS) obtained from slide 6 software and PLAXIS 2D software; it was found that LEM provided a slightly higher FOS. The analysis also revealed that the FEM approach provides more comprehensive information on the failure surface, including stress, strain, deformation, and displacement at any point in a slope section.
- Finally, the remedial measures analysis identified that flattening the slope angle, lowering the slope angle, and benching the slope section have a significant influence on slope stability.

6.2. Recommendation

Based on the outcome and findings of the present study, the following recommendations were forwarded.

- Based on the present study, it has been concluded that certain rock slope sections in the study area are only partially unstable under certain conditions. To mitigate further failures and stabilize the slope, it is recommended to implement shotcrete, rock bolts, and retaining walls with anchors.
- Combining two or three methods with engineering and economic considerations is highly recommended. Reshaping bench and slope geometry is also recommended to mitigate instability problems caused by the slope height and slope angle.
- Further study is required to identify the effect of surface and groundwater on stability condition; particularly the study area is highly susceptible to slope failure during the rainy season.
- Further geotechnical investigations, geophysical surveys, and topographic surveys should be performed to better evaluate the influence of critical factors for slope instability. Additionally, a well-designed drainage system is necessary for the area, as it is highly affected by poor drainage due to its undulated landscape.
- Finaly the road under study area has many problems as shown (fig 7.1) related to landslide downstream of the road due to mountainous terrain of the road section and heavy rainfall of this summer. So that these failures need more investigation in terms of budget and instrumentation. Due to that these section needs more field investigations and Solution.

Figure 7-1 Qune-Bedesa Road section failure in July 2024 which needs Further explorations.

References

Abbate, A., Longoni, L., Ivanov, V. I., & Papini, M. (2019). Wildfire impacts on slope stability triggering in mountain areas. *Geosciences, 9*(10), 417.

Abramson, L. W., Lee, T. S., Sharma, S., & Boyce, G. M. (2002). *Slope Stablity and stablization technique* (Vol. Volume 2). New York: John wily and Sons.

Albataineh, N. (2006). *SLOPE STABILITY ANALYSIS USING 2D AND 3D METHODS [Master's thesis,University of Akron].* Akron: University of Akron and OhioLINK.

Ambassa, Z., & Amba, J. C. (2022). Towards an Advanced New Emerging Method of Determination of Mohr–Coulomb Parameters of Soils from at the Oedometric Test: Case Study-Lateritic Soils of Cameroon. *Mathematical Problems in Engineering, 2022*.

Ameratunga, J., Sivakugan, N., & Das, B. M. (2016). Correlations of soil and rock properties in geotechnical engineering.

Anbalagan, R. (1992). Landslide hazard evaluation and zonation mapping in mountainous terrain. . *Engineering geology*, *32*(4), 269-277.

Ayalew, L. (1999). The effect of seasonal rainfall on landslides in the highlands of Ethiopia. *Bull Eng Geol env*, 58, 9–19.

Aydan, O. (2016). Large rock slope failures induced by recent earthquakes. *Rock Mechanics and Rock Engineering*, *49*(6), 2503-2524.

BAYOU, N. B. (2020). EVALUATION OF SLOPE STABILITY CONDITIONS BY NUMERICAL ANALYSIS, A CASE OF OTOLO-SAWLA ASPHALT ROAD PROJECT, SOUTHERN PART OF ETHIOPIA (Doctoral dissertation).

Bekele, A., & Meten, M. (2022). Modeling rock slope stability using kinematic, limit equilibrium and finite-element methods along Mertule Maryam–Mekane Selam road, central Ethiopia. *Modeling Earth system and Enviroment*, 1-27.

Bekele, A., & Meten, M. (2022). Modeling rock slope stability using kinematic, limit equilibrium and finite-element methods along Mertule Maryam–Mekane Selam road, central Ethiopia. *Modeling Earth Systems and Environment*, 1-27.

Berg, R. R., Christopher, B. R., & Samtani., N. C. (2009). *Design and Construction of Mechanically Stabilized Earth Walls and Reinforced Soil Slopes – Volume I.* Washington DC: Ryan R. Berg & Associates, Inc.

BGS. (2024, 9 11). *British geological survey*. Retrieved from Understanding our world: https://www.bgs.ac.uk/discovering-geology/earth-hazards/landslides/how-to-classify-a-landslide/

Caroles, L. (2023). Probabilistic Seismic Hazard Analysis on Pavement Failure Restoration; Case Study of Sorong–Makbon Road. Sustainability. *15*(7), 5994.

Casagrande, A. (1932). Research of Atterberg Limits of Soils Public Roads. *13*(8), 121-213.

Chango, Z., Huang, F., Huang, J., Jiang, S. H., Zhou, C., & Zhu, L. (2021). Experimental study of the failure mode and mechanism of loess fill slopes induced by rainfall. *Engineering Geology, 280*. doi: 105941

Chatterjee, D., & Murali Krishna, A. (2019). Effect of slope angle on the stability of a slope under rainfall infiltration. *Indian Geotechnical Journal*, *49*(6), 708-717.

Chen, H., Qin, S., Xue, L., & Xu, C. (2021). Why the Xintan landslide was not triggered by the heaviest historical rainfall: Mechanism and review. *Engineering Geology, 294*, 106379.

Christian, J. T. (2004). Geotechnical engineering reliability: How well do we know what we are doing? *Journal of geotechnical and geoenvironmental engineering, 130*(10), 985-1003.

D.V. Griffiths, P. L. (1999). Slope stability analysis by finite elements. *Geotechnique, 49*(3), pp. 387-403.

Das, B. M. (2002). Soil Mechanics Laboratory Manual. *Oxford University Press, New York, 6th Edition*, 8-9.

Dietze, M., Bel, R., Ozturk, U., Cook, K. L., Andermann, C., & Beer, A. R. (2022). .More than heavy rain turning into fast-flowing water–a landscape perspective on the 2021 Eifel floods. *Natural Hazards and Earth System Sciences*, *22*(6), 1845-1856.

Diro, G. A., Kabeta, W. F., & Teshager, D. K. (2020). Assessments of Geotechnical Conditions and Slope Stability Analysis: Case Study in Gedo town, Ethiopia. *Int. J. Sci. Res. Eng. Trends*, *6*(3), 1250-1258.

El Jazouli, A., Barakat, A., & Khellouk, R. (2022). Geotechnical studies for Landslide susceptibility in the high basin of the Oum Er Rbia river (Morocco). *Geology, Ecology, and Landscapes, 6*(1), 40-47.

Eleyas, A. L. (2016). Discussion on the Analysis, Prevention, and Mitigation Measures of Slope Instability Problems: A case of Ethiopian Railways. *Electronic Journal of Geotechnical Engineering, (21.12), ,* pp 4101-4119.

Fathiyah, H. &. (2017). *Parametric Study on the Effect of Rainfall Pattern to Slope Stability.* University of Indonesia.: Department of Civil Engineering, .

Fentahun. A. (2020). *SLOPE STABILITY ANALYSIS AND EVALUATION OF ROAD CUT SLOPE.* Adama, Ethiopia: Adama Science and Technology University.

Gallage, C., Abeykoon, T., & Uchimura, T. (2021). Instrumented model slopes to investigate the effects of slope inclination on rainfall-induced landslides. *Soils and foundations, 61*(1), 160-174.

Gao, W., Yang, H., Hu, R. W., & Hu, R. (2022). Soil–rock mixture slope stability analysis bymicrotremor survey and discrete element method. *Bulletin of Engineering Geology and the Environment, 81*(3), 1-17.

Getachew, N., & Meten , M. (2021). Weights of evidence modeling for landslide susceptibility mapping of Kabi-Gebro locality, Gundomeskel area, Central Ethiopia. *Geoenvironmental Disasters, 8*(1), 1-22.

Gidday, B. G., Ayothiraman, R., Ramaiah, B. J., & Ramana, G. V. (2023). Physical and numerical modeling of rainfall triggered shallow landslides in central highlands, Ethiopia. *Bulletin of Engineering Geology and the Environment, 82*(7), 239.

Gutierrez-Martin, A. (2020). A GIS-physically-based emergency methodology for predicting rainfall-induced shallow landslide zonation. *Geomorphology, 359,* 107121.

Hamza, T., & Raghuvanshi, T. K. (2017). GIS based landslide hazard evaluation andzonation–a case from Jeldu District, central Ethiopia. *Journal of KingSaudVUniversity-Science, 29*(2).

Hansen, A. (1984.). Landslide hazard analysis. *Slope Instability* (pp. 523-602). New York: John Wiley.

Havaej, M., & Stead, D. (2016). Investigating the role of kinematics and damage in the failure of rock slopes. *Computers and Geotechnics, 78*, 181-193.

He, Y., Cai, Z., Wang, F., Guo, C., Xiang, B., & He. (2023). Numerical investigation on slope stability influenced by seismic load and discontinuity with a continuous-discontinuous method. *Bulletin of Engineering Geology and the Environment, 82*(3), 70.

Highland, L. M., and Bobrowsky, Peter,. (2008). *The landslide handbook - A guide to understanding landslides:*. Reston, Virginia, U.S: Geological Survey Circular 1325, 129 p.

Hossain, M., Islam, M. A., Badhon, F. F., & Imtiaz, T. (2021). Hydrometer Analysis. *Properties and Behavior of Soil-Online Lab Manual*.

Ibrahim, M. B., Salisu, S. A., Musa, A. A., Abussalam, B., & Hamza, S. M. (2022). Framework for the identification of shallow ground movement in modified slopes (an expert opinion). *In IOP Conference Series: Earth and Environmental Science , 106*(1), 12055.

Kabeta, W. F., Tamiru, M., Tsige, D., & Ware, H. (2023). An integrated geotechnical and geophysical investigation of landslide in Chira town, Ethiopia. *Heliyon, 9*(7).

Kazmi, D., Qasim, S., Harahap, I. S., Baharom, S., Mehmood, M., Siddiqui, F. I., & Imran, M. (2017). Slope remediation techniques and overview of landslide risk management. *Civil engineering journal, 3*(3), 180-189.

Khan, M., & Wang, S. (2021, May 17). Stability Analysis to Correlate Shear Strength with Slope Angle and Shear Stress by Considering Saturated and Unsaturated Seismic Conditions. pp. Appl. Sci. 2021, 11, 4568. https://doi.org/10.3390/app11104568.

Kumar, M. (2022). M. Factors Affecting Slope Stability of an Opencast Mine: A Brief Study. *Int. J. Innov. Sci. Res. Technol, 7*, 878-882.

Lazarte, C. A., & Helen Robinson, e. (2015). *GEOTECHNICAL ENGINEERING CIRCULAR NO. 7 OIL NAIL WALLS - REFERENCE MANUAL.* Washington DC: Schnabel Engineering, Rockville, MD 20850.

Liang, Y. C. (2023). Shear behavior of bedding fault material on the basal layer of DGB landslide. *Scientific Reports*, 13(1), 233.

Luna, P., Dakoulas, P., Zheng, W., Çetin, K. O., Perlea, M., Kung, G. T., & Barani, S. (2010). General Report—Session 4.

Mebrahtu, T. K., Heinze, T., Wohnlich, S., & Alber. (2022). Slope stability analysis of deep-seated landslides using limit equilibrium and finite element methods in Debre Sina area, Ethiopia. *Bulletin of Engineering Geology and the Environment, 81*(10), 403.

Mebrahtu, T., Banning, A., Girmay, H. E., & Wohnlich, S. (2021). The effect of hydrogeological and hydrochemical dynamics on landslide triggering in the central highlands of Ethiopia. *Hydrogeology Journal*, 29(3), 1239-1260.

Meko, L. M. (2023). Road cut slope stability analysis for static and dynamic (pseudo-static analysis) loading conditions. *Open Geosciences, 15*, 20220561.

Mengesha, T., Tadiwos, C., Workineh, H., Negusssie, T., & Kebede, W. (1996). *Geological map of Ethiopia* (Vol. 2nd edition). Addis Ababa: Geological Survey of Ethiopia.

MIDAS GEOTECH. (2021, 09 09). Retrieved from www.midasgeotech.com: https://www.midasgeotech.com/blog/slope-stability-analysis-and-design

Mizal-Azzmi, N. M.-N. (2011). Geotechnical Approaches for Slope Stabilization in Residential Area. *Procedia Engineering, 20*, Pages 474-482.

NZGS. (2023). *SLOPE STABILITY GEOTECHNICAL GUIDANCE SERIES.* Wellington 6013: New Zealand Geotechnical Society.

Pandit, K., Singh, M., Sharma, S., Sandhu, H. A., & Sahoo, J. (2021). Back-Analysis of a Debris Slopethrough Numerical Methods and Field Observations of Slope Displacements. *Indian Geotechnical Journal, 51*(4), 811-828.

Pantelidis, L. (2009). Rock slope stability assessment through rock mass classification. *International Journal of Rock Mechanics and Mining Sciences 46(20)*, 315-325.

Pauli, A., Kraus, M. A., & Siebert, G. (2021). Experimental and numerical investigations on glass fragments: shear-frame testing and calibration of Mohr–Coulomb plasticity model. *Glass Structures & Engineering, 6*, 65-87.

Popescu, M. (2001). A Suggested Method for Reporting Landslide Remedial Measures. *International Union of Geological Sciences Working Group on Landslides.* Commission on Landslide Remediation.

Raghuvanshi, T. K. (2014). Slope stability susceptibility evaluation parameter (SSEP) rating scheme–an approach for landslide hazard zonation. *Journal of African Earth Sciences, 99*, 595-612.

Raghuvanshi, T. K. (2017). Plane failure in rock slopes–A review on stability analysis techniques. *Journal of King Saud University-Science*.

Sara, B. (2012, April). Retrieved from ResearchGate: https://www.researchgate.net/figure/Classification-of-type-of-landslides-modified-after-Varnes-1978_fig3_258614998

Savi, S., Comiti, F., & Strecker, M. R. (2021). Pronounced increase in slope instability linked to global warming: A case study from the eastern European Alps. *Earth Surface Processes and Landforms, 46*(7), 1328-1347.

Searom, G. (2017). *Landslide hazard evaluation and zonation in and Around Hagereselam Town Doctoral dissertation.* Ethiopia: Addis Ababa University.

Shariati, M. & Fereidooni, D. (2021). Rock slope stability evaluation using kinematic and kinetic methods along the Kamyaran-Marivan road, west of Iran. *Journal of Mountain Science, 18*(3), 779-793.

Shi, K. W. (2019). Grain-size effect on rare earth elements in Pahang River and Kelantan River, Peninsular Malaysia. *Continental Shelf Research*, 103977.

Shiferaw. (2021). Study on the influence of slope height and angle on the factor of safety and shape of failure of slopes based on strength reduction method of analysis. *Journal of Basic and Applied Sciences*.

Siddique, T., Pradhan, S. P., Vishal, V., & Mondal, .. (2019). Stability assessment of Himalayan road cut slopes along National Highway 58, India. *Environmental Earth Sciences*, *76*, 1-18.

Vanneschi, C., Rindinella, A., & Salvini, R. (2022). Hazard Assessment of Rocky Slopes: An Integrated Photogrammetry–GIS Approach Including Fracture Density and Probability of Failure Data. *Remote Sensing*, *14*(6), 1438.

Woldearegay, K. (2013). Review of the occurrences and influencing factors of landslides in the highlands of Ethiopia. *Momona Ethiopian Journal of Science*, 3-31.

Zhao, L., & Karim, M. A . (2018). Use of geosynthetic materials in solid waste landfill design: A review of geosynthetic related stability issues. *Annals of Civil Environmental Engineering*(2), 6-15.

APPENDIXS

Appendix A: The location of the critical soil slope sections of the study area.

Sample Code	Northing	Easting	Altitude (m)	Sampling method
SS1	8°58’55.13’’	40°51’09.15’’	2236	Disturbed sample from natural soil deposit depth of 1m.
SS2	8°58’55.62’’	40°51’31.89’’	2287	Disturbed sample from natural soil deposit depth of 1m.
SS3	8°58’55.37’’	40°51’31.40’’	2485	Disturbed sample from natural soil deposit depth of 1m.
SS4	8°58’55.62’’	40°51’31.74’’	2260	Disturbed sample from natural soil deposit depth of 1m.
SS= Soil slope section				

Appendix B: Soil Particle Size Analysis Result (Sieve and Hydrometer analysis)

Test pit one (SS1)							
Sieve No.	Opening (mm)	Mass of empty Sieve	Mass of soil + Sieve	Mass of Soil Retained	% Retained	Cumulative retained	% Passing
4	4.75	594.4	695.1	100.7	10.07	10.07	89.93
10	2	1080	1294.4	214.4	21.44	31.51	68.49
16	1.18	522	756.4	234.4	23.44	54.95	45.05
20	0.6	462.3	641.4	179.1	17.91	72.86	27.14
40	0.425	850.9	919.6	68.7	6.87	79.73	20.27
60	0.25	443.2	494.1	50.9	5.09	84.82	15.18
200	0.075	421.6	538.8	117.2	11.72	96.54	3.46
Pan		408.4	443	34.6	3.46	100.00	0.00
Sum				1000			

Test pit Two (SS2)							
Sieve No.	Opening (mm)	Mass of empty Sieve	Mass of soil+ Sieve	Mass of Soil Retained	% Retained	Cumulative retained	% Passing
4	4.75	594.4	725.6	131.2	13.12	13.12	86.88
10	2	1080	1274.5	194.5	19.45	32.57	67.43
16	1.18	522	756.8	234.8	23.48	56.05	43.95
20	0.6	462.3	764.3	302	30.20	86.25	13.75
40	0.425	850.9	891.2	40.3	4.03	90.28	9.72
60	0.25	443.2	472	28.8	2.88	93.16	6.84
200	0.075	421.6	471.1	49.5	4.95	98.11	1.89
Pan		408.4	427.3	18.9	1.89	100.00	0.00
Sum				1000			

Test pit Three (SS3)							
Sieve No.	Opening (mm)	Mass of empty Sieve	Mass of soil+ Sieve	Mass of Soil Retained	% Retained	Cumulative retained	% Passing
4	4.75	594.4	745.5	151.1	15.11	15.11	84.89
10	2	1080	1198.3	118.3	11.83	26.94	73.06
16	1.18	522	745.6	223.6	22.36	49.30	50.70
20	0.6	462.3	641.4	179.1	17.91	67.21	32.79
40	0.425	850.9	865.5	14.6	1.46	68.67	31.33
60	0.25	443.2	654.3	211.1	21.11	89.78	10.22
200	0.075	421.6	485	63.4	6.34	96.12	3.88
Pan		408.4	447.2	38.8	3.88	100.00	0.00
Sum				1000			

Test pit Four (SS4)							
Sieve No.	Opening (mm)	Mass of empty Sieve	Mass of soil+ Sieve	Mass of Soil Retained	% Retained	Cumulative retained	% Passing
4	4.75	594.4	715.3	120.9	12.09	12.09	87.91
10	2	1080	1165.35	85.35	8.53	20.63	79.38
16	1.18	522	856.2	334.2	33.42	54.05	45.96
20	0.6	462.3	687.03	224.73	22.47	76.52	23.48
40	0.425	850.9	898.5	47.6	4.76	81.28	18.72
60	0.25	443.2	524.03	80.83	8.08	89.36	10.64
200	0.075	421.6	497.14	75.54	7.55	96.92	3.08
Pan		408.4	439.25	30.85	3.09	100.00	0.00
Sum				1000			

Appendix C: Specific gravity of soil

Specific Gravity Test													
S. N	**Description**	**Determination No**											
		11+820			12+078			12+420			13+507		
		1	2	3	1	2	3	1	2	3	1	2	3
1	Weight of bottle	109.3	107.9	109.4	109.3	107.9	109.4	109.3	107.9	109.4	109.3	107.9	109.4
2	Weight of bottle + Dry soil	116.9	117.4	119.5	120.9	117.9	119.5	116.9	116.9	119.5	116.9	109.5	119.5
3	Weight of bottle + soil + Water	384.8	390.4	387.1	389.8	388.5	393.21	395.3	380.5	387.1	384.8	382	387.1
4	Weight of Water + bottle	379.6	388.3	381	379.6	385.3	382	379.6	382.9	381	379.6	388.4	389
Calculation													
1	Specific Gravity	2.68	2.73	2.68	2.69	2.71	2.74	2.78	2.64	2.68	2.68	2.72	2.68
2	Average G	2.68			2.71			2.70			2.69		

Appendix D: Water Content Results

Water Content Test													
S N	**Description**	**Determinations**											
		11+820			**12+078**			**12+420**			**13+507**		
		B10	A10	S10	A3	N20	A20	B10	A10	S10	A3	N20	A20
1	Weight of Empty Container W1 in g	29.3	26.5	30.3	42.7	43.8	39.6	32.8	38.56	32.65	42.7	43.8	39.6
2	Weight of Container + wet soil W2 in g	58.1	50.4	68.8	80.2	84.8	94.8	58.1	48.36	68.8	65	75.8	89.36
3	Weight of Container + Dry soil W3 in g	52.1	45.5	60.7	75.7	80	88.9	55.64	46.32	65.4	59.36	68.6	84.78
Calculation													
4	weight of Water = W2-W3	6	4.9	8.1	4.5	4.8	5.9	2.46	2.04	3.4	5.64	7.2	4.58
5	weight of Solid = W3-W1	22.8	19	30.4	33	36.2	49.3	22.84	7.76	32.75	16.66	24.8	45.18
6	weight of Water = (W2-W3/W3-W1) *100	26.32	25.79	26.64	13.64	13.26	11.97	10.77	26.29	10.38	33.85	29.03	10.14
	Average	26.25			12.95			15.81			24.34		

Appendix D: Atterberg limit test results

Atterberg Limits							
S. N	**Observation**	**SS1**					
		Liquid limit			**Plastic Limits**		
		1	2	3	1	2	3
1	Water content can No.	M67	M60	M10	R30	M32	N20
2	Number of blows (N)	34	27	22			
3	Mass of empty can (M1)	22.1	22.6	22.3	9.86	9.41	9.65
4	Mass of can + wet soil (M2)	50.5	59.1	55.2	14.32	13.6	12.4
5	Mass of can + dry soil (M3)	39.3	44.5	41.9	13.22	12.63	11.8
	Calculation						
6	Mass of water = M2 - M3	11.2	14.6	13.3	1.1	0.97	0.56
7	Mass of dry soil = M3 - M1	17.2	21.9	19.6	3.36	3.22	2.15
8	Water content = [(6) / (7)] x 100	65.12	66.67	67.86	32.74	30.12	26.05
9	Liquid Limit	63.40			29.64		

Atterberg Limits							
S. N	**Observation**	**SS2**					
		Liquid limit			**Plastic Limits**		
		1	2	3	1	2	3
1	Water content can No.	A1	A3	S2	R30	M32	N20
2	Number of blows (N)	32	27	21			
3	Mass of empty can (M1)	22.1	22.4	22.8	9.5	9.3	9.4
4	Mass of can + wet soil (M2)	63.5	67.5	64.32	13.1	12.5	12.9
5	Mass of can + dry soil (M3)	51.98	51.23	52.2	12.3	11.8	12.1
	Calculation						
6	Mass of water = M2 - M3	11.52	16.27	12.12	0.8	0.7	0.8
7	Mass of dry soil = M3 - M1	29.88	28.83	29.4	2.8	2.5	2.7
8	Water content = [(6) / (7)] x 100	38.55	56.43	41.22	28.57	28.00	29.63
9	Liquid Limit	44.4			28.73		

Atterberg Limits							
S. N	**Observation**	**SS3**					
		Liquid limit			**Plastic Limits**		
		1	2	3	1	2	3
1	Water content can No.	A4	A5	A6	M50	M52	M53
2	Number of blows (N)	32	26	23			
3	Mass of empty can (M1)	22.1	22.4	22.8	22.1	22.6	22.3
4	Mass of can + wet soil (M2)	61.87	65.36	65.23	50.5	56.36	55.2
5	Mass of can + dry soil (M3)	51.2	54.3	52.2	45.3	48.96	48.3
	Calculation						
6	Mass of water = M2 - M3	10.67	11.06	13.03	5.2	7.4	6.9
7	Mass of dry soil = M3 - M1	29.1	31.9	29.4	23.2	26.36	26
8	Water content = [(6) / (7)] x 100	36.67	34.67	44.32	22.41	28.07	26.54
9	Liquid Limit	38.65			25.68		

Atterberg Limits							
S. N	**Observation**	**SS4**					
		Liquid limit			**Plastic Limits**		
		1	2	3	M54	M55	M56
1	Water content can No.	B1	B2	B3	M67	M60	M10
2	Number of blows (N)	32	27	21			
3	Mass of empty can (M1)	22.1	22.4	22.8	22.1	22.6	22.3
4	Mass of can + wet soil (M2)	69.8	67.3	65.5	45.32	47.36	48.8
5	Mass of can + dry soil (M3)	51.2	54.3	52.2	39.3	44.5	41.9
	Calculation						
6	Mass of water = M2 - M3	18.6	13	13.3	6.02	2.86	6.85
7	Mass of dry soil = M3 - M1	29.1	31.9	29.4	17.2	21.9	19.6
8	Water content = [(6) / (7)] x 100	63.92	40.75	45.24	35.00	13.06	34.95
9	Liquid Limit	52.3			27.67		

Appendix F: Compaction tests results

Laboratory Compaction test of Soil	**Pit 1 at SS1**				**Pit 2 at SS2**			
Compacted Soil - Sample no.	1	2	3	4	1	2	3	4
w = Assumed water content, w%	10	12	14	16	4	6	8	10
Actual average water content, w%	28.36	29	30.52	32.7	15.63	16.9	18.74	21.7
Mass of compacted soil and mold (grams)	8974	9115	9214	9182	9315	9389	9541	9436
Mass of mold (grams)	5172	5172	5172	5172	5172	5172	5172	5172
Wet mass of soil in mold (grams)	3802	3943	4042	4010	4143	4217	4369	4264
Volume of mold(cm3)	2137				2137			
Wet density, ρ , (g/cm3)	1.78	1.85	1.89	1.88	1.94	1.97	2.04	2.00
Dry density, ρd , (g/cm3)	1.39	1.43	1.45	1.41	1.68	1.69	1.72	1.64
Optimum Moisture Content	35.89%				24.38%			
Maximum Dry Density	1.45				1.74			

Laboratory Compaction test of Soil	**SS3**				**SS4**			
Compacted Soil - Sample no.	1	2	3	4	1	2	3	4
w = Assumed water content, w%	10	12	14	16	4	6	8	10
Actual average water content, w%	16.87	18.43	19.65	25.34	25.96	27.85	28.21	32.54
Mass of compacted soil and mold (grams)	9041	9211	9596	9615	9125	9365	9465	9465
Mass of mold (grams)	5172	5172	5172	5172	5172	5172	5172	5172
Wet mass of soil in mold (grams)	3869	4039	4424	4443	3953	4193	4293	4293
Volume of mold(cm3)	2137				2137			
Wet density, ρ , (g/cm3)	1.81	1.89	2.07	2.08	1.85	1.96	2.01	2.01
Dry density, ρd , (g/cm3)	1.55	1.60	1.73	1.66	1.47	1.53	1.57	1.52
Optimum Moisture Content	26.51%				31.54%			
Maximum Dry Density	1.72				1.53			

Appendix G: Plasticity Chart (Das, 2002)

Plasticity index (PI)	Descriptions
0	Non plasticity
1-5	Slight plasticity
5-10	Low plasticity
10-20	Medium plasticity
20-40	High plasticity
>40	Very high plasticity

Appendix H: Temperature recorded in the study area (2000-2021)

ST. Name	Tep.Max	Years	Jan	Feb	Mar	Apr	May	Jun	Jul	Aug	Sep	Oct	Nov	Des
Qune	Tep.Max	2000	30	30.4	29.2	28.2	28.2	29	30	30	31	30.4	30.4	29
Qune	Tep.Max	2001	30.2	31.2	31.5	29	31.2	29.5	30.8	31.1	32.6	32.2	31.5	29
Qune	Tep.Max	2002	28.4	29.6	31	33	35	33	32.2	30	30	30	29	29.5
Qune	Tep.Max	2003	30	31.2	31	30.4	32.2	31.8	28.6	28	29.4	30.4	30.2	30
Qune	Tep.Max	2004	30.2	28.8	30	29.8	32	31.2	29	27.4	28.2	28.4	30.2	31
Qune	Tep.Max	2005	30	33	31	30	30.2	30	31	31	30.2	30	30	27
Qune	Tep.Max	2006	29.8	30.2	31.2	31	31	31	29	29	29.2	30.4	28.8	28.4
Qune	Tep.Max	2007	27.8	31	32	30.2	29.4	29.6	29.8	28.2	28.4	29.2	28.4	28
Qune	Tep.Max	2008	29	30.1	32	31.2	32	37.3	33.6	26.8	29.4	28.2	28.2	28.8
Qune	Tep.Max	2009	33	31	33	31.5	32.4	34.8	33.6	26.8	29.4	28.2	28.2	28.8
Qune	Tep.Max	2010	28.2	28	28.4	29	29.4	29.4	30	28.2	29	29	28	29
Qune	Tep.Max	2011	29	29.4	30	31.2	32	30	30.5	30.5	30	30	29.5	27.5
Qune	Tep.Max	2012	26.5	29.5	30	29.5	29.5	31.2	30.5	30	30.5	30	30	29.5
Qune	Tep.Max	2013	30.5	29.5	30	30.8	30.2	31	31.5	30	30	31	31	29.6
Qune	Tep.Max	2014	30	31.6	32.6	31.1	30.3	32.8	30.6	29	30.3	30.4	30.3	28.1
Qune	Tep.Max	2015	27.4	32.7	32.7	32.6	31.6	32	30.3	29.7	29.3	30.4	29.7	28.4
Qune	Tep.Max	2016	29	31.2	33.6	32.2	29.4	29.4	28.8	30.2	32.5	29	27.4	28
Qune	Tep.Max	2017	28.5	29.4	32.8	31.5	31.4	32.2	31.4	31	27.5	29.2	27.4	27
Qune	Tep.Max	2018	28.6	31.3	28.6	28.6	28.6	28.6	29.4	28.7	28.6	31.3	28.6	28.7
Qune	Tep.Max	2019	31.4	32.3	34.2	33.4	33.6	32.1	30.9	27.8	28.2	28	28.2	25.6
Qune	Tep.Max	2020	28.1	29.3	27.8	31	31.1	30.1	30.2	29.6	28.7	28.1	29.3	27.8
Qune	Tep.Max	2021	27.4	29.2	31	32.3	32.1	29.2	31	32.3	32.1	31.2	29.1	30
Qune	Tep.Max	2022	29	29.2	29.9	28.7	28.9	30	32.4	29.9	28.7	29.4	29.4	29.4
		Average	29.22	30.40	31.02	30.70	30.94	31.10	30.66	29.36	29.70	29.76	29.25	28.61

ST. Name	Tep. Min	Years	Jan	Feb	Mar	Apr	May	Jun	Jul	Aug	Sep	Oct	Nov	Des
Qune	Tep. Min	2000	12	15.2	14	14.5	13	15.4	16	14	16	15	14.3	14.8
Qune	Tep. Min	2001	10.4	15	10	15	9.4	11	14	14.8	11	12.5	12.4	11.8
Qune	Tep. Min	2002	9	8.6	13	13	14.2	16	15	14.2	11.8	11.2	14	11.9
Qune	Tep. Min	2003	14.4	15	13.6	14.2	14.8	13.8	14	14.6	15.6	12	14.6	10.8
Qune	Tep. Min	2004	10	11.2	10.4	14.4	12.6	12	10.2	1.2	13.6	13.6	10.6	12.8
Qune	Tep. Min	2005	10.2	11.2	15	14.6	14.8	15.2	15	15	15	14.8	10.1	8.4
Qune	Tep. Min	2006	12	17	10	14	14.2	14	14	14	14.2	13.4	12	10.8
Qune	Tep. Min	2007	10.2	15.2	15	14.2	14.4	14.5	14.2	14.7	13	10.1	9.2	8
Qune	Tep. Min	2008	9	7.3	9.4	11.2	14	13	7.5	8.5	9	10	10.2	11
Qune	Tep. Min	2009	9.5	11	11	14.5	14	15.4	14.2	15	15	10.2	10.5	13.5
Qune	Tep. Min	2010	9.5	13.2	14	15	15	16	15	14	15	15	12	10
Qune	Tep. Min	2011	12	14.8	14.8	12.8	12	14	14	13.5	14	13.5	13.5	8.5
Qune	Tep. Min	2012	9.5	9.8	11	12	13	14	11.5	14	14	12	13	13
Qune	Tep. Min	2013	13.5	11.5	12.5	13.5	14	15	14	14	14	12	12	8.4
Qune	Tep. Min	2014	8.5	11.3	12.4	13	13.8	14.3	14	14	14	10.4	9.5	7
Qune	Tep. Min	2015	7	8.2	11.8	12	14	14.8	14.6	13.8	13.7	13	10.2	10.6
Qune	Tep. Min	2016	10	10	14.8	15.2	15	15	14.8	14	14	13	11.2	12
Qune	Tep. Min	2017	11	10.2	11.8	13.7	14.8	15	14.3	13.5	13	10	7.8	5.5
Qune	Tep. Min	2018	11	12	13	10.4	9	9.6	13.4	12	8.4	9.2	8.7	10
Qune	Tep. Min	2019	7	10	13.5	12.5	13.7	14.4	13.2	13	13.1	9.8	9.7	8
Qune	Tep. Min	2020	12	11	10.2	12.4	13.5	13.8	13	11.8	13	9.9	7.8	6.8
Qune	Tep. Min	2021	4.1	4.3	10	13	12.1	12.5	12	11	12	8	6.5	6
Qune	Tep. Min	2022	7	7.2	7.2	7.2	7.2	13	12	13	12	13	12	13
		Average	9.95	11.31	12.10	13.14	13.15	13.99	13.47	12.94	13.23	11.81	10.95	10.11

ST. Name	Tep. Max	Years	Jan	Feb	Mar	Apr	May	Jun	Jul	Aug	Sep	Oct	Nov	Des
Badesa	Tep. Max	2000	29	29.6	28.4	28	31.5	29.9	28.7	30.4	29.3	27.5	28.6	31.3
Badesa	Tep. Max	2001	29.5	31	29	29	30.3	37.2	32.5	29.9	30.2	30	31.3	31.3
Badesa	Tep. Max	2002	29.4	32.4	32.2	31.4	32.2	32	30.4	30	30	31	31	30.4
Badesa	Tep. Max	2003	32	32.8	33	33	32	32	28.4	30	30	31.4	33	32
Badesa	Tep. Max	2004	31.4	32.2	34	29.4	31.5	31.5	30.3	29	28.9	29.2	30.4	29
Badesa	Tep. Max	2005	29.8	33.5	31.5	37	29.3	29.6	29	29.6	28.6	30.4	29.4	29.4
Badesa	Tep. Max	2006	30.6	31.7	31.5	29.8	29.8	31	30	28.4	27.6	29.2	29.2	27.6
Badesa	Tep. Max	2007	30.7	32.6	33	30.4	31.6	30.4	29.5	28	28.2	28.8	29	29.2
Badesa	Tep. Max	2008	30.7	31.2	33	31.3	30.8	32.2	29.8	29.5	29.4	30.8	28.2	29.4
Badesa	Tep. Max	2009	29.8	32.2	33.8	31.2	39.8	32.4	30.4	29.9	30.1	30.4	30.5	29.2
Badesa	Tep. Max	2010	30.4	32.2	29	29.4	30.4	31.2	29.4	28.7	29	29.3	29.5	29.8
Badesa	Tep. Max	2011	30.7	32.2	32.6	33	34	31.4	30.4	30.4	28.4	30.8	31	29.8
Badesa	Tep. Max	2012	30	31.8	32.2	30.2	33.8	32.8	30.4	29.3	28.8	29.3	30	29.8
Badesa	Tep. Max	2013	32.6	32.8	32.5	29.6	28.8	28.6	31.5	27.5	29.6	29.4	29	28.7
Badesa	Tep. Max	2014	29.9	31.5	32	30	29.4	32.6	31.6	28.6	28.8	30	30.3	29.6
Badesa	Tep. Max	2015	30.6	32.3	32.7	33.5	32.1	31	31.6	31.3	30.4	31.3	37.2	31.3
Badesa	Tep. Max	2016	33.4	32.5	34.6	32.5	30.4	30	29.8	29.7	30.6	32	32.5	32.3
Badesa	Tep. Max	2017	30	32.5	33.7	32	31	32.5	30.8	31.2	32	31.2	29.9	30.7
Badesa	Tep. Max	2018	31	31	31	31	30.9	29.7	29.3	30	30.2	31.3	30.2	32
Badesa	Tep. Max	2019	32.7	33	33.8	33.8	34.4	30	30	28.7	28.7	30	30	29.5
Badesa	Tep. Max	2020	32	33	33.5	32.2	29.4	30.4	30.4	30.4	28.7	31	30.3	30.4
Badesa	Tep. Max	2021	30.2	31.3	32	30	30	29.4	29.4	29.4	29.4	31.5	31.5	31.5
Badesa	Tep. Max	2022	34.5	34.5	34.5	34.5	34.5	30	29.2	29.3	29.3	29.3	29.3	29.3
		Average	30.91	32.17	32.33	31.40	31.65	31.21	30.12	29.53	29.40	30.22	30.49	30.15

ST. Name	Tep. Min	Years	Jan	Feb	Mar	Apr	May	Jun	Jul	Aug	Sep	Oct	Nov	Des
Badesa	Tep. Min	2000	11.5	10	11.7	12	11.6	10.3	12	10.2	12.3	11.8	13.2	12.5
Badesa	Tep. Min	2001	11	10.5	10	10	8.5	11	12	10.5	8.4	13.7	13.5	11.9
Badesa	Tep. Min	2002	6.5	6	7	11.5	13	11.5	13	13.2	9.5	6	7	9.5
Badesa	Tep. Min	2003	5	10	11	11.8	10	12	13	10	11.5	5.5	6.5	4.5
Badesa	Tep. Min	2004	7	6	5	9	10	11.4	12.5	11	11	10	5.9	5.3
Badesa	Tep. Min	2005	7	5	8.9	10	11.5	11.8	11.2	11.7	9.7	6.5	5	3
Badesa	Tep. Min	2006	5.3	9.4	8	10	10	10.9	9.5	11.5	11	8.4	7.2	6.7
Badesa	Tep. Min	2007	6.2	9	8.8	7.2	11.7	12	10.2	11.7	10.5	4.6	4.5	4.3
Badesa	Tep. Min	2008	5.4	5.5	6	8	12	10.5	11	8.9	10	7.2	4.5	3.7
Badesa	Tep. Min	2009	4.5	7	9.5	11.3	11.6	8.4	13.2	12.5	10	6.5	5.4	10
Badesa	Tep. Min	2010	4.4	9.4	7.2	6.8	10.3	13.7	13.3	12.2	8.5	9	6	2.5
Badesa	Tep. Min	2011	5.5	6.7	9.4	11	12	13.5	13	10.7	11	7.5	5	4.5
Badesa	Tep. Min	2012	6	6.5	7.5	12.5	10.2	11.9	11.5	12	11.6	5.3	4.9	6.4
Badesa	Tep. Min	2013	4.5	6.3	10.2	12.6	12.3	13	13.6	10	11.2	7	6	5
Badesa	Tep. Min	2014	5.3	8.4	10.6	12	11.8	11	13	11.2	12.5	7.2	7.6	5.6
Badesa	Tep. Min	2015	5.9	6.4	10.4	11.5	13.2	13.6	13	13.4	12.5	9.2	7.5	9.5
Badesa	Tep. Min	2016	15.4	7.5	14.3	14.8	12.5	10	13.6	12.8	11.9	11	7.2	7
Badesa	Tep. Min	2017	9	9.4	11	11.4	12	13.7	13.2	9	8	8.4	5.5	3.6
Badesa	Tep. Min	2018	2	5	6	9	11.6	12.5	13.2	12.2	10	8.9	7	8
Badesa	Tep. Min	2019	5	7.5	11	12.9	12	12.9	12	12.9	13.9	9	5.2	4.5
Badesa	Tep. Min	2020	9	8	10.5	12.3	11.3	12	12	13	13	13	6.3	5
Badesa	Tep. Min	2021	6.5	7	12.3	12.2	10.7	8.5	7	7.5	10	8.3	9	10
Badesa	Tep. Min	2022	12	12.2	12.6	14	13	13	11	11	12	12	12	12
		Average	6.95	7.77	9.52	11.03	11.43	11.70	12.04	11.27	10.87	8.52	7.04	6.74

Appendix I: Rainfall recorded in the study area (2000-2021)

ST. Name	Prcip	Years	Jan	Feb	Mar	Apr	May	Jun	Jul	Aug	Sep	Oct	Nov	Des
Qune	Prcip	2000	50.5	40	124	39.7	70.1	101.9	27.6	135.8	17.4	27.4	35	10
Qune	Prcip	2001	36.1	98.4	47	0	9.7	51.8	49	46	33.7	123	31.5	101.8
Qune	Prcip	2002	70.5	0	174	49.7	73.1	121.9	27.6	145.8	17.4	17.4	25	20
Qune	Prcip	2003	3.2	53.1	54.5	112.7	25.2	105	205.4	225	140.8	0	30	15.8
Qune	Prcip	2004	51.4	0	73.4	164.8	2.4	36.1	125.6	1446	246.8	99	17	28
Qune	Prcip	2005	0	14.8	107.6	173.6	208.8	98.4	215.6	87.6	171	4.8	12.4	0
Qune	Prcip	2006	12	33.4	130	88	63.4	47	140.8	243.3	101.1	133	0	73.2
Qune	Prcip	2007	18.2	0	148.4	285.4	43.4	0	192.3	200.9	147.2	16.2	0	0
Qune	Prcip	2008	11.6	0	18.5	105.4	118.9	9.7	0	0	0	0	0	0
Qune	Prcip	2009	32	10.1	42.2	71.1	0	51.8	93.7	95.6	58.2	59.9	54.5	63.3
Qune	Prcip	2010	2.5	85.8	199.2	87.2	65.1	49	133	103	211.2	0	3	0
Qune	Prcip	2011	0	0	43.2	36	110.4	46	98.5	141.5	57.5	0	0	0
Qune	Prcip	2012	0	0	0	95.5	44	33.7	88.5	192	108.5	13	1.6	7
Qune	Prcip	2013	26.7	2	7	51.5	20	123	58	69	146.5	5	41	40
Qune	Prcip	2014	0	3.1	172.9	174.8	190.7	31.5	181.5	205	108.4	147.3	8.9	3.1
Qune	Prcip	2015	0	0	9	42.6	131	101.8	49.8	236.5	105.2	2.6	0	18.8
Qune	Prcip	2016	5.3	36.6	39.6	254.4	220.8	87.7	205.8	119.1	116.2	28.2	12	0
Qune	Prcip	2017	0	39.1	24.5	35.5	77.6	20.9	86.2	162.9	186.9	11	0	0
Qune	Prcip	2018	0	0	0	0	0	0	67.2	50	102.7	69.2	29.9	0
Qune	Prcip	2019	0	12.7	56.8	90.2	188.4	138.6	130.6	194.8	209.4	95.5	91.4	25.8
Qune	Prcip	2020	0	0	0	56.5	162.1	143.7	60.8	175.1	263.4	119.8	13.4	4.4
Qune	Prcip	2021	11.5	0	4.7	3.8	98.9	0	0	176.2	138.1	0	0	0
Qune	Prcip	2022	131.3	0	0	0	0	89.3	110.4	83.1	0	0	0	0
		Average	20.12	18.66	64.20	87.76	83.65	64.73	102.08	197.13	116.85	42.27	17.68	17.88

ST. Name	Prcip	Years	Jan	Feb	Mar	Apr	May	Jun	Jul	Aug	Sep	Oct	Nov	Des
Qune	Prcip	2000	50.5	40	124	39.7	70.1	101.9	27.6	135.8	17.4	27.4	35	10
Qune	Prcip	2001	36.1	98.4	47	0	9.7	51.8	49	46	33.7	123	31.5	101.8
Qune	Prcip	2002	70.5	0	174	49.7	73.1	121.9	27.6	145.8	17.4	17.4	25	20
Qune	Prcip	2003	3.2	53.1	54.5	112.7	25.2	105	205.4	225	140.8	0	30	15.8
Qune	Prcip	2004	51.4	0	73.4	164.8	2.4	36.1	125.6	1446	246.8	99	17	28
Qune	Prcip	2005	0	14.8	107.6	173.6	208.8	98.4	215.6	87.6	171	4.8	12.4	0
Qune	Prcip	2006	12	33.4	130	88	63.4	47	140.8	243.3	101.1	133	0	73.2
Qune	Prcip	2007	18.2	0	148.4	285.4	43.4	0	192.3	200.9	147.2	16.2	0	0
Qune	Prcip	2008	11.6	0	18.5	105.4	118.9	9.7	0	0	0	0	0	0
Qune	Prcip	2009	32	10.1	42.2	71.1	0	51.8	93.7	95.6	58.2	59.9	54.5	63.3
Qune	Prcip	2010	2.5	85.8	199.2	87.2	65.1	49	133	103	211.2	0	3	0
Qune	Prcip	2011	0	0	43.2	36	110.4	46	98.5	141.5	57.5	0	0	0
Qune	Prcip	2012	0	0	0	95.5	44	33.7	88.5	192	108.5	13	1.6	7
Qune	Prcip	2013	26.7	2	7	51.5	20	123	58	69	146.5	5	41	40
Qune	Prcip	2014	0	3.1	172.9	174.8	190.7	31.5	181.5	205	108.4	147.3	8.9	3.1
Qune	Prcip	2015	0	0	9	42.6	131	101.8	49.8	236.5	105.2	2.6	0	18.8
Qune	Prcip	2016	5.3	36.6	39.6	254.4	220.8	87.7	205.8	119.1	116.2	28.2	12	0
Qune	Prcip	2017	0	39.1	24.5	35.5	77.6	20.9	86.2	162.9	186.9	11	0	0
Qune	Prcip	2018	0	0	0	0	0	0	67.2	50	102.7	69.2	29.9	0
Qune	Prcip	2019	0	12.7	56.8	90.2	188.4	138.6	130.6	194.8	209.4	95.5	91.4	25.8
Qune	Prcip	2020	0	0	0	56.5	162.1	143.7	60.8	175.1	263.4	119.8	13.4	4.4
Qune	Prcip	2021	11.5	0	4.7	3.8	98.9	0	0	176.2	138.1	0	0	0
Qune	Prcip	2022	131.3	0	0	0	0	89.3	110.4	83.1	0	0	0	0
		Average	20.12	18.66	64.20	87.76	83.65	64.73	102.08	197.13	116.85	42.27	17.68	17.88